



POLITECNICO  
DI TORINO

POLITECNICO DI TORINO

Master Degree course in Mechatronics Engineering

Master Degree Thesis

**Development and Validation of a  
Test Rig for Thermal Management  
System Evaluation in Electric  
Powertrains**

**Supervisors**

Prof. Gianmario PELLEGRINO

Eng. Jiri PIKULA

Eng. Zdenek MACH

**Candidate**

Sara FRANCHINA

ACADEMIC YEAR 2025-2026

# Acknowledgements

*Ai miei genitori, **Daniela e Giuseppe.***

*A mia sorella **Giulia.***

*A **Greta e Alessia.***

*Per il supporto, la pazienza e la fiducia che  
non mi avete mai fatto mancare.*

## **Abstract**

The primary objective of this thesis is the development of a dedicated thermal test rig intended for the experimental evaluation of key components of an electric powertrain lubrication circuit under controlled temperature and pressure conditions.

The setup was designed and assembled at Garrett Advancing Motion with the purpose of enabling systematic and repeatable characterization of the electric oil pump, oil filter and heat exchanger, which represent critical elements for the reliability and overall efficiency of modern electrified powertrains.

The rig, developed at Garrett Advancing Motion, is specifically designed to test the oil pump, oil filter, and heat exchanger, components essential to the reliability and efficiency of electric powertrain systems.

Garrett Motion operates as a global engineering company in the automotive sector, with established expertise in turbocharging technologies and an increasing focus on electrification solutions. Within this context, the test bench supports development activities by providing a laboratory-scale platform where both individual components and their interaction inside a closed-loop lubrication system can be investigated under operating conditions comparable to those encountered in service.

The facility allows detailed analysis of hydraulic behaviour, thermal response and long-term performance, with particular attention to effects associated with temperature variation and continuous operation. The experimental data obtained from these campaigns serve to guide component validation and to improve the robustness and efficiency of future thermal-management architectures for next-generation electric vehicles.

# Contents

<b>List of Figures</b>	5
<b>List of Tables</b>	9
<b>Glossary</b>	11
<b>1 Introduction</b>	13
1.1 Context and Objectives . . . . .	13
1.2 Thesis Structure . . . . .	14
<b>2 Technical Background and Literature Review</b>	15
2.1 Lubrication systems in automotive applications . . . . .	15
2.2 Electric oil pumps . . . . .	16
2.3 Control strategies for electric oil pumps . . . . .	16
2.4 Low-temperature operation and cold-start conditions . . . . .	17
2.5 Pump performance characterization . . . . .	17
2.6 State of the art of experimental test approaches . . . . .	18
<b>3 Design and Development of the Thermal Test Rig</b>	19
3.1 Project Background and Objectives . . . . .	19
3.2 Design Requirements and Boundary Conditions . . . . .	22
3.2.1 Thermal Requirements . . . . .	22
3.2.2 Hydraulic Requirements . . . . .	23
3.2.3 Pressure and Flow Measurement Requirements . . . . .	25
3.2.4 Component Compatibility and Material Selection . . . . .	26
3.3 System Architecture and Layout . . . . .	27
3.3.1 Overall Layout of the Test Rig . . . . .	27
3.3.2 Hydraulic Circuit Configuration . . . . .	29
3.3.3 Main Mechanical Components . . . . .	30
3.3.4 Modularity of the Rig . . . . .	32
3.4 Measurement System . . . . .	33
3.4.1 Measured Quantities . . . . .	34

3.4.2	Pressure Measurement System . . . . .	34
3.4.3	Temperature Measurement System . . . . .	36
3.4.4	Flow Rate Measurement . . . . .	37
3.4.5	Sensor Placement Strategy . . . . .	37
3.4.6	Data Acquisition Overview . . . . .	38
3.5	Power Supply and Protection System . . . . .	38
3.5.1	Electrical Architecture Overview . . . . .	38
3.5.2	EOP Power Supply . . . . .	39
3.5.3	Auxiliary Power Supplies . . . . .	40
3.5.4	Protection Devices . . . . .	40
3.5.5	Emergency Stop System . . . . .	41
3.5.6	Grounding and Electrical Safety Measures . . . . .	41
3.6	Design Iteration and Improvements Based on Preliminary Testing . . . . .	42
3.6.1	Initial Rig Configuration . . . . .	42
3.6.2	Preliminary Leakage Tests and Root Cause Identification . . . . .	43
3.6.3	Adapter Design Improvement . . . . .	44
3.6.4	O-ring Design and Sizing Criteria . . . . .	44
3.6.5	Final Configuration Validation . . . . .	47
<b>4</b>	<b>Software Architecture and System Monitoring</b>	<b>49</b>
4.1	LabVIEW Control Interface . . . . .	49
4.2	Software Architecture and Block Diagram Description . . . . .	51
4.3	Data acquisition and Signal Management . . . . .	52
<b>5</b>	<b>HSE and CE Marking</b>	<b>57</b>
5.1	The importance of HSE . . . . .	57
5.2	Local HSE Approval and Mandatory Safety Documentation . . . . .	58
5.3	Hazard Identification and Risk Assessment . . . . .	59
5.4	CE Marking of the Thermal Test Rig . . . . .	61
<b>6</b>	<b>Test Procedure</b>	<b>63</b>
6.1	Preparation and Setup checks . . . . .	63
6.2	Test Sequence Execution . . . . .	64
6.2.1	Manual Test Execution . . . . .	65
6.2.2	Automatic Test Execution . . . . .	66
6.2.3	Selection of Executed Test Conditions . . . . .	68
6.3	Step Management and Fault Handling . . . . .	69
6.3.1	Test Step Definition . . . . .	69
6.3.2	Stabilization Criteria . . . . .	70
6.3.3	Manual Step Transition Logic . . . . .	70

6.3.4	Fault Detection and Alarm Management . . . . .	71
6.3.5	Safety Actions and Protective Measures . . . . .	71
6.3.6	Test Interruption and Data Integrity . . . . .	71
<b>7</b>	<b>Experimental Results and Discussion</b>	<b>73</b>
7.1	Experimental campaign overview . . . . .	73
7.2	Results for EOP1 . . . . .	74
7.3	Results for EOP2 . . . . .	75
7.4	Comparative analysis between EOP1 and EOP2 . . . . .	77
7.5	Filter and HE results . . . . .	78
7.6	Validation of the thermal test rig . . . . .	79
<b>8</b>	<b>Conclusion and additional steps for the future</b>	<b>81</b>
<b>A</b>	<b>Test EOP1</b>	<b>83</b>
A.1	Operating point maps . . . . .	83
A.2	Pressure–flow characteristic curves . . . . .	88
A.3	Efficiency maps . . . . .	91
A.4	Filter and heat exchanger results . . . . .	96
<b>B</b>	<b>Test EOP2</b>	<b>99</b>
B.1	Operating point maps . . . . .	99
B.2	Pressure–flow characteristic curves . . . . .	102
B.3	Efficiency maps . . . . .	104
B.4	Filter and heat exchanger results . . . . .	109
	<b>Bibliography</b>	<b>111</b>

# List of Figures

3.1	Previous experimental test rig configuration used for standalone electric oil pump testing. . . . .	19
3.2	Electrical heater installed on the lubrication circuit to provide controlled thermal conditioning of the oil during hot soak tests. . . . .	22
3.3	Simplified functional layout of the lubrication circuit, showing the main components and oil flow direction. . . . .	24
3.4	Flowmeter installed in the hydraulic circuit for oil flow rate measurement. . . . .	26
3.5	Globe valve used for pressure regulation: original component (left), integrated heating solution with thermal insulation (center) and additional protection used during cold starts. . . . .	27
3.6	Overall layout of the test rig . . . . .	28
3.7	Test rig installed inside the catch basin . . . . .	29
3.8	Hydraulic schematic of the test rig with flow direction . . . . .	29
3.9	Custom mechanical components: oil tank and adapters . . . . .	31
3.10	Improved single-piece EOP adapter design for the first EOP tested. . . . .	32
3.11	Improved single-piece EOP adapter design for the second EOP tested. . . . .	32
3.12	Final configuration of the rig. . . . .	33
3.13	Pressure sensor installation detail on the hydraulic circuit . . . . .	35
3.14	Custom holder used for pressure sensor mounting . . . . .	35
3.15	K-type thermocouple installation detail on the test rig . . . . .	36
3.16	Electrical cabinet housing power supply and protection components . . . . .	39
3.17	Emergency stop push-button located outside the climatic chamber . . . . .	41
3.18	Initial adapter–tank interface design . . . . .	43
3.19	Improved adapter design with integrated O-ring groove . . . . .	44
3.20	Static axial O-ring sealing configuration . . . . .	45
3.21	Catalogue reference for static axial O-ring groove dimensions . . . . .	46
3.22	O-ring compression and gland fill verification using calculation tool . . . . .	47
4.1	LabVIEW control interface used to operate the test rig and monitor the main signals during testing activities. . . . .	50

4.2	LabVIEW block diagram illustrating the modular software architecture of the control and monitoring system. . . . .	51
4.3	Pressure and temperature sensors on the rig. . . . .	53
6.1	Test rig in the climatic chamber during tests. . . . .	64
6.2	Example of electric oil pump (EOP) performance map obtained at an oil temperature of $-20\text{ }^{\circ}\text{C}$ , reported as a visual reference to illustrate the manual mapping procedure described in this section. A complete set of performance maps is provided in the Appendix. . . . .	67
6.3	Rectangular automatic test profile selected for endurance-oriented test planning. The profile represents repeated cycles between predefined operating levels, resulting in sustained loading at peak conditions. . . . .	68
7.1	Conditions of the rig after reaching $T = -40^{\circ}\text{C}$ without the EOP running. . . . .	76
A.1	EOP1 – Operating point map at $T = 0^{\circ}\text{C}$ . . . . .	84
A.2	EOP1 – Operating point map at $T = -10^{\circ}\text{C}$ . . . . .	85
A.3	EOP1 – Operating point map at $T = -20^{\circ}\text{C}$ . . . . .	86
A.4	EOP1 – Operating point map at $T = -30^{\circ}\text{C}$ . . . . .	86
A.5	EOP1 – Operating point map at $T = -40^{\circ}\text{C}$ . . . . .	87
A.6	EOP1 – Pressure–flow characteristic at $T = 0^{\circ}\text{C}$ . . . . .	88
A.7	EOP1 – Pressure–flow characteristic at $T = -10^{\circ}\text{C}$ . . . . .	88
A.8	EOP1 – Pressure–flow characteristic at $T = -20^{\circ}\text{C}$ . . . . .	89
A.9	EOP1 – Pressure–flow characteristic at $T = -30^{\circ}\text{C}$ . . . . .	89
A.10	EOP1 – Pressure–flow characteristic at $T = -40^{\circ}\text{C}$ . . . . .	90
A.11	EOP1 – Cubic efficiency map at $T = 0^{\circ}\text{C}$ . . . . .	91
A.12	EOP1 – Linear efficiency map at $T = 0^{\circ}\text{C}$ . . . . .	92
A.13	EOP1 – Cubic efficiency map at $T = -10^{\circ}\text{C}$ . . . . .	92
A.14	EOP1 – Linear efficiency map at $T = -10^{\circ}\text{C}$ . . . . .	93
A.15	EOP1 – Cubic efficiency map at $T = -20^{\circ}\text{C}$ . . . . .	93
A.16	EOP1 – Linear efficiency map at $T = -20^{\circ}\text{C}$ . . . . .	94
A.17	EOP1 – Cubic efficiency map at $T = -30^{\circ}\text{C}$ . . . . .	94
A.18	EOP1 – Linear efficiency map at $T = -30^{\circ}\text{C}$ . . . . .	95
A.19	EOP1 – Linear efficiency map at $T = -40^{\circ}\text{C}$ . . . . .	95
A.20	EOP1 – Filter and heat exchanger results at $T = 0^{\circ}\text{C}$ . . . . .	96
A.21	EOP1 – Filter and heat exchanger results at $T = -10^{\circ}\text{C}$ . . . . .	96
A.22	EOP1 – Filter and heat exchanger results at $T = -20^{\circ}\text{C}$ . . . . .	97
A.23	EOP1 – Filter and heat exchanger results at $T = -30^{\circ}\text{C}$ . . . . .	97
A.24	EOP1 – Filter and heat exchanger results at $T = -40^{\circ}\text{C}$ . . . . .	98
B.1	EOP2 – Operating point map at $T = 0^{\circ}\text{C}$ . . . . .	100

B.2	EOP2 – Operating point map at $T = -10^{\circ}\text{C}$ .	100
B.3	EOP2 – Operating point map at $T = -20^{\circ}\text{C}$ .	101
B.4	EOP2 – Operating point map at $T = -30^{\circ}\text{C}$ .	101
B.5	EOP2 – Pressure–flow characteristic at $T = 0^{\circ}\text{C}$ .	102
B.6	EOP2 – Pressure–flow characteristic at $T = -10^{\circ}\text{C}$ .	102
B.7	EOP2 – Pressure–flow characteristic at $T = -20^{\circ}\text{C}$ .	103
B.8	EOP2 – Pressure–flow characteristic at $T = -30^{\circ}\text{C}$ .	103
B.9	EOP2 – Cubic efficiency map at $T = 0^{\circ}\text{C}$ .	104
B.10	EOP2 – Linear efficiency map at $T = 0^{\circ}\text{C}$ .	105
B.11	EOP2 – Cubic efficiency map at $T = -10^{\circ}\text{C}$ .	105
B.12	EOP2 – Linear efficiency map at $T = -10^{\circ}\text{C}$ .	106
B.13	EOP2 – Cubic efficiency map at $T = -20^{\circ}\text{C}$ .	106
B.14	EOP2 – Linear efficiency map at $T = -20^{\circ}\text{C}$ .	107
B.15	EOP2 – Cubic efficiency map at $T = -30^{\circ}\text{C}$ .	107
B.16	EOP2 – Linear efficiency map at $T = -30^{\circ}\text{C}$ .	108
B.17	EOP2 – Filter and heat exchanger results at $T = 0^{\circ}\text{C}$ .	109
B.18	EOP2 – Filter and heat exchanger results at $T = -10^{\circ}\text{C}$ .	109
B.19	EOP2 – Filter and heat exchanger results at $T = -20^{\circ}\text{C}$ .	110
B.20	EOP2 – Filter and heat exchanger results at $T = -30^{\circ}\text{C}$ .	110



# List of Tables

3.1	Comparison between the previous experimental test rig and the newly developed thermal test rig . . . . .	21
3.2	Thermal operating requirements of the test rig . . . . .	22
3.3	Thermal design strategy for high- and low-temperature operation . . . . .	23
3.4	Main hydraulic components of the test rig . . . . .	30
3.5	Measured quantities and main purpose . . . . .	34
3.6	Pressure measurement system overview . . . . .	36
3.7	Temperature measurement system overview . . . . .	37
3.8	Measurement locations for component-level evaluation . . . . .	37
3.9	Main electrical protection devices . . . . .	41
3.10	Summary of adapter design modifications . . . . .	44
4.1	Overview of acquired signals and instrumentation . . . . .	54
6.1	Summary of the main test typologies performed on the thermal test rig . . . . .	65
6.2	Objectives of manually executed test categories [2] . . . . .	65
6.3	Overview of planned and executed tests and associated limitations . . . . .	69
7.1	Overview of experimental tests . . . . .	74
7.2	Maximum measured efficiency values for EOP1 . . . . .	75
7.3	Maximum measured efficiency values for EOP2 . . . . .	76
7.4	Comparison between EOP1 and EOP2 . . . . .	78



# Glossary

**EOP** Electric Oil Pump. Electric pump used to circulate lubricating oil within the thermal management and lubrication system under test.

**HE** Heat Exchanger. Component used to exchange thermal energy between the oil circuit and the external environment.

**HSE** Health, Safety and Environment. Set of procedures and regulations aimed at ensuring safe working conditions and environmental protection.

**CE Marking** Conformité Européenne Marking. Certification indicating compliance with European safety directives.

**MRA** Machine Risk Assessment. Methodology used to identify hazards and evaluate machinery-related risks.

**NVH** Noise, Vibration and Harshness. Characteristics related to acoustic and vibrational behavior of systems.

**PPE** Personal Protective Equipment. Protective devices worn by operators during testing activities.

**CAN** Controller Area Network. Communication protocol used for data exchange between electronic devices.

**RPM** Revolutions Per Minute. Unit used to express rotational speed.

**DAQ** Data Acquisition. System used to acquire and record sensor signals.

**TDMS** Technical Data Management Streaming. Binary file format developed by National Instruments for structured storage and high-speed streaming of measurement data.

**SSR** Solid State Relay. Electronic switching device for high-power loads.

**TPM** Total Productive Maintenance. Maintenance strategy focused on reliability and safety.

**SOS** Safety Operating Sheet. Step-by-step guide for safe machine operation.



# Chapter 1

## Introduction

### 1.1 Context and Objectives

Garrett Advancing Motion has been operating in the automotive industry for over six decades, developing advanced engineering solutions with a strong focus on efficiency, reliability and performance. The company is historically recognised for its expertise in turbocharging technologies, particularly in applications requiring high power density and operation at elevated rotational speeds.

With the advent of electrification in the automotive sector, these competencies have been progressively extended to the development of solutions for electrified powertrains, addressing the new technical challenges associated with electric propulsion systems. In this context, Garrett has developed an integrated e-powertrain architecture combining the electric motor, inverter and gearbox into a compact 3-in-1 system. This design achieves a significant reduction in weight and size compared to conventional systems, while maintaining controlled NVH behaviour and satisfying performance and efficiency specifications. [7]

The reliable operation of such highly integrated systems relies not only on the core powertrain components, but also on dedicated auxiliary subsystems. Among these, the lubrication system plays a key role in ensuring both mechanical durability and thermal control, particularly for the gearbox and related components operating under variable load and temperature conditions. The system is designed to operate across a wide range of temperatures and pressures, providing sufficient oil flow and effective heat dissipation to maintain stable performance under real-world operating conditions.

In this context, the present project focuses on the experimental testing of the lubrication system, consisting of the oil pump, oil filter, and heat exchanger. The test bench provides a controlled and repeatable environment to monitor key performance indicators such as oil pressure, temperature distribution, and thermal efficiency. The objective is to evaluate the system's performance under representative operating conditions and to

verify its ability to meet the required functional and thermal targets.

## **1.2 Thesis Structure**

The thesis is organized into several chapters, each addressing a specific aspect of the project. This section provides a brief overview of the scope and contents of each chapter.

Chapter 3 presents the design procedure, providing a detailed description of the development process followed to realize the mechanical components of the test rig. Initial tests evaluating the robustness of the mechanical design are described, along with the solutions implemented to enhance reliability prior to performing the full experimental tests. The test environment is also introduced, including the selection of sensors used to record data during the experiments.

Chapter 4 focuses on the software developed to implement the control and monitoring strategy for the test rig, with particular emphasis on the user interface created to facilitate the execution of the tests.

Chapter 5 addresses the procedures and documentation required to obtain local approval for performing tests in the laboratory. It also describes the actions taken to achieve CE marking, which is necessary to replicate the rig at other Garrett facilities and to allow future testing with different components.

Chapter 6 provides a detailed description of the test procedures, with particular attention to manual operations, step management, and fault handling.

Finally, Chapter 7 presents the analysis of the data obtained from the tests, including the methods used to interpret the results and evaluate the performance of the lubrication system.

# Chapter 2

## Technical Background and Literature Review

This chapter provides the theoretical and technological background required to properly frame the experimental work presented in this thesis. The main concepts related to automotive lubrication systems, electric oil pumps and their control strategies are introduced, with particular emphasis on low-temperature operating conditions and pump performance characterization.

The state of the art concerning experimental approaches for electric oil pump testing is also reviewed in order to highlight the motivations behind the development of the thermal test rig described in the following chapters.

### 2.1 Lubrication systems in automotive applications

Lubrication systems play a fundamental role in modern automotive powertrains, ensuring the reduction of friction and wear between moving components, promoting heat removal and contributing to overall system durability. Engine oil is typically delivered to critical components through a pressure-fed lubrication circuit composed of an oil pump, filter, heat exchanger and distribution galleries.

The effectiveness of the lubrication process strongly depends on the oil flow rate and pressure available at each lubrication point. Insufficient oil supply may result in increased friction, accelerated wear or catastrophic component failure, while excessive flow leads to unnecessary energy consumption.

Traditional lubrication systems rely on mechanically driven oil pumps directly coupled to engine speed. Although robust, this configuration produces oil flow proportional to engine rotational speed rather than to actual lubrication demand, leading to efficiency penalties under partial-load conditions.

In response to increasingly stringent efficiency requirements, electrically driven oil

pumps have been introduced as an alternative solution capable of decoupling oil delivery from engine speed and enabling demand-based lubrication strategies [13, 14].

## 2.2 Electric oil pumps

Electric oil pumps (EOPs) are electromechanical devices designed to provide controlled oil circulation independently of engine operating conditions. Their adoption has grown significantly in recent years, particularly in hybrid and electric vehicles, where engine operation may be intermittent or completely absent.

Compared to conventional mechanical pumps, EOPs offer several advantages, including on-demand lubrication, improved thermal management and reduced parasitic losses. These benefits contribute directly to fuel consumption reduction and improved system efficiency [13].

From a constructive point of view, EOPs are commonly based on positive-displacement pump architectures such as gear, gerotor or vane designs. The selection of the pump type affects volumetric efficiency, noise characteristics and sensitivity to oil viscosity variations.

Despite their advantages, EOPs introduce additional challenges related to electric motor sizing, thermal management and control complexity. In particular, the performance of EOPs is strongly influenced by lubricant properties and operating temperature, making their behaviour at cold-start conditions a critical design aspect [14].

## 2.3 Control strategies for electric oil pumps

The performance of an electric oil pump is not only determined by its hydraulic design but also by the adopted control strategy. Modern EOPs typically employ closed-loop control algorithms implemented within an electronic control unit.

Two main control approaches are commonly adopted. In speed-controlled systems, the pump rotational speed is directly commanded by the control unit, resulting in pressure and flow rates that vary according to hydraulic load conditions. This approach produces classical pressure–flow characteristics similar to those of mechanical pumps.

Alternatively, flow-controlled strategies aim at maintaining a target oil flow rate through internal regulation algorithms. In this case, pump speed is continuously adjusted to compensate for pressure variations and viscosity changes, resulting in flatter pressure–flow curves within the regulation capability of the system.

Communication interfaces such as LIN or CAN are typically employed for command and diagnostic purposes. The chosen interface influences the achievable control resolution, response time and diagnostic functionality [6].

Protection strategies are also embedded within EOP controllers to prevent damage

under critical operating conditions. These include current limitation, thermal protection and stall detection, which may significantly affect pump operability under extreme temperature conditions.

## 2.4 Low-temperature operation and cold-start conditions

Low-temperature operation represents one of the most critical conditions for automotive lubrication systems. Cold-start events are typically defined as engine start-up occurring at ambient temperatures below  $-20^{\circ}\text{C}$ , with extreme design targets reaching  $-30^{\circ}\text{C}$  or  $-40^{\circ}\text{C}$  depending on vehicle application and market requirements.

At low temperatures, lubricant viscosity increases exponentially, resulting in a dramatic rise in hydraulic losses within the lubrication circuit. This behaviour leads to increased pump torque demand, reduced flow delivery and elevated electrical power consumption.

In electric oil pumps, these effects may cause activation of protection mechanisms, including current limitation or stall shutdown. As a consequence, the ability of the pump to guarantee sufficient oil circulation during cold-start conditions becomes a key performance indicator.

Several studies have demonstrated that oil circulation behaviour at low temperature has a significant impact on overall system performance and thermal stability [5]. The combined influence of oil viscosity, pump architecture and control logic defines the effective low-temperature operating envelope of an EOP.

These considerations motivate the need for experimental testing under controlled low-temperature conditions in order to properly evaluate pump behaviour beyond nominal operating points.

## 2.5 Pump performance characterization

Electric oil pump performance is commonly characterized through pressure–flow maps, efficiency curves and operating envelopes. The pressure–flow characteristic describes the relationship between delivered flow rate and outlet pressure at a given rotational speed or control command.

Efficiency is typically defined as the ratio between hydraulic output power and electrical input power. Due to the relatively low power levels involved, efficiency measurements are particularly sensitive to instrumentation accuracy and operating conditions.

Performance maps are usually generated by acquiring multiple steady-state operating points under controlled temperature, pressure and speed conditions. Interpolation

techniques are then employed to construct continuous efficiency surfaces.

The interpretation of these maps provides insight into pump behaviour, operating limits and sensitivity to external parameters such as temperature and hydraulic load [14].

## **2.6 State of the art of experimental test approaches**

Experimental characterization of electric oil pumps is commonly performed using dedicated test benches capable of controlling oil temperature, pressure and flow rate. In many laboratory setups, pumps are tested as standalone components under simplified hydraulic conditions.

Although suitable for basic performance assessment, such configurations often fail to represent realistic system-level interactions. In particular, the influence of auxiliary components such as oil filters and heat exchangers is frequently neglected.

Furthermore, low-temperature testing below  $-20^{\circ}\text{C}$  is rarely addressed due to the complexity of thermal conditioning and instrumentation reliability.

Recent academic studies and industrial test platforms have highlighted the importance of integrated lubrication circuit testing to accurately assess component interaction and system behaviour [15].

These limitations motivate the development of advanced thermal test rigs capable of operating over extended temperature ranges while enabling both component-level and system-level analysis, forming the basis of the experimental work presented in this thesis.

# Chapter 3

## Design and Development of the Thermal Test Rig

### 3.1 Project Background and Objectives

The development of the thermal test rig aims to extend the experimental capabilities already available with the goal of testing lubrication components used in electric powertrain applications. Prior to this project, the available rig was able to support experimental testing on the EOP exclusively and with limited instrumentation.

The previous configuration is shown in Figure 3.1, this was limited to standalone pump testing and did not allow system-level evaluation.

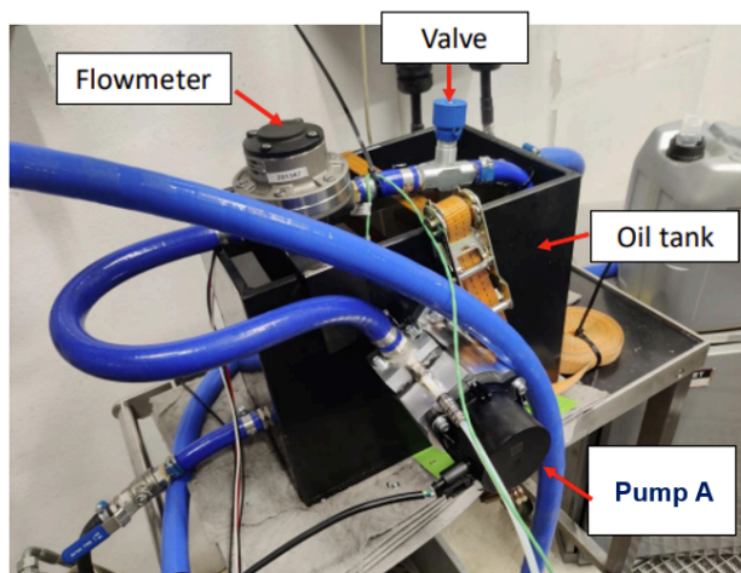


Figure 3.1. Previous experimental test rig configuration used for standalone electric oil pump testing.

While this approach was sufficient for preliminary functional verification, it did not

allow a comprehensive evaluation of component behaviour under representative operating conditions. The main limit for the previous configuration is the impossibility to test additional components such as the oil filter and the heat exchanger, and therefore it did not allow the assessment of pressure losses, thermal interactions, or system-level performance.

With the advancement in the e-PWT project, it became necessary to develop a more advanced experimental platform capable of reproducing realistic operating scenarios.

The primary objective of this project was to design and realize a thermal test rig capable of reproducing a wide range of temperature, pressure, and flow conditions. The design of the rig aims to support the experimental characterization of the electric oil pump, oil filter, and heat exchanger, both as individual components and as part of an integrated lubrication circuit.

In addition to performance evaluation, the test rig was required to meet several practical and organizational constraints. It had to be compatible with the climatic chambers available in the Brno laboratory, allow safe operation in compliance with internal HSE requirements, and offer sufficient flexibility to accommodate future component variants and testing campaigns.

The main differences between the previous configuration and the newly developed thermal test rig are summarized in Table [3.1](#).

Table 3.1. Comparison between the previous experimental test rig and the newly developed thermal test rig

<b>Aspect</b>	<b>Previous Test Rig</b>	<b>New Thermal Test Rig</b>
Tested components	Electric oil pump (EOP) only	EOP, oil filter, and heat exchanger
System configuration	Standalone component testing	Integrated lubrication circuit
Thermal design approach	Components selected without low-temperature design constraints	Entire rig designed and validated for operation down to $-40^{\circ}\text{C}$
Pressure measurement layout	Single pressure measurement point located downstream of the pump	Pressure measurement points located both upstream and downstream of the pump
Leakage behaviour	Oil leakages observed due to a non-optimized pump adapter design	Pump adapter redesigned to improve sealing performance and eliminate leakages
Flow control device	Ball valve used for flow regulation, with limited precision	Globe valve adopted to ensure accurate and repeatable flow control
Flow regulation strategy	Coarse flow adjustment	Fine flow modulation enabling stable pressure mapping
Instrumentation layout	Limited sensor positioning flexibility	Optimized sensor placement to support system-level analysis
System-level evaluation	Limited capability to evaluate component interactions	Assessment of pressure losses and thermal interactions within the lubrication circuit
Expandability	Fixed configuration	Modular layout allowing future component integration

## 3.2 Design Requirements and Boundary Conditions

A key phase in the development of the thermal test rig is represented by the definition of design requirements, during which functional targets and operational limits are established to guide the subsequent design activities. The requirements were defined considering three main aspects: the experimental objectives of the test campaign, the operating conditions of the lubrication components under investigation, and the physical and organizational constraints associated with laboratory operation.

### 3.2.1 Thermal Requirements

One of the most critical aspects in the experimental campaign was the requirement regarding the temperature range, in fact the rig is required to operate under testing conditions spanning from  $-40\text{ }^{\circ}\text{C}$  oil temperature to  $+125\text{ }^{\circ}\text{C}$ .

Table 3.2. Thermal operating requirements of the test rig

Parameter	Specification
Minimum oil temperature	$-40\text{ }^{\circ}\text{C}$
Maximum oil temperature	$+125\text{ }^{\circ}\text{C}$
Temperature reference	Oil temperature inside the circuit
Accepted temperature deviation	$\pm 1.5\text{ }^{\circ}\text{C}$ during testing
Thermal environment	Climatic chamber

For the upper thermal limit, potential issues are addressed through the integration of a heater in the system. This tool allows to raise the temperature of the lubricant independently of the surrounding environment, allowing the chamber to maintain an ambient temperature. As a result, all instrumentation and electronic components can remain within standard laboratory ambient conditions, typically in the range of  $20\text{--}25\text{ }^{\circ}\text{C}$ , reducing thermal stress and improving system reliability.

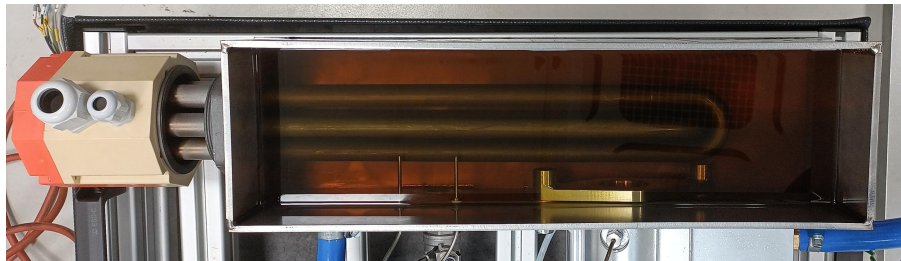


Figure 3.2. Electrical heater installed on the lubrication circuit to provide controlled thermal conditioning of the oil during hot soak tests.

The low-temperature operating limit introduces additional design challenges. It is

important to highlight that the specified temperature range refers to the oil temperature under test conditions. Consequently, the oil must remain at the target temperature even during pump operation.

The role of the climatic chamber is fundamental in this phase. The environmental temperature set inside the chamber must be lower than the target oil temperature in order to compensate for heat generation and guarantee stable thermal conditions throughout the test sequence.

The goal is to choose components and materials able to operate under these critical conditions. In particular, hoses, fittings and elastomeric seals were selected to maintain mechanical integrity and sealing performance at low temperature, avoiding brittleness and excessive stiffness.

Table 3.3. Thermal design strategy for high- and low-temperature operation

Aspect	High-temperature operation	Low-temperature operation
Main challenge	Oil overheating	High oil viscosity and material stiffness
Temperature control method	Electric heater integrated in oil circuit	Climatic chamber cooling
Environment temperature	Maintained at ambient level	Lower than target oil temperature
Design focus	Local oil heating	Material compatibility and insulation
Primary mitigation strategy	Heater integration	Component selection and thermal protection

### 3.2.2 Hydraulic Requirements

The hydraulic design of the thermal test rig was developed with the objective of reproducing representative lubrication system behaviour under controlled laboratory conditions. The circuit was required to guarantee stable oil circulation, accurate pressure generation and repeatable flow behaviour over a wide range of operating points.

A simplified functional representation of the lubrication system adopted for the experimental activity is shown in Figure 3.3. The diagram illustrates the sequential arrangement of the main components under investigation, namely the electric oil pump, oil filter and heat exchanger, as well as the direction of the oil flow within the circuit.

One of the primary hydraulic requirements was the ability to control outlet pressure independently from the pump rotational speed. This capability is essential during performance mapping activities, where pressure–flow characteristics must be evaluated

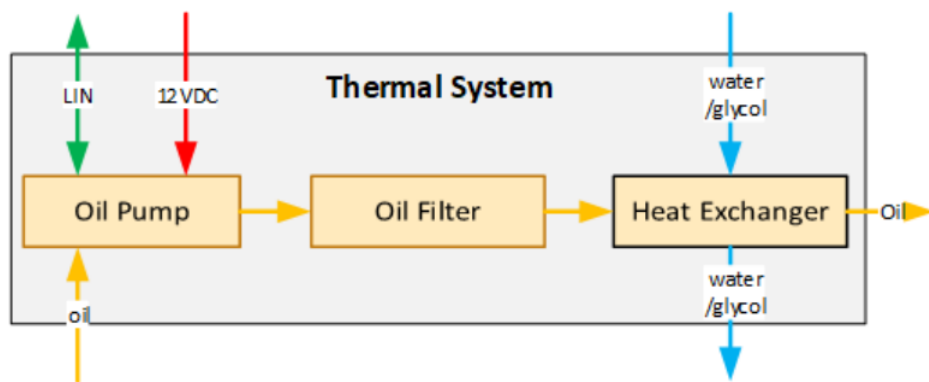


Figure 3.3. Simplified functional layout of the lubrication circuit, showing the main components and oil flow direction.

at constant temperature and rotational speed. For this reason, pressure regulation is achieved by modifying the hydraulic resistance of the circuit rather than altering the pump speed.

The hydraulic layout was also designed to support the integration of multiple components in series. The combined presence of the oil filter and heat exchanger introduces additional pressure losses and affects the global system response. Consequently, the rig enables both component-level and system-level investigations, allowing the assessment of pressure drops and interaction effects between the different elements of the lubrication circuit.

Particular attention was dedicated to flow stability. Unstable conditions such as pressure oscillations or cavitation phenomena were considered unacceptable, as they may compromise data quality and repeatability. The routing of hydraulic lines was therefore designed to minimize abrupt directional changes and ensure uniform flow distribution throughout the system.

### **3.2.3 Pressure and Flow Measurement Requirements**

Accurate measurement of hydraulic parameters represents a fundamental requirement for the experimental characterization of the thermal test rig. In particular, pressure and flow rate are the key quantities used to evaluate component performance, pressure losses, and overall system behaviour under different operating conditions.

Pressure measurements are required at several locations along the lubrication circuit in order to enable a detailed analysis of the system. Dedicated pressure sensors were therefore installed both upstream and downstream of the main hydraulic components, including the electric oil pump, oil filter, and heat exchanger. This configuration allows the identification of localized pressure drops, supports component-level efficiency evaluation, and enables comparison between different operating points during performance mapping activities.

Flow rate represents the second key hydraulic parameter. The selected flow measurement solution was required to operate reliably across a wide operating envelope, covering both low-flow conditions typical of cold start tests and higher nominal flow rates occurring at elevated pump speeds. Particular attention was paid to ensuring stable and repeatable measurements despite significant variations in oil viscosity caused by temperature changes.

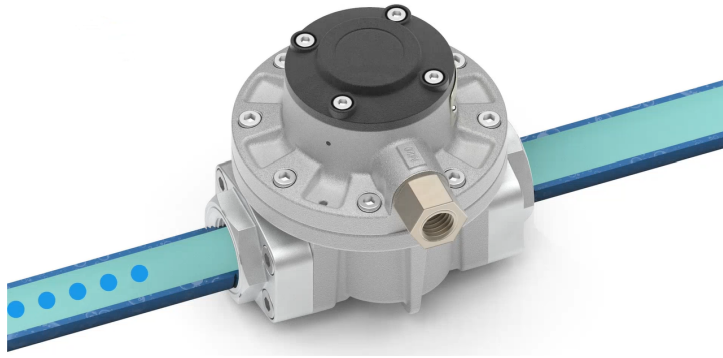


Figure 3.4. Flowmeter installed in the hydraulic circuit for oil flow rate measurement.

The flowmeter was installed along a straight section of the hydraulic line in order to minimize measurement disturbances related to flow turbulence and secondary velocity components. This installation strategy improves measurement accuracy and repeatability, especially during steady-state acquisition phases where flow stabilization is required before data logging.

Both pressure and flow signals are continuously acquired by the data acquisition system and made available for real-time monitoring through the LabVIEW interface. The same signals are simultaneously recorded for post-processing and performance analysis, ensuring consistency between online visualization and stored experimental data.

The combined availability of distributed pressure measurements and accurate flow rate acquisition enables detailed hydraulic characterization of the test rig. This configuration supports pressure–flow mapping of the EOP, evaluation of component-induced losses, and assessment of system behaviour over the full range of operating conditions defined for the experimental campaign.

### **3.2.4 Component Compatibility and Material Selection**

Component compatibility and material selection represent key boundary conditions for the design of the thermal test rig. All elements in contact with the lubricant were required to maintain mechanical integrity, sealing capability and dimensional stability throughout repeated thermal cycles.

Material selection was carried out considering both chemical compatibility with the lubricant and mechanical behaviour at extreme temperatures. Elastomeric components were identified as particularly sensitive, as their mechanical properties may vary significantly at low temperatures, potentially leading to leakage or loss of functionality.

Hoses and fittings were therefore selected to guarantee sufficient flexibility during cold operation while maintaining adequate pressure resistance at elevated temperatures.

Metallic components were chosen to provide structural robustness and corrosion resistance, particularly in areas subjected to thermal gradients and pressure fluctuations.

A representative example of this design philosophy is provided by the globe valve adopted for pressure regulation. According to the manufacturer technical documentation, the minimum allowable operating temperature of the component is 0 °C. In order to extend its operational range and ensure reliable performance during cold-start tests, a dedicated heating element was integrated directly on the valve body.

An additional external insulation cover was implemented to reduce thermal losses and provide further protection during low-temperature operation. This solution enabled the globe valve to operate reliably under the full thermal range required by the experimental campaign.

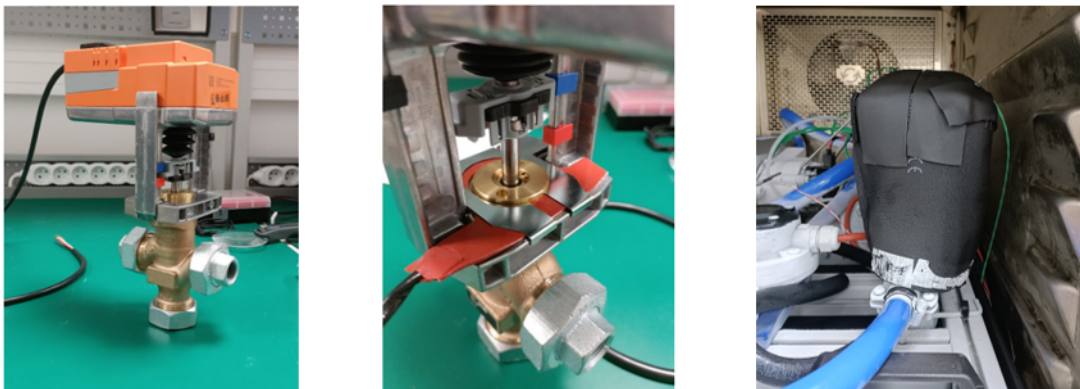


Figure 3.5. Globe valve used for pressure regulation: original component (left), integrated heating solution with thermal insulation (center) and additional protection used during cold starts.

### 3.3 System Architecture and Layout

From a structural point of view, the test rig integrates mechanical, hydraulic and thermal subsystems within a compact layout compatible with the dimensional constraints of the climatic chambers available in the Brno laboratory.

This chapter describes how the rig is physically constructed, focusing on the overall layout, the hydraulic circuit configuration, the main mechanical components and the modular architecture adopted for the experimental activity.

#### 3.3.1 Overall Layout of the Test Rig

The overall layout of the experimental bench is shown in Figure 3.6.

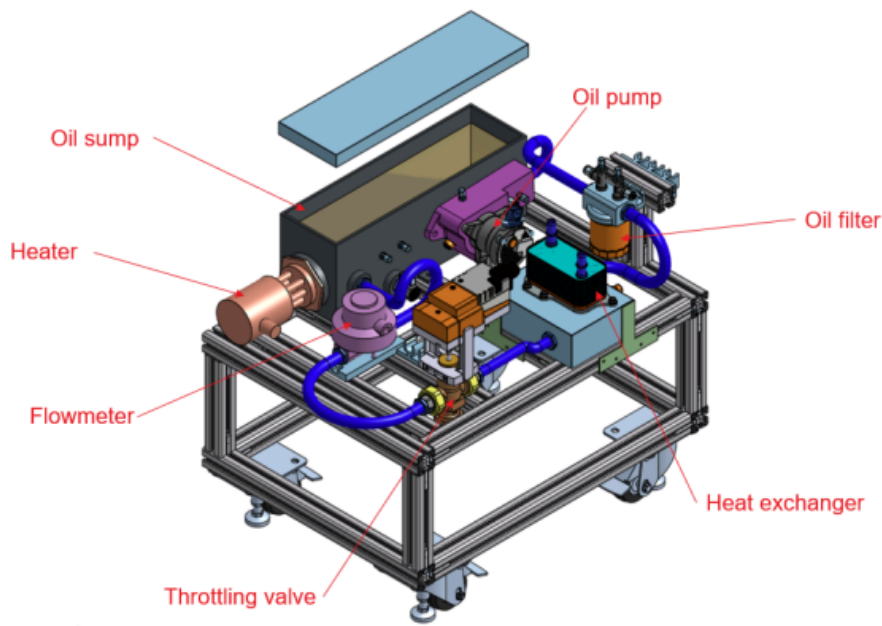


Figure 3.6. Overall layout of the test rig

All hydraulic components are mounted on a rigid support frame made of modular aluminium profiles. This solution provides sufficient mechanical stiffness while maintaining a relatively low overall weight, facilitating handling operations and installation inside the climatic chamber.

The layout of the frame was defined to ensure a clear physical organization of the system and to support both assembly and maintenance activities. In particular, the following design criteria were considered during the definition of the component arrangement:

- compatibility with the internal dimensions of the climatic chamber;
- accessibility of hydraulic connections and fittings;
- minimization of pressure losses through reduced hose length and limited bends;
- ease of maintenance and component replacement.

The entire rig is positioned inside a dedicated catch basin, as shown in Figure 3.7. The purpose of this basin is to contain possible oil leakages during testing activities, preventing contamination of the climatic chamber and improving overall operational safety.

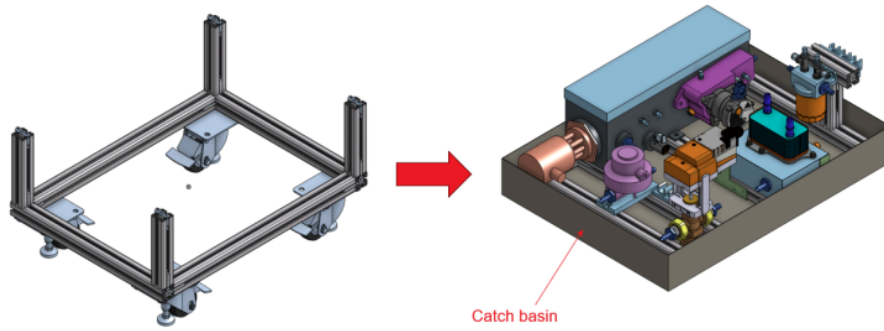


Figure 3.7. Test rig installed inside the catch basin

The spatial arrangement of the components follows the oil flow direction in a linear and intuitive manner. This design choice reduces unnecessary hose routing, limits pressure losses caused by sharp bends and simplifies troubleshooting during experimental campaigns.

Adequate spacing between components was also maintained to allow visual inspection of fittings and to minimize thermal interaction between heated elements and surrounding parts.

### 3.3.2 Hydraulic Circuit Configuration

The hydraulic circuit represents the core of the experimental setup. A simplified schematic of the system is shown in Figure 3.8.

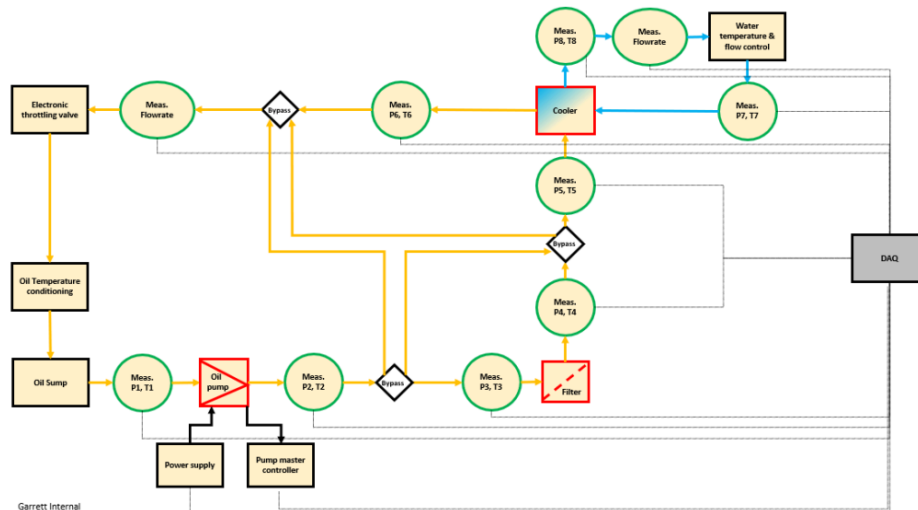


Figure 3.8. Hydraulic schematic of the test rig with flow direction

The circuit is based on a closed-loop configuration. Oil is stored in a dedicated tank, which acts both as reservoir and thermal buffer. From the tank, the lubricant is drawn

by the EOP, which represents the primary active component of the system.

Downstream of the EOP, the oil flows through the oil filter and the HE, which are installed in series. After passing through the HE, the oil returns to the tank, completing the hydraulic loop.

This configuration reproduces a typical lubrication circuit architecture and allows continuous oil circulation under stable hydraulic and thermal operating conditions.

A throttling valve is installed at the outlet of the circuit. By progressively increasing the hydraulic resistance, the outlet pressure can be regulated independently from the EOP rotational speed. This feature is essential for EOP characterization tests, where pressure–flow relationships must be evaluated at constant speed and temperature.

Straight pipe sections were introduced upstream and downstream of critical components in order to reduce flow disturbances and improve hydraulic stability during measurements.

For clarity, Table 3.4 summarizes the main hydraulic elements integrated into the circuit and their respective functions.

Table 3.4. Main hydraulic components of the test rig

<b>Element</b>	<b>Function</b>
Oil tank	Oil storage and thermal buffer
EOP	Oil circulation within the circuit
Oil filter	Particle filtration
HE	Thermal regulation of the lubricant
Throttle valve	Pressure control

### 3.3.3 Main Mechanical Components

The mechanical structure of the rig consists of both commercial hardware and custom-designed parts developed specifically for this project.

The main mechanical elements include:

- aluminium support frame;
- oil tank;
- pump adapters;
- HE support structure;
- hydraulic fittings and flanges.

Custom adapters were designed to ensure correct mounting of the EOPs and to provide standardized interfaces between components. Particular attention was paid to sealing

surfaces and sensor integration points in order to guarantee oil tightness over the entire operating temperature range.

The oil tank was designed to accommodate the required oil volume and to integrate multiple interfaces, including inlet and outlet ports, heater installation and temperature measurement locations.

Standardized hydraulic fittings were adopted throughout the system, allowing rapid disassembly and reconfiguration of the circuit without requiring structural modifications.

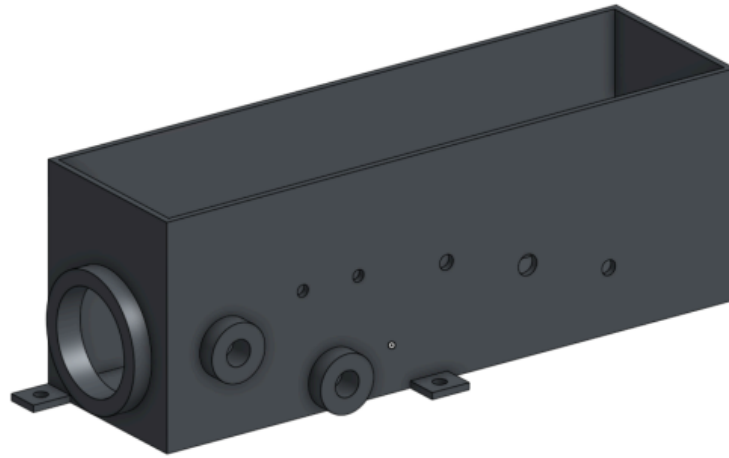


Figure 3.9. Custom mechanical components: oil tank and adapters

As highlighted in Table 3.1, the previous experimental test rig presented several limitations from a design point of view. One representative example is the adapter used for mounting the two EOP models.

In the previous configuration, the adapter was composed of two separate parts assembled together and sealed using a thick layer of silicone in order to prevent oil leakages. During experimental activity, however, leakages were repeatedly detected at the interface between the two components, especially during high-temperature tests.

To overcome this issue, the adapter design was revised and replaced with a single-piece component. The new adapter integrates all hydraulic interfaces within a unique solid body, eliminating the sealing surface previously located between the two parts.

This design modification significantly improved the reliability of the system. During the subsequent test campaigns, no oil leakages were detected at the adapter interface, confirming the effectiveness of the updated solution.

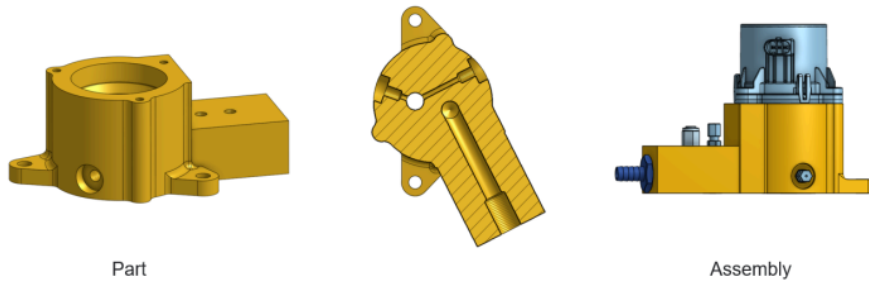


Figure 3.10. Improved single-piece EOP adapter design for the first EOP tested.

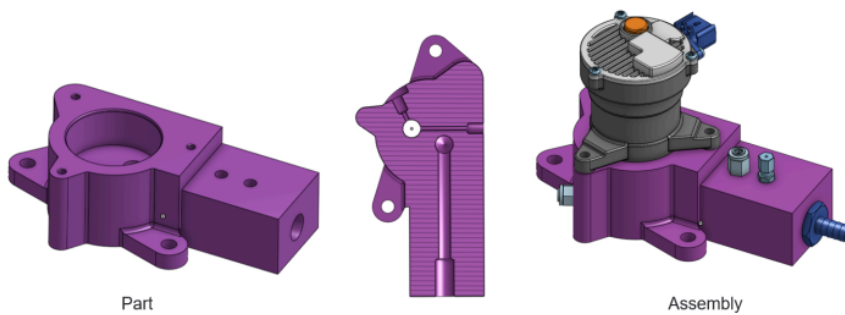


Figure 3.11. Improved single-piece EOP adapter design for the second EOP tested.

### 3.3.4 Modularity of the Rig

The test rig was developed following a modular design philosophy aimed at maximizing experimental flexibility.

Hydraulic connections are based on standardized fittings, allowing individual components to be removed or replaced without disassembling the entire system. This approach enables rapid configuration changes between different test campaigns.

The modular architecture allows:

- testing of the EOP alone;
- evaluation of oil filter and EOP or HE and EOP as independent subsystems;
- full system testing with all components integrated.

This flexibility represents a significant improvement compared to the previous experimental setup, which allowed only standalone EOP testing and offered limited instrumentation capabilities.

Overall, the adopted architecture provides a robust and adaptable experimental platform suitable for both development and validation activities.

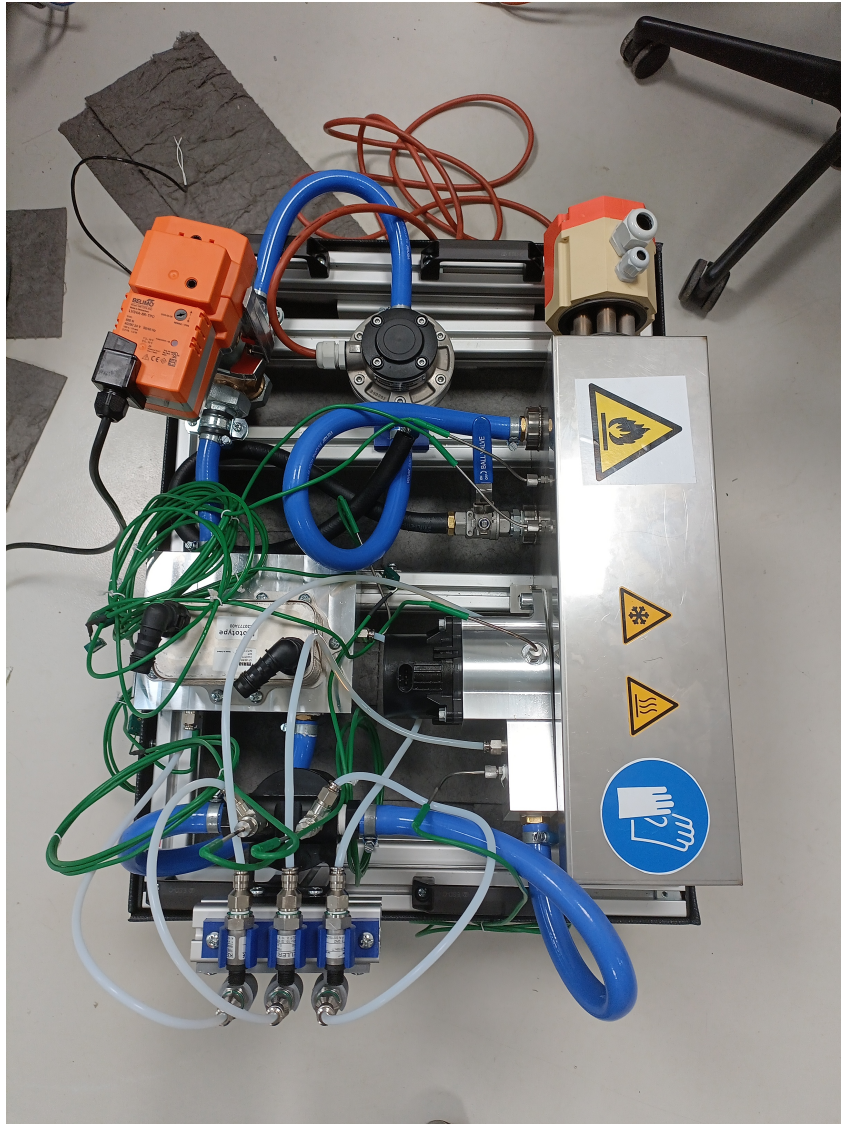


Figure 3.12. Final configuration of the rig.

### 3.4 Measurement System

The experimental characterization of the thermal test rig requires a reliable measurement system capable of monitoring the main hydraulic and thermal variables governing the behaviour of the lubrication circuit.

For this reason, a dedicated instrumentation architecture was implemented to ensure accurate and repeatable acquisition of pressure, temperature and flow rate data over the full operating range of the system. These measurements represent the basis for the evaluation of EOP performance, pressure losses across the oil filter and the HE, as well as the thermal behaviour of the lubrication circuit under controlled boundary conditions.

Particular attention was paid to sensor selection, positioning and integration within the rig, in order to minimize measurement uncertainty while limiting interference with

the hydraulic behaviour of the system.

### 3.4.1 Measured Quantities

During experimental operation, the following physical quantities are monitored:

- lubricant pressure,
- lubricant temperature,
- volumetric flow rate.

Pressure measurements are required to evaluate the hydraulic performance of the EOP and to quantify pressure losses introduced by the oil filter and the HE. Temperature measurements provide information on the thermal state of the lubricant and allow the analysis of heat generation and heat exchange phenomena occurring within the circuit. The flow rate is a key variable to define the operating points and construct EOP performance maps.

For clarity, Table 3.5 summarizes the measured quantities and their main purpose within the experimental activity.

Table 3.5. Measured quantities and main purpose

Measured quantity	Purpose in the test rig
Pressure ( $p$ )	EOP hydraulic characterization and pressure loss evaluation across oil filter and HE
Temperature ( $T$ )	Monitoring of bulk oil temperature and component-level thermal gradients
Volumetric flow rate ( $Q$ )	Definition of operating points, EOP mapping and hydraulic power estimation

### 3.4.2 Pressure Measurement System

Oil pressure is measured using piezoresistive pressure sensors installed at selected locations along the hydraulic circuit.

The sensors are connected to the main oil line through PTFE tubing, allowing flexible positioning of the sensing elements and reducing direct exposure to elevated oil temperatures. This solution also facilitates maintenance activities and component replacement.



Figure 3.13. Pressure sensor installation detail on the hydraulic circuit

To ensure mechanical stability and repeatable positioning, dedicated mounting solutions were adopted for the sensors.

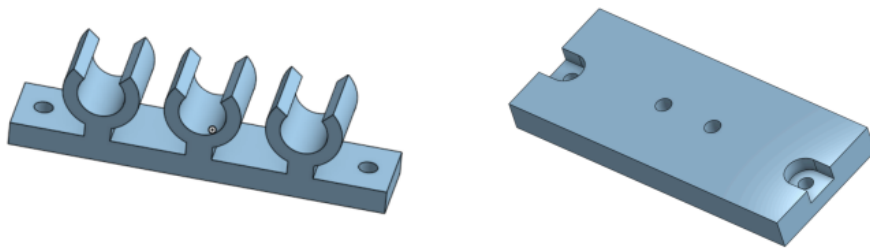


Figure 3.14. Custom holder used for pressure sensor mounting

Pressure measurement points are located upstream and downstream of the main components (EOP, oil filter and HE). This configuration enables direct evaluation of:

- pressure rise generated by the EOP,
- pressure drops introduced by the oil filter and the HE,
- overall circuit pressure level under different operating points.

Table 3.6 summarizes the adopted pressure sensing approach.

Table 3.6. Pressure measurement system overview

Sensor / method	Installation	Notes
KELLER PAA21Y (piezoresistive)	Remote-mounted, connected via PTFE tubing	Used to acquire oil pressure at multiple locations along the circuit

### 3.4.3 Temperature Measurement System

Oil temperature is monitored using K-type thermocouples distributed throughout the hydraulic circuit.

Thermocouples are installed inside the oil tank to monitor the bulk lubricant temperature and at selected points along the circuit (inlet/outlet of the main components) to capture local thermal variations and temperature gradients.

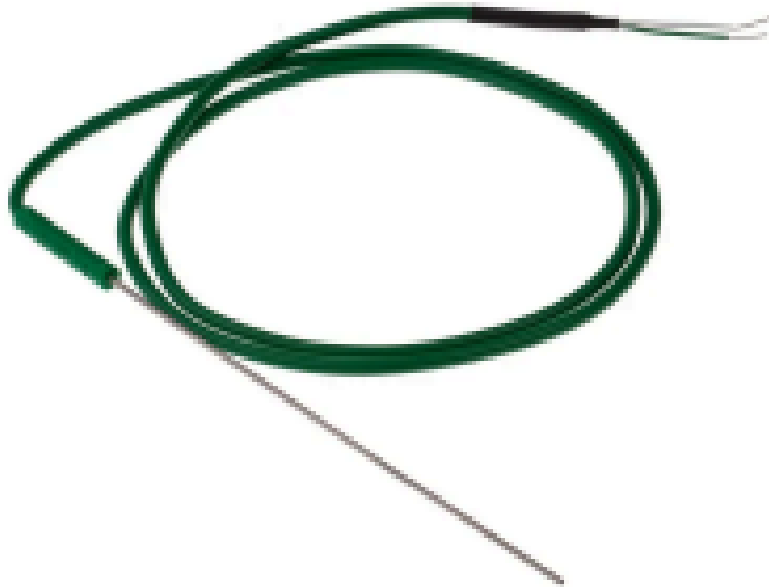


Figure 3.15. K-type thermocouple installation detail on the test rig

This measurement layout supports the evaluation of:

- thermal stabilization of the lubricant before and during tests,
- thermal gradients across the HE,
- temperature changes due to hydraulic losses and EOP operation.

Table 3.7 summarizes the adopted temperature sensing approach.

Table 3.7. Temperature measurement system overview

Sensor / method	Installation	Notes
K-type thermocouples	Oil tank and circuit measurement ports	Used to monitor bulk oil temperature and local thermal gradients

### 3.4.4 Flow Rate Measurement

The lubricant volumetric flow rate is measured using a dedicated flowmeter integrated into the hydraulic circuit. The flowmeter provides continuous monitoring of the circuit flow rate during both transient and steady-state operation.

The flow measurement is used for EOP mapping activities and for post-processing calculations requiring flow rate as input (e.g., pressure–flow relationships and hydraulic power estimation).

### 3.4.5 Sensor Placement Strategy

The instrumentation layout was defined to ensure accurate measurements while limiting the impact of sensor integration on the hydraulic behaviour of the circuit.

Pressure measurement points were positioned as close as possible to the inlet and outlet of each component, enabling direct quantification of individual pressure losses. Temperature measurement points were distributed to capture both global oil temperature and localized thermal effects across the circuit.

A schematic overview of the measurement point distribution is reported in Figure 3.3.

For clarity, Table 3.8 summarizes the measurement locations adopted for component-level evaluation.

Table 3.8. Measurement locations for component-level evaluation

Location	Measured variables
Oil tank	Bulk oil temperature (and reference pressure level when required)
EOP inlet / outlet	Pressure and temperature for EOP characterization
Oil filter inlet / outlet	Pressure drop and temperature across the oil filter
HE inlet / outlet	Pressure drop and temperature gradient across the HE
Flowmeter section	Volumetric flow rate $Q$

### **3.4.6 Data Acquisition Overview**

All sensor signals are acquired through the laboratory data acquisition system and recorded continuously during testing.

Pressure, temperature and flow signals are logged simultaneously to enable synchronized analysis of hydraulic and thermal behaviour. Continuous acquisition allows evaluation of both transient phenomena (e.g., start-up and stabilization phases) and steady-state operating conditions.

The acquired dataset constitutes the basis for the experimental analysis presented in the following chapters.

## **3.5 Power Supply and Protection System**

The operation of the thermal test rig requires a dedicated electrical system capable of supplying power to the EOP, auxiliary devices and measurement equipment while ensuring safe operation under a wide range of experimental conditions.

For this reason, a specific power supply and protection architecture was developed. The electrical system was designed to guarantee reliable power delivery, adequate protection against fault conditions and safe interaction between the test rig and the laboratory infrastructure.

This chapter describes the electrical architecture of the rig, focusing on the power supply layout, protection strategies and safety measures implemented during experimental activity.

### **3.5.1 Electrical Architecture Overview**

The electrical architecture of the test rig is organized around a centralized electrical cabinet, which houses the main power supply components, protection devices and control interfaces.

The cabinet is positioned outside the climatic chamber in order to avoid exposure of electrical equipment to extreme temperatures and to allow safe access during testing operations.

Power and signal cables are routed from the cabinet to the rig through dedicated feedthrough ports available on the climatic chamber walls, ensuring environmental sealing while maintaining electrical continuity.

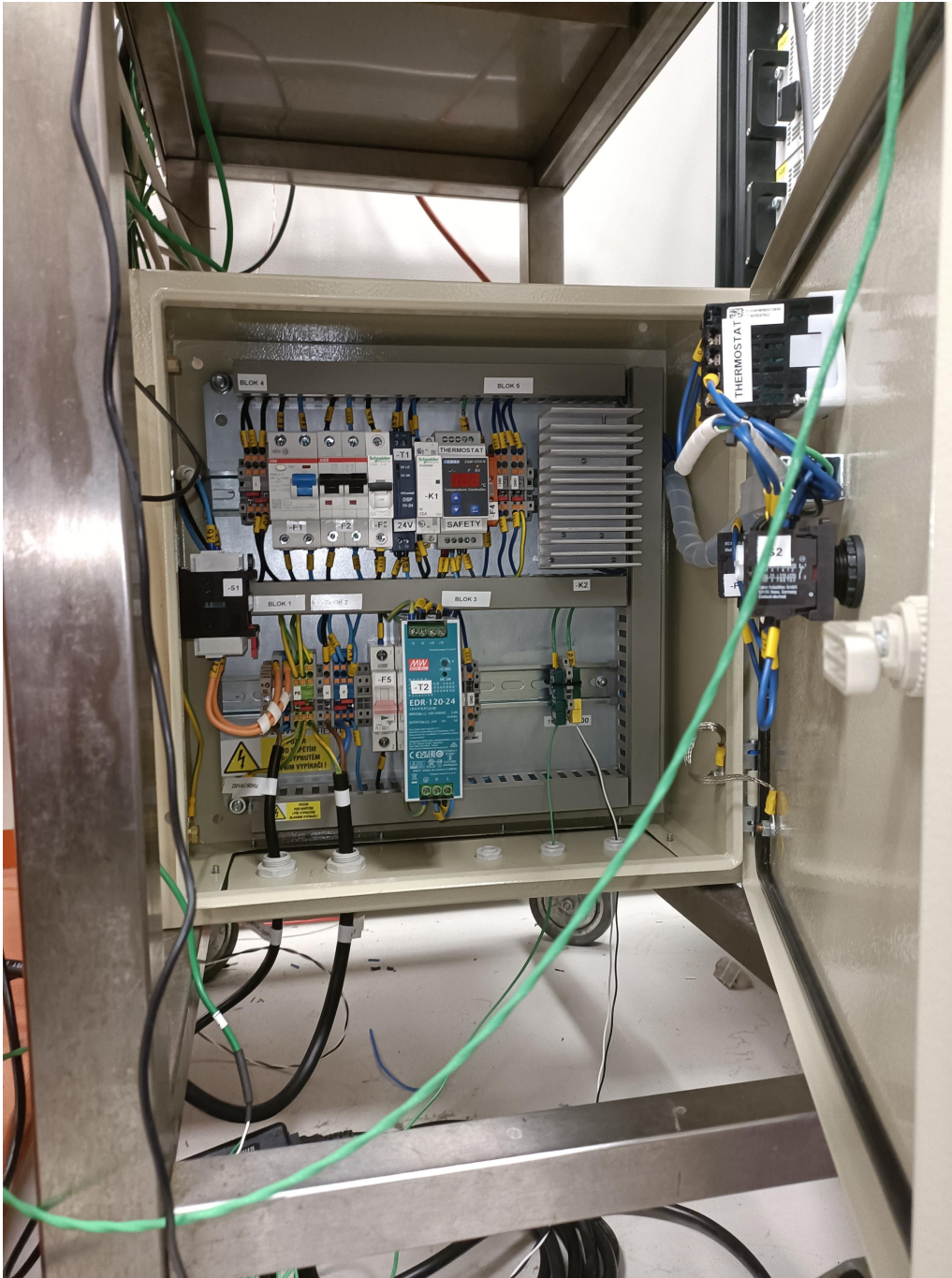


Figure 3.16. Electrical cabinet housing power supply and protection components

The electrical system supports the simultaneous operation of the EOP, heating devices and instrumentation while maintaining electrical separation between power circuits and measurement signals.

### 3.5.2 EOP Power Supply

The EOP is supplied through a dedicated power line designed to support the required voltage and current levels during operation.

The power supply system allows control of the EOP operating conditions during testing, including constant-speed operation and transient start-up phases.

Electrical connections between the cabinet and the EOP are realized using shielded cables and industrial connectors, ensuring reliable operation and minimizing electromagnetic interference with measurement signals.

The separation between power cables and sensor wiring was carefully maintained along the entire routing path to reduce noise coupling effects.

### **3.5.3 Auxiliary Power Supplies**

In addition to the EOP, several auxiliary devices require electrical power during operation of the test rig. These include:

- electrical immersion heater installed in the oil tank,
- globe valve actuator used for flow regulation,
- data acquisition and signal conditioning devices.

Each auxiliary component is supplied through an independent protected circuit, allowing individual activation and isolation when required.

This modular power distribution strategy improves operational flexibility and simplifies troubleshooting during experimental activity.

### **3.5.4 Protection Devices**

To ensure safe operation of the experimental setup, multiple protection devices were integrated into the electrical architecture.

The implemented protection strategy includes:

- circuit breakers for overcurrent protection,
- residual current devices for personnel safety,
- emergency stop circuit for immediate system shutdown.

Circuit breakers are sized according to the nominal operating current of each device and provide protection against short-circuit and overload conditions.

Residual current devices are used to detect leakage currents and ensure compliance with laboratory electrical safety regulations.

Table 3.9. Main electrical protection devices

Device	Function
Circuit breaker	Protection against overcurrent and short circuit
Residual current device	Personnel protection against electric shock
Emergency stop circuit	Immediate shutdown of all powered components
Fuses	Local protection of auxiliary circuits

### 3.5.5 Emergency Stop System

An emergency stop system was implemented to allow immediate interruption of all powered devices in case of unsafe operating conditions.

The emergency stop button is located outside the climatic chamber in an easily accessible position. When activated, the system disconnects the main power supply to the EOP and all auxiliary devices.

This solution ensures rapid response during abnormal events and complies with standard laboratory safety procedures.



Figure 3.17. Emergency stop push-button located outside the climatic chamber

### 3.5.6 Grounding and Electrical Safety Measures

All metallic structures of the test rig, including the aluminium frame, oil tank and hydraulic components, are connected to a common protective earth.

Proper grounding reduces the risk of electric shock and limits potential differences between components during operation.

Cable routing, connector selection and enclosure design were implemented in accordance with standard laboratory electrical safety practices, ensuring safe long-term operation of the experimental setup.

## **3.6 Design Iteration and Improvements Based on Preliminary Testing**

The development of the thermal test rig followed an iterative design approach. An initial configuration was first assembled and experimentally evaluated in order to verify mechanical integrity, sealing performance and general robustness prior to the execution of the complete test campaign.

Preliminary testing activities allowed early identification of critical issues, leading to targeted design improvements implemented on the same rig architecture.

### **3.6.1 Initial Rig Configuration**

In the initial design of the thermal test rig, the interface between the oil tank and the EOP adapter was realized through a dedicated flange.

The flange geometry was derived from the design previously adopted in earlier experimental setups, allowing reuse of an already validated mechanical concept and reducing development time.

The initial configuration was characterized by the following features:

- mechanical connection between tank and adapter ensured by a bolted flange;
- sealing based solely on surface contact between mating parts;
- absence of dedicated elastomeric sealing elements at the interface.

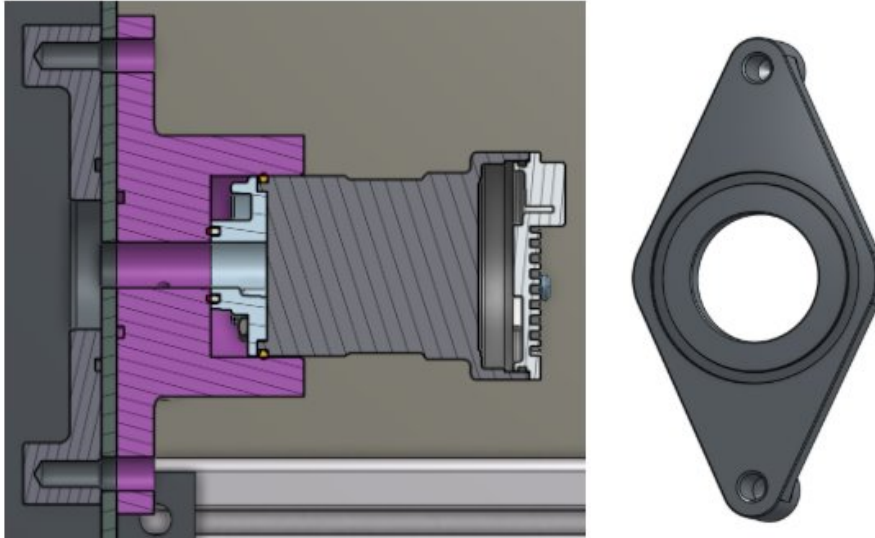


Figure 3.18. Initial adapter-tank interface design

### 3.6.2 Preliminary Leakage Tests and Root Cause Identification

After assembly of the initial configuration, preliminary leakage tests were performed before activating the EOP and thermal systems.

The tests consisted of:

- complete filling of the oil tank with lubricant;
- static pressurization due to fluid head;
- long-duration monitoring, including overnight tests conducted over multiple days.

The objective of these tests was to verify sealing integrity under static conditions and to identify potential leakage paths prior to dynamic operation. During these tests, significant oil leakages were observed in the region between the tank and the EOP adapter.

Following the detection of leakages, a systematic analysis was conducted to identify the root cause of the phenomenon.

The investigation highlighted the following aspects:

- oil migration occurred from the internal tank volume towards the adapter interface;
- the leakage path was located at the flange contact surface;
- no structural damage or manufacturing defects were observed.

The root cause was therefore attributed to the absence of a defined sealing element capable of preventing fluid passage between the tank cavity and the adapter body under static pressure.

### 3.6.3 Adapter Design Improvement

Based on the outcomes of the leakage analysis, the adapter geometry was revised in order to improve sealing performance at the tank–adapter interface.

The implemented design modifications are summarized in Table 3.10.

Table 3.10. Summary of adapter design modifications

Aspect	Modification
Sealing concept	Introduction of elastomeric O-ring
Sealing position	Groove machined on adapter side
Interface type	Defined radial sealing surface
Assembly	Controlled compression during bolted assembly

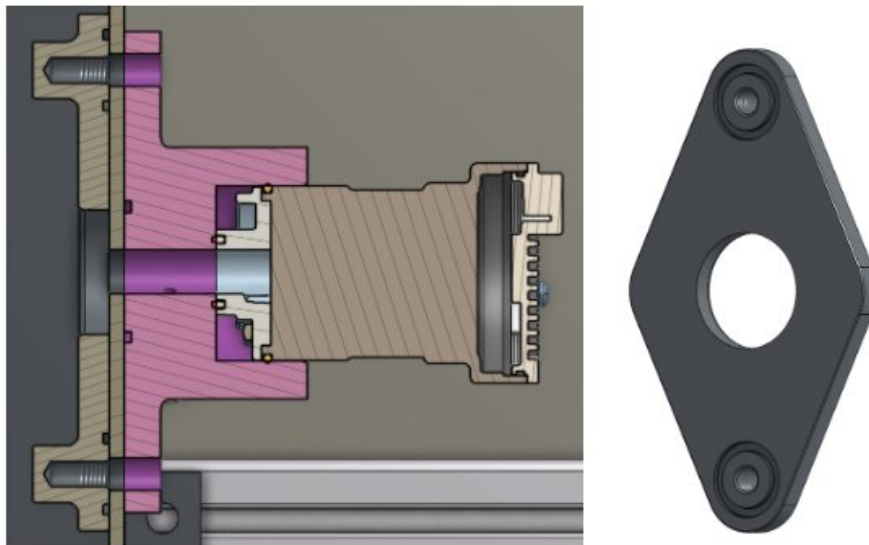


Figure 3.19. Improved adapter design with integrated O-ring groove

### 3.6.4 O-ring Design and Sizing Criteria

In order to guarantee reliable sealing performance at the interface between the EOP adapter and the mating component, a dedicated O-ring sealing system was introduced in the redesigned adapter.

The sealing configuration adopted in the present project is a static axial seal, where the compression of the elastomer is generated by the tightening of the bolted joint. A schematic representation of the axial sealing principle is shown in Figure 3.20.

## Těsnění statické - axiální

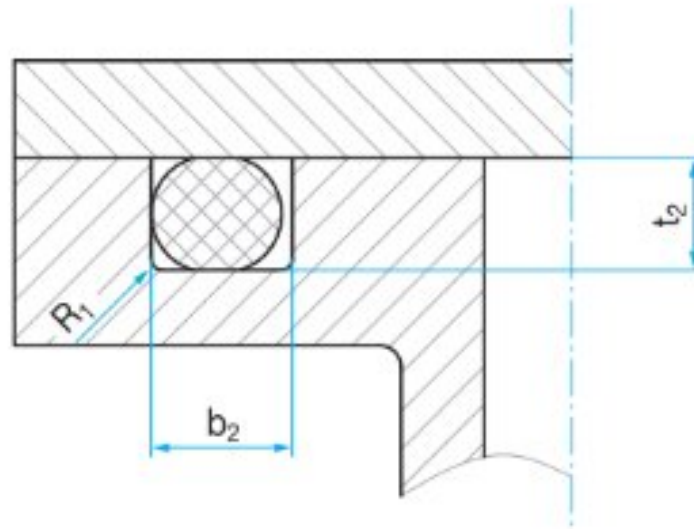


Figure 3.20. Static axial O-ring sealing configuration

In this configuration, the O-ring is positioned inside a dedicated groove and compressed in axial direction between two rigid surfaces. This solution is particularly suitable for static applications, providing high sealing reliability with limited sensitivity to pressure variations.

### Sizing Criteria and Catalogue Selection

The preliminary sizing of the O-ring groove was performed following standard industrial guidelines for static axial sealing applications.

The O-ring cross-section diameter and the corresponding groove dimensions were selected using manufacturer catalogue data. Table-based design recommendations were adopted to define the groove depth and width as a function of the O-ring cross-section diameter.

An extract of the catalogue used for the final selection is shown in Figure 3.21.

Průměr průřezu $d_2$ [mm]	Statická aplikace[mm]			
	radiálně		axiálně	
	$t_1 + 0,05$	$b_1 + 0,25$	$t_2 + 0,05$	$b_2 + 0,25$
1,00	0,8	1,3	0,75	1,4
1,25	0,9	1,7	0,90	1,7
1,50	1,1	2,0	1,10	2,1
1,78	1,3	2,4	1,30	2,5
1,80	1,3	2,4	1,30	2,6
2,00	1,5	2,6	1,50	2,8
2,20	1,7	3,0	1,60	3,1
2,40	1,8	3,2	1,80	3,3
2,50	1,9	3,3	1,90	3,5
2,62	2,0	3,5	2,00	3,7
2,65	2,0	3,6	2,00	3,8
3,00	2,3	3,9	2,30	4,1

Figure 3.21. Catalogue reference for static axial O-ring groove dimensions

Based on the available installation space and the target compression range, the final O-ring size was selected to ensure adequate squeeze while avoiding excessive gland filling.

### Design Verification and Compression Evaluation

After the preliminary geometric definition, the sealing configuration was verified using a dedicated O-ring calculation tool.

The verification focused on the main design parameters governing static sealing behaviour, namely:

- compression ratio (squeeze);
- absolute compression value;
- gland fill percentage;
- installation stretch.

The calculation tool allowed verification that all parameters remained within the recommended ranges for static axial sealing applications.

Figure 3.22 shows the calculation results obtained for the selected geometry, confirming acceptable compression levels and gland fill values over the expected operating conditions.






Calculation Results		Axial Sealing	
		Min.	Max.
Compression (%)		17.01	26.64
Compression (mm)		0.41	0.69
Housing Fill (%)		60.97	78.24
Stretch OR Inside-Ø (%)		-	0.84
Compression OR Outside-Ø (%)		-	-
Groove Width $b_4$ (mm)		3.50	3.55
Total Compression Force (N)		101	255

Figure 3.22. O-ring compression and gland fill verification using calculation tool

The adoption of a single-piece adapter combined with a properly sized O-ring sealing system eliminated the critical sealing interface present in the previous design and significantly improved the robustness and reliability of the hydraulic connection.

### 3.6.5 Final Configuration Validation

After implementation of the O-ring sealing solution, the rig was reassembled and subjected to the same leakage test procedure previously applied.

The validation tests included:

- complete tank filling;
- extended static monitoring periods;
- visual inspection of all interfaces.

No oil leakages were observed at the tank–adapter interface during the validation phase.

The modified configuration was therefore considered reliable and was adopted as the final design for all subsequent experimental activities.



# Chapter 4

## Software Architecture and System Monitoring

The thermal test rig is operated through a LabVIEW-based control and monitoring software environment developed within the CTC department [10]. Together with the design phase, the control phase represents one of the two key steps of the experimental activity. The software enables the operator to control the main actuators of the rig, monitor the system behaviour in real time, and acquire the data required for post-processing and analysis.

Within the scope of this thesis, the software was configured, validated, and used to execute the experimental campaign described in Chapter 6. For this reason, Chapter 4 focuses on the software architecture, the control logic, and the monitoring functionalities that supported the experimental activity.

The main objective of the software is to provide a stable and reliable interface between the operator and the physical system, ensuring repeatability of the tests, real-time visibility of critical parameters, and safe operation of the rig under a wide range of operating conditions.

### 4.1 LabVIEW Control Interface

The LabVIEW control interface constitutes the primary interaction point between the operator and the thermal test rig. The goal of its design is to support both manual and automatic test execution; however, during this experimental campaign, its primary use was related to manual testing, which represents the core of the internship project.

Through the interface, the operator is able to directly control the main active components of the system. In particular, the EOP rotational speed and outlet pressure can be both regulated through specific control elements, the first has a dedicated command while the control of the second can be achieved by the voltage-based command of the

throttle valve, that changes its position. The goal of this control configuration is to allow the definition of precise operating points in terms of rotational speed, pressure, and flow rate.

In parallel, the interface provides real-time visualization of the main physical quantities measured on the rig. On the screen there is a dedicated section for the visualization of the numerical values, both set and actual values are displayed; on the other side the same values are shown as time-based trends, allowing continuous comparison between target setpoints and actual measured signals. This aspect is particularly important during stabilization phases, where the test can only proceed once temperature, speed and pressure have reached steady values.

With this configuration, the operator is in constant control of the test progression. The design of the interface doesn't allow automatic transitions between tests step, and the decision to move to a new operating point is left to the test engineer based on the observed system behaviour. This choice increases flexibility during experimental testing and allows immediate reaction to unexpected conditions.

A representative view of the LabVIEW user interface is shown in Figure 4.1, where the main control inputs, real-time indicators, and waveform charts can be identified.

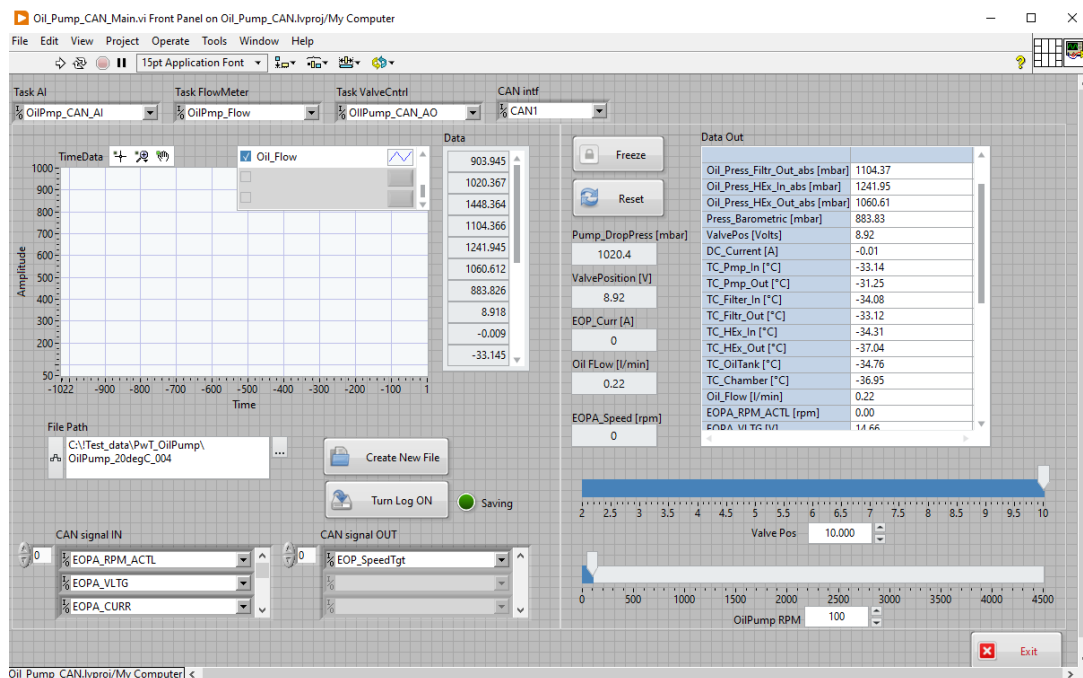


Figure 4.1. LabVIEW control interface used to operate the test rig and monitor the main signals during testing activities.

## 4.2 Software Architecture and Block Diagram Description

The internal organization of the software follows a modular structure, as illustrated in the LabVIEW block diagram shown in Figure 4.2. From the block diagram, it is possible to recognize several groups of elements, divided into different functional levels, each associated with a specific role within the control and monitoring framework.

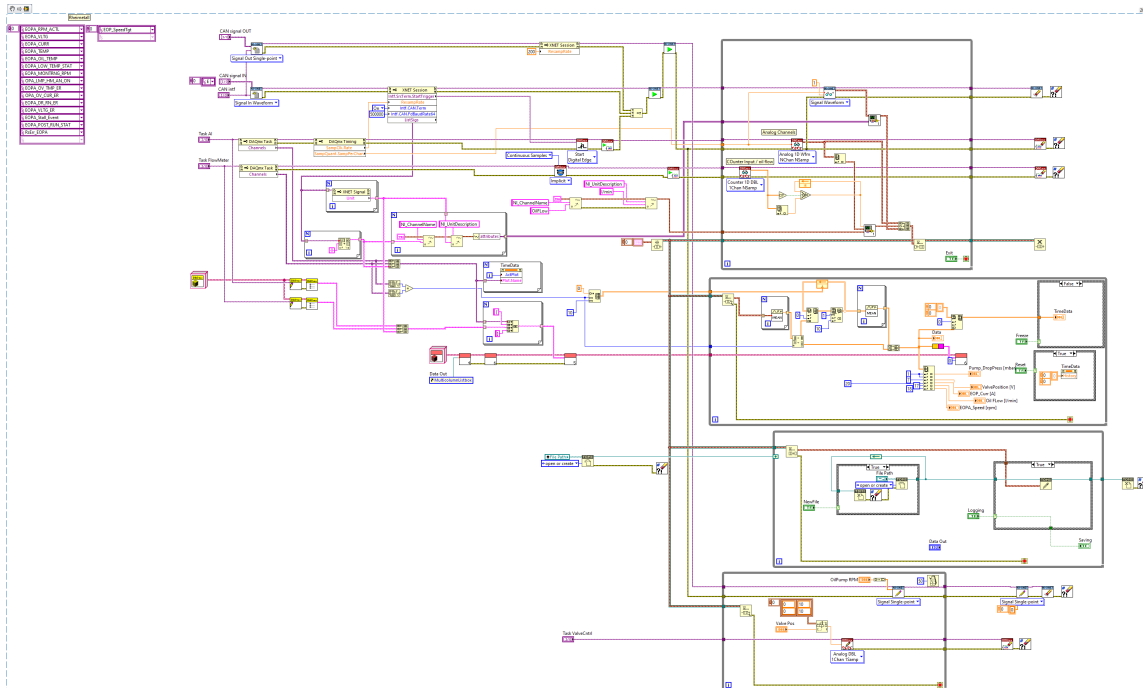


Figure 4.2. LabVIEW block diagram illustrating the modular software architecture of the control and monitoring system.

The software architecture can be divided into four main sections:

- **Signal input and acquisition**

On the left side of the diagram, a table reports the list of sensor measurements and CAN signals from the test rig, including pressure, temperature, flow rate, voltage, current, and rotational speed. These signals, representing the primary source of information, are collected through dedicated acquisition tasks and describe the state of the system.

- **Control signal generation**

The software architecture is designed to ensure that control actions remain logically decoupled from measurement activities, preserving the integrity of the acquired data. To achieve this result, the setpoints inserted by the operator through the interface are processed independently from the acquisition chain and converted into

control commands for the physical actuators, such as the EOP controller and the throttle valve.

- **Real-time monitoring and visualization**

Constant monitoring of the signals is mandatory during this experimental test campaign. This level supports test supervision, which is particularly important during stabilization phases, and allows verification that the system is operating under the intended conditions. The signals acquired in the first level are directed to numerical indicators and waveform charts that enable the operator to continuously observe both instantaneous values and time-based trends.

- **Data logging and file management**

In this level, the logging modules store the signals coming from the real-time monitoring data stream into structured files for post-processing and analysis, using the National Instruments TDMS file format [11]. This approach guarantees consistency between visualized and recorded data while avoiding duplication or loss of information.

Finally, synchronization across all functional levels is ensured by the structure of the software loop, which updates control outputs and reads sensor inputs at a fixed and configurable sampling rate. This ensures consistent time alignment of the recorded signals and enables reliable comparison between commanded setpoints and measured values.

The block diagram also integrates basic logical checks, such as limit verification and signal validation, which contribute to safe operation of the system during testing.

### 4.3 Data acquisition and Signal Management

The data acquisition system represents a fundamental element of the thermal test rig, as it enables continuous monitoring and recording of all relevant physical quantities during the execution of the experimental campaign. Its primary role is to provide a reliable interface between the instrumentation installed on the rig and the software environment used for control, supervision, and data analysis.

The experimental activity requires the simultaneous acquisition of hydraulic, thermal, and electrical parameters in order to characterize the behaviour of the lubrication system under different operating conditions. For this reason, the acquisition architecture was designed to manage multiple signal types in parallel, ensuring temporal coherence among all measured quantities.

The monitored signals can be grouped into the following main categories:

- pressure measurements, used to evaluate absolute pressure levels and pressure drops across the main components of the circuit;

- temperature measurements, acquired at several locations to monitor oil temperature and thermal gradients;
- flow rate measurement, required to characterize the hydraulic performance of the system;
- electrical quantities, including supply voltage and current absorbed by the electric oil pump;
- rotational speed signals, allowing comparison between commanded and actual pump speed.

All sensors are connected to the data acquisition hardware through dedicated input channels. Analog signals are scaled according to sensor-specific calibration parameters, while digital and communication-based signals are handled through appropriate interfaces. This configuration allows all measurements to be processed within a single acquisition framework.

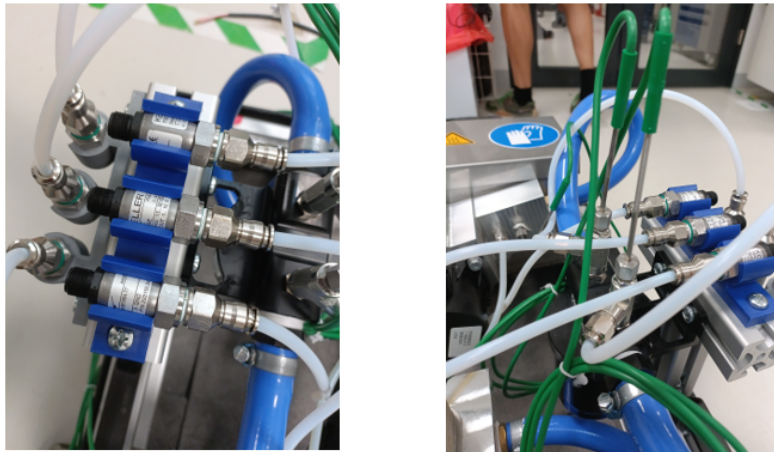


Figure 4.3. Pressure and temperature sensors on the rig.

A key requirement of the system is signal synchronization. All channels are sampled within the same software loop, guaranteeing that pressure, temperature, flow rate, and electrical signals share a common time reference. This aspect is essential for the correct interpretation of transient phenomena and for the accurate comparison between setpoints and measured values.

The acquired data are simultaneously routed to two parallel processing paths: real-time visualization and data logging. This structure ensures that the operator can continuously monitor the system behaviour during testing while preserving the same information for post-processing, without data duplication or loss.

Table 4.1 summarizes the main measured quantities, the corresponding sensor types, and their role within the experimental activity.

Table 4.1. Overview of acquired signals and instrumentation

Measured Quantity	Sensor Type	Purpose
Pressure	Pressure transducers	Evaluation of absolute pressure levels and pressure drops across system components
Temperature	Thermocouples	Monitoring of oil temperature and thermal gradients within the circuit
Flow rate	Flowmeter	Hydraulic performance characterization and flow stability verification
Voltage	Electrical measurement	Monitoring of pump supply conditions
Current	Electrical measurement	Evaluation of pump electrical load and operating limits
Rotational speed	Internal pump signal (CAN)	Comparison between target and actual pump speed

The adopted acquisition strategy provides a robust and flexible framework capable of supporting both manual and automatic test procedures, ensuring reliable data quality and traceability throughout the entire experimental campaign.



# Chapter 5

## HSE and CE Marking

### 5.1 The importance of HSE

This section provides an overview of the documentation and procedures necessary to safely perform experimental tests, highlighting the work carried out during the internship. The development of a thermal test rig requires careful identification of potential hazards, starting from the mechanical design and the electrical circuits, and extending to the operational environment, in this case the Brno Laboratory. Assessing these risks ensures that all tests are conducted safely and reliably.

A thermal test rig involves multiple potential sources of harm. Mechanical hazards include sharp edges and materials that may reach extreme temperatures during operation, while electrical hazards arise when high voltages are used. The operational environment is equally important in mitigating these risks. In this project, the use of a climatic chamber provides an inherent safety measure, as it isolates the rig during tests and prevents accidental contact with hazardous components.

Safe operation of the test rig also requires strict adherence to internal company safety rules. These rules ensure that all personnel can operate the system properly and without risk of injury, in line with Garrett's global HSE policy. Compliance depends not only on the implementation of safety procedures by the company, but also on the cooperation and awareness of all employees, emphasizing the shared responsibility of supervisors and operators in maintaining a safe workplace.

Finally, achieving CE marking requires evaluation by an external company with expertise in Czech safety regulations. This assessment focuses on both mechanical and electrical safety aspects and is essential for replicating the rig in other facilities and continuing its use for testing different components. CE compliance guarantees that the system meets European safety standards and allows trained personnel to operate the rig safely.

## 5.2 Local HSE Approval and Mandatory Safety Documentation

The thermal test rig has been operated in the Brno Laboratory. Prior to the start of testing activities, all documentation must be approved by the HSE department and subsequently released, so that all operators can become familiar with it before performing any activity on the bench. This approach reflects the company's HSE policy, which prioritizes injury prevention and the protection of employees and visitors before any operational activity. [8]

In order to obtain local HSE approval, it is mandatory to provide three main documents, which translate Garrett's Cardinal Safety Rules into practical operating procedures:

- **Safety Components Inspection (Kontrola bezpečnostních prvků).** This document contains a checklist used to verify the correct installation and proper functioning of all safety-related components. In the case of the thermal test rig, particular attention is given to the general condition of the machine, the electrical cabinet together with the emergency stop system, and the presence of appropriate labels and safety signs. This inspection ensures that safety devices are not missing, damaged, or bypassed, since it is forbidden to perform any operation without safeguards. [8]
- **Safety Operating Sheet (SOS).** This document provides a step-by-step guide for the safe operation of the test rig. The operator must fully understand the operational limits of the system, covering all phases from start-up to shutdown. The document also specifies the personal protective equipment (PPE) required during these activities. Since each machine requires dedicated procedures, the SOS includes the steps for transporting the rig from the workshop floor to the climatic chamber, with the objective of avoiding oil spills, as the oil can be toxic to the skin.
- **TPM (Údržba TPM).** This document describes routine maintenance activities aimed at ensuring reliability, longevity, and safe operation of the test rig. In this application, particular emphasis is placed on oil-related components, including inspection of the oil tank to verify the integrity of its walls, checking O-rings to prevent leakages, and monitoring oil colour to detect potential contamination.

To prevent discrepancies between documentation and the actual condition of the machine, the HSE department performs a direct inspection of the rig in the Brno facility. Once all approvals are obtained, the operator—usually a test or development engineer—is authorized to perform the tests autonomously, in compliance with the approved procedures. [8]

## 5.3 Hazard Identification and Risk Assessment

The risk assessment is performed prior to the testing phase. If, during the inspection, a component does not meet the safety requirements, it is necessary to return to the design phase until every aspect of the rig is compliant with safety requirements. The existence of a machine risk assessment is an essential requirement of the Garrett Machinery Safety Procedure (HSEMS 305). [9]

The goal of this activity is to identify the main sources of hazard for the operators, in order to eliminate them where possible or to mitigate the risk through protective measures. Garrett follows the European standard ISO 12100, which is a basic safety standard Type A addressing risk assessment and risk reduction for machinery. [9] The standard defines the methodology for the design of safe machines, the application of risk assessment, and the hierarchical use of risk reduction measures.

The method used to classify and assess risks is the Machine Risk Assessment (MRA). This approach is designed to evaluate machines with respect to proper safeguarding and supports the identification of potential hazards and the implementation of appropriate protective measures to ensure operator safety. [9] The MRA confirms whether the existing protective measures are adequate and identifies whether additional protective measures are required, as well as the designated person responsible for their implementation.

After identifying the potential hazards, the associated risks are estimated through a numerical assessment based on the following parameters:

- **Severity (S)**: pressure mark, minor or severe fracture, loss of one or two fingers or toes, leg or hand amputation, etc.
- **Frequency of Exposure (FE)**: yearly, monthly, weekly, daily, hourly.
- **Probability of Occurrence (PO)**: almost impossible, unlikely, possible, probable, certain.
- **Possibility of Avoidance (PA)**: possible, possible under certain circumstances, not possible.

The hazard rating (HR) is evaluated using the following relation:

$$HR = S \times PO \times FE \times PA \quad (5.1)$$

The resulting value is classified according to the following ranges [9]:

- 0.005–10: Negligible risk
- 11–20: Very low risk
- 21–45: Low risk

- 46–160: Significant risk
- 161–500: High risk
- > 500: Very high risk

The subsequent step aims to identify the most effective controls to eliminate or reduce the risk to an acceptable level. To achieve this objective, the 3-step method [9] defined by ISO 12100 is applied:

- **Step 1:** Evaluation of the applicability of inherently safe design measures.
- **Step 2:** Consideration of technical protective measures and safeguarding solutions.
- **Step 3:** If residual risks remain, they are addressed through information for use and operational instructions.

After implementation of these measures, several hazards and corresponding mitigation actions were identified for the thermal test rig developed during the internship, as summarized below.

**Mechanical hazards – sharp edges** A simple rectangular aluminium structure is placed under the rig to collect possible oil leakages. The risks associated with the sharp edges of the aluminium profile were mitigated by applying rubber seals along the exposed edges.

**Thermal hazards – materials at high and low temperatures** The test rig is designed to operate within a temperature range from  $-40^{\circ}\text{C}$  to  $125^{\circ}\text{C}$ , requiring specific precautions after test completion. Two test scenarios are considered, leading to different risk conditions. During cold tests, the entire climatic chamber is cooled, exposing the catch basin and chamber walls to low temperatures. During hot tests, the heater is activated and only specific components of the oil circuit reach elevated temperatures.

The climatic chamber itself acts as a safety measure: during operation, the door must remain closed and the trained operator does not access the chamber. After each test, the LabVIEW interface displays the internal chamber temperature, allowing the operator to verify when it is safe to interact with the rig. In emergency situations, operators are required to use appropriate PPE, stop the activities using the emergency protocol, and wait until safe temperature conditions are restored before direct intervention.

**Electrical hazards** Electrical risks are mainly associated with the use of a 231 V heater:

- **Heater operation:** Risks include electric shock due to faulty wiring or improper grounding, short circuits, overheating, and potential fire hazards. These risks were

mitigated by installing the heater inside the oil sump, implementing protected cable routing, and designing the electrical cabinet in accordance with EN ISO 60204-1.

- **Thermostat malfunction:** A failure scenario in which the primary thermostat remains stuck in the closed position could disrupt the control of the solid-state relay (SSR) and associated relays, preventing correct regulation of the heating elements. This risk is mitigated through the use of a secondary thermostat acting as a backup and continuous temperature monitoring via sensors installed on the rig.
- **SSR short circuit:** In this scenario, the heater would operate at full power for the entire duration of the test. A secondary thermostat connected to a dedicated safety relay is set to a critical temperature threshold and interrupts the heater power supply if this limit is reached.

**Pressure and fluid-related hazards – pump failure** Pump failure may lead to high-pressure oil leakages, representing a critical risk especially at elevated temperatures. The climatic chamber acts as a primary safety barrier by isolating the rig during operation, while the emergency stop button allows immediate interruption of the test in the event of anomalies. Pressure sensors enable continuous monitoring of operating conditions, allowing prompt detection of abnormal behavior.

In addition to its role in ensuring operator safety, the Machine Risk Assessment represents a fundamental requirement of the CE marking procedure and is prescribed by the Machinery Directive 2006/42/EC. It provides documented evidence that the essential health and safety requirements of the directive, as well as other applicable regulations, have been fulfilled.

## 5.4 CE Marking of the Thermal Test Rig

The CE marking represents the manufacturer’s declaration that a product complies with all applicable European Union legislation concerning health, safety, and environmental protection. For machinery intended to be placed into service within the European Union, CE marking is a mandatory requirement prior to operation [16].

The thermal test rig developed within this project falls within the scope of the Machinery Directive 2006/42/EC. According to Article 2(a) of the directive, a machine is defined as an assembly of linked components, powered by energy other than directly applied human effort, designed to perform a specific application and including at least one moving part [12]. Based on this definition, the test rig is classified as a machine, as it consists of interconnected mechanical and electrical components, is electrically powered,

includes moving parts such as the oil pump and fluid circulation, and performs a clearly defined testing function.

The rig is intended to operate as a complete and autonomous system and does not require integration into another machine to perform its function. For this reason, it is not classified as partly completed machinery. The Machinery Directive therefore applies in full, and compliance with its Essential Health and Safety Requirements is mandatory.

In addition to the Machinery Directive, other European directives were evaluated to determine their applicability. Electrical safety and electromagnetic compatibility aspects were considered based on the operating voltage, control architecture, and intended use of the system. This evaluation ensured that all relevant regulatory requirements were addressed prior to commissioning the test rig.

A fundamental element of the CE marking process is the execution of a Machine Risk Assessment in accordance with ISO 12100. The risk assessment provides a structured methodology to identify hazards, evaluate associated risks, and implement appropriate risk reduction measures, thereby demonstrating compliance with the Essential Health and Safety Requirements defined by the Machinery Directive.

The conformity assessment procedure adopted for the test rig is based on internal production control, supported by verification activities carried out by a specialized external company. The technical documentation includes design drawings, electrical schematics, risk assessment documentation, operating instructions, and maintenance procedures. Upon completion of the conformity assessment process, the Declaration of Conformity is issued and the CE marking is applied to the test rig.

CE marking is essential not only to ensure compliance with European legislation, but also to enable the replication of the test rig in other Garrett facilities. A CE-compliant design ensures that the system can be safely operated, modified, and reused for future testing activities involving different components or operating conditions.

**Current Status of CE Compliance** At the current stage of the project, the CE marking has been formally obtained on *10/12/2025*. During the conformity assessment process, a single recommendation was issued, concerning the installation of a dedicated support for the electrical cabinet. The purpose of this requirement is to ensure that the cabinet is positioned in a stable environment and remains easily accessible to the operator during normal operation and in emergency conditions.

The implementation of this modification is currently in the design phase and will be integrated into the final configuration of the test rig. Once completed, the solution will fully address the recommendation raised during the CE assessment, without affecting the overall functionality or safety performance of the system.

# Chapter 6

## Test Procedure

### 6.1 Preparation and Setup checks

The tests on the thermal rig are performed in the CTC department, within the climatic chambers area. The selection of the climatic chamber is carried out considering the temperature range required for the experimental campaign.

For the required tests, the most critical operating condition corresponds to an oil temperature of  $-40^{\circ}\text{C}$ . Since this value refers to the oil temperature inside the circuit, the climatic chamber must be capable of reaching lower ambient temperatures in order to guarantee stable and uniform thermal conditions during the test execution.

Before introducing the rig into the climatic chamber, a series of preliminary preparation and setup checks is performed. The rig is positioned into a catch basin, designed to collect possible oil leakages, and it is mounted on a wheeled kart with locked wheels. The catch basin and the kart are mechanically secured to prevent relative movement during transport and operation. A visual inspection of the rig is carried out to verify the integrity of the mechanical components, the absence of visible leakages, and the correct positioning of sensors and hydraulic connections. In addition, the oil level inside the tank is checked to ensure that it complies with the operating requirements of the test.

Once the preliminary checks confirm that the rig is in suitable condition, it is transferred from the laboratory floor to the climatic chamber using a motorized lifting table. As discussed in Chapter 5, it is mandatory to avoid any possible hazards; for this reason, this step is also considered an integral part of the preparation procedure. The goal is always to minimize risks for the operator first and for the equipment.

After positioning the rig inside the climatic chamber, the electrical and instrumentation connections are completed. The sensors installed on the rig are connected to the electrical cabinet, which is located outside the climatic chamber. The routing of the cables is performed through a dedicated opening on the side of the chamber, allowing proper connection without compromising the chamber insulation or operator safety. Once the

connections are established, the LabVIEW control interface is used to verify the correct acquisition of signals, ensuring that all sensors are properly connected and operational.

The test engineer is responsible for activating the climatic chamber and setting the target temperature using the chamber control panel. The stabilization of the oil temperature is monitored through the LabVIEW interface, which provides real-time feedback on the measured values. Only after the target temperature is reached and stable, and all preparation checks have been successfully completed, the system is considered ready for the execution of the test sequence.

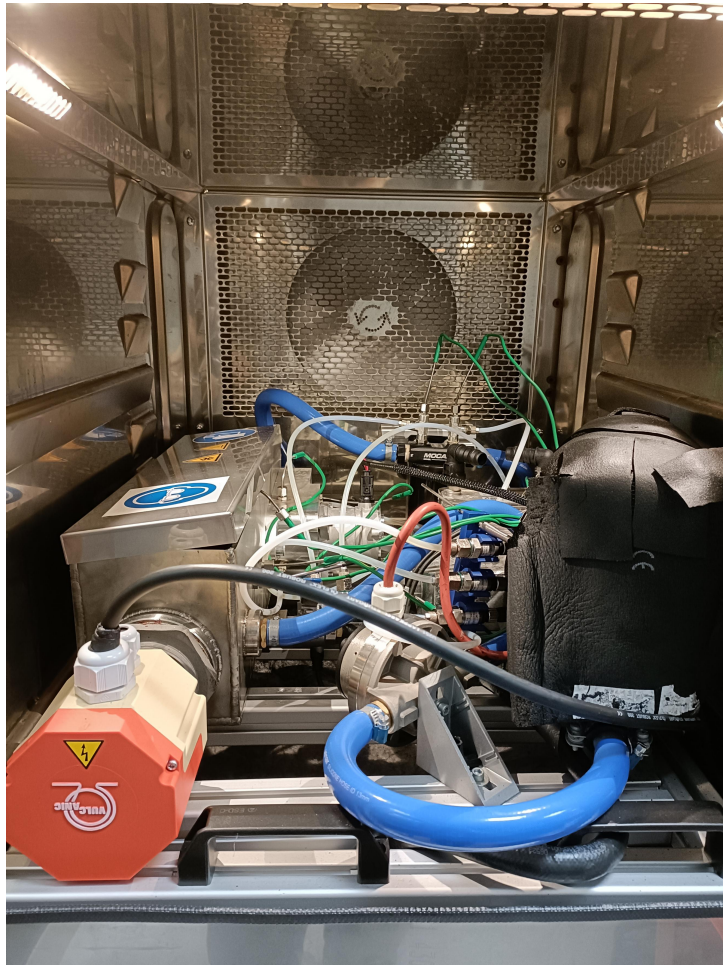


Figure 6.1. Test rig in the climatic chamber during tests.

## 6.2 Test Sequence Execution

In order to obtain a comprehensive experimental characterization of the lubrication system and its components, the test campaign was initially planned to include different test typologies. Each test type was designed to investigate specific operating conditions and performance aspects, ranging from low-temperature start-up behavior to high-temperature operation and long-term endurance. The planned test categories and their

main characteristics are summarized in Table 6.1. Not all planned test conditions were ultimately executed, as discussed later in this section, due to safety considerations and practical constraints.

Table 6.1. Summary of the main test typologies performed on the thermal test rig

Test category	Cold Start Test	Hot Soak Test	Endurance Test
Type of test	Manual test	Manual test	Automatic test
Temperature range	−40 °C to 0 °C	125 °C	−40 °C to 125 °C
Focus	Pump behavior with high-viscosity oil	System thermal response at upper temperature limits	Long-term performance degradation
Main checks / method	Startup success, current peaks, potential stalling	Heater performance, overheating	Automated thermal step cycles

### 6.2.1 Manual Test Execution

The performance tests are performed to obtain accurate and repeatable measurements at predefined operating points. In particular, the adopted procedure is based on mapping the electric oil pump (EOP) by progressively increasing the outlet pressure while keeping the oil temperature and rotational speed constant.

The two categories of tests performed manually are cold start tests and hot soak tests. A summary of the objectives associated with each test category is reported in Table 6.2.

Table 6.2. Objectives of manually executed test categories [2]

Test category	Objective
Cold start tests	Evaluation of start-up performance with high-viscosity oil, including detection of hard starts, motor overload conditions, and potential pump stalling.
Hot soak tests	Evaluation of system behaviour at thermal limits, with focus on component deformation, seal degradation, and overheating phenomena.

The goal of this test campaign is to provide validation data for the main components of the rig at a specific working temperature. For this reason, each test sequence starts with the activation of the climatic chamber by setting the target temperature. The thermal

stabilization phase allows preliminary checks of the system, including verification of the EOP signals and the correct operation of the climatic chamber through the environmental temperature sensors.

The oil temperature, measured by a dedicated sensor installed in the oil tank, is considered the reference parameter for test execution. A tolerance of  $\pm 1.5$  °C is accepted during the test, for instance to account for temperature variations caused by pump operation. Once the target oil temperature is reached and confirmed through the LabVIEW interface, the throttle valve position is set to its fully open condition, corresponding to a control voltage of 10 V. This condition must be verified at the beginning of each test sequence.

Subsequently, the pump rotational speed is set directly through the LabVIEW interface. The waveform chart allows the operator to follow the evolution of the measured signals and to verify that the target rotational speed is reached and stabilized before starting data acquisition. In order to ensure an efficient organization of the recorded data, one data file is created for each rotational speed level.

With constant oil temperature and rotational speed, the outlet pressure is varied in predefined increments, typically in steps of 0.5 bar. This is achieved by progressively closing the throttle valve, resulting in a reduction of the control voltage from 10 V downward. After each adjustment, the system is allowed to stabilize for at least 30 s, and a minimum data logging time of 60 s is ensured before proceeding to the next setpoint.

For each operating point, the corresponding flow rate and all relevant signals are recorded and associated with the specific test condition. The procedure is repeated until the operational limits of the EOP are reached. Once the maximum rotational speed is achieved, the throttle valve is returned to the fully open position before either proceeding to the next test sequence or concluding the test. [1]

An example of an electric oil pump performance map is reported in Figure 6.2 as a visual reference to support the description of the manual mapping procedure. A complete set of performance maps generated during the experimental campaign is provided in the Appendix.

## 6.2.2 Automatic Test Execution

To address endurance requirements, automatic cycling tests were considered during the planning of the experimental campaign, with the objective of reproducing repeated operating conditions representative of long-term system usage. The goal is to highlight gradual degradation phenomena, aging effects, and potential performance drift of the components under test [4].

During the planning phase, two different automatic test profiles were evaluated: a rectangular profile and a triangular profile. The rectangular profile is based on operating

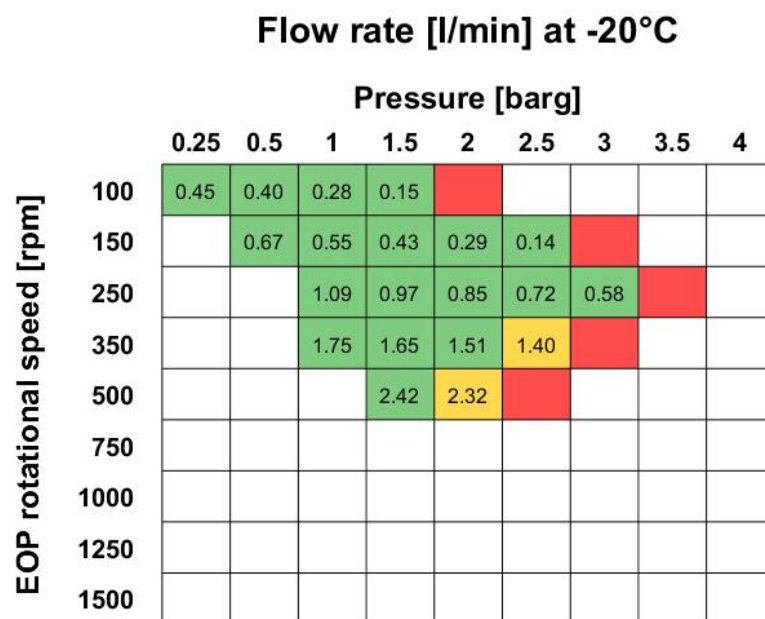


Figure 6.2. Example of electric oil pump (EOP) performance map obtained at an oil temperature of  $-20\text{ }^{\circ}\text{C}$ , reported as a visual reference to illustrate the manual mapping procedure described in this section. A complete set of performance maps is provided in the Appendix.

the system at fixed load levels for a defined duration, followed by a rapid transition to the next level. Conversely, the triangular profile involves a continuous and linear variation of the operating conditions between minimum and maximum values within each cycle.

The main difference between the two approaches lies in the time spent at extreme operating conditions. The rectangular profile is generally associated with a more severe loading condition, as the system remains at peak operating levels for a longer fraction of each cycle. This characteristic can accelerate the accumulation of thermal and mechanical stress, making such profiles suitable for endurance-oriented evaluations. Triangular profiles tend to distribute the load more gradually over time, potentially reducing the time spent at extreme operating conditions [3].

Based on these considerations, the rectangular test profile was selected as the reference solution for the automatic test planning, as it was considered more effective for endurance-oriented evaluations where accelerated stress accumulation is desirable. The triangular profile was therefore not retained for further development.

Figure 6.3 illustrates the rectangular automatic test profile selected during the planning phase, reported as a reference to clarify the cyclic loading strategy considered for endurance testing.

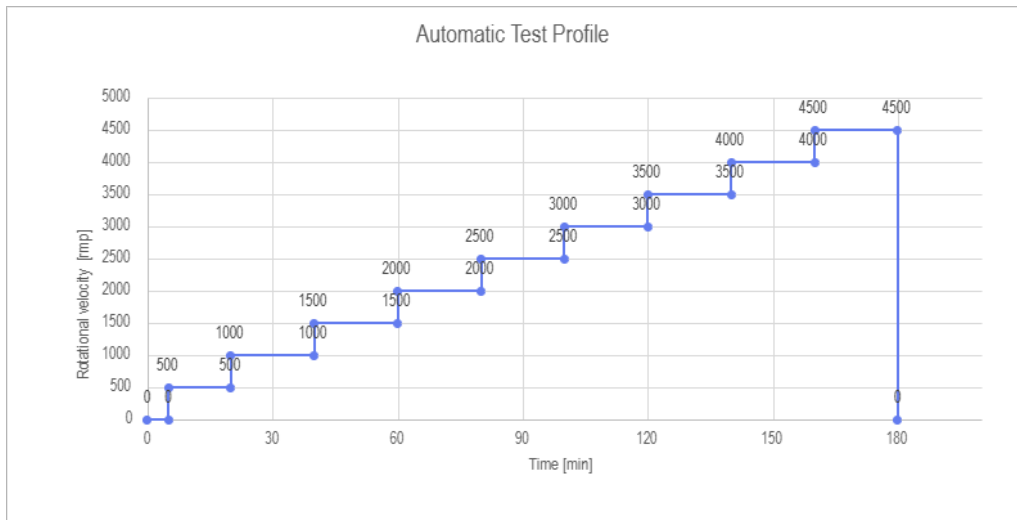


Figure 6.3. Rectangular automatic test profile selected for endurance-oriented test planning. The profile represents repeated cycles between predefined operating levels, resulting in sustained loading at peak conditions.

### 6.2.3 Selection of Executed Test Conditions

Despite the detailed planning of the experimental campaign, it was not possible to execute all the originally planned tests. With the exception of the cold start tests – the only test fully performed – the remaining test typologies were only partially executed or not performed.

The tests at hot temperature were only partially performed, the functionality of the heating system was initially verified at an intermediate temperature level of 50 °C. A second test at target temperature of 125 °C was performed but interrupted due to hardware limitations. As the pump rotational speed was increased, the EOP internal signal “xxx” was activated, shifting from value 1 to value 2 and indicating an overcurrent condition. As a consequence, the internal protection logic of the pump was activated, limiting the maximum rotational speed to 792 rpm limit and preventing the continuation of the test.

Following this event, the team decided to not proceed further hot temperature tests on this pump. At the time of writing, a technical discussion with the pump supplier is ongoing. This scenario applies for pump 1, and based on these results no hot tests were planned for the second pump.

Regarding the automatic endurance tests, these have been postponed due to time constraints associated with the available testing window. The execution of these tests has been scheduled for a subsequent test campaign, currently planned for March.

Table 6.3 provides a concise overview of the planned test activities, the tests actually executed, and the main reasons for any deviations from the original test plan.

Table 6.3. Overview of planned and executed tests and associated limitations

Planned test	Execution status	Main cause
Full cold performance tests	Performed with operational point mapping	–
Full hot soak performance tests	Partial test: heater validation only	Hardware limitations prevented full execution
Automated endurance profile	Not performed	Postponed due to time constraints

## 6.3 Step Management and Fault Handling

The execution of the experimental campaign requires a structured management of the individual test steps, together with continuous monitoring of the system behaviour in order to guarantee both measurement reliability and operational safety.

Since the test activities were mainly performed in manual mode, particular attention was given to the definition of clear stabilization criteria and to the implementation of protective actions capable of preventing unsafe operating conditions.

### 6.3.1 Test Step Definition

Each experimental test is divided into a sequence of operating steps, where every step is characterized by a predefined combination of:

- EOP rotational speed;
- outlet pressure level;
- target oil temperature.

These parameters define the operating point at which the system is required to operate for data acquisition. During each step, all sensor signals are continuously recorded and stored for post-processing and performance evaluation.

The transition between consecutive steps is not time-driven, but condition-driven, and depends on the stabilization of the main physical quantities of the system.

### 6.3.2 Stabilization Criteria

Before proceeding to the next operating point, the system is required to reach steady-state conditions. Stabilization is evaluated by monitoring the real-time trends displayed on the control interface.

In general, an operating point is considered stable when the following conditions are simultaneously satisfied:

- oil temperature variation remains within a limited range around the target value;
- outlet pressure does not exhibit oscillations beyond sensor noise;
- flow rate shows stable behaviour without significant fluctuations;
- EOP speed remains constant at the commanded setpoint.

A minimum stabilization time of approximately 30–60 seconds is typically observed before enabling data logging for each test step, ensuring repeatable and comparable measurements across the experimental campaign.

### 6.3.3 Manual Step Transition Logic

The progression between test steps is performed manually by the operator through the LabVIEW control interface.

This design choice allows full supervision of the system behaviour and provides high flexibility during experimental testing. The operator can decide when to advance to the next step based on the observed trends, or interrupt the test if abnormal conditions are detected.

Manual step management also enables immediate reaction to unexpected phenomena, such as pressure instabilities or temperature deviations, which could compromise test integrity or component safety.

### 6.3.4 Fault Detection and Alarm Management

During operation, the control system continuously monitors the main physical quantities of the test rig, including:

- oil temperature at different locations;
- inlet and outlet pressure levels;
- oil flow rate;
- electrical signals related to the EOP and heating system.

Each signal is associated with predefined warning and safety thresholds. When a signal exceeds its allowable operating range, visual alarms are displayed on the control interface to alert the operator.

Depending on the severity of the deviation, the system may require manual intervention or automatically trigger protective actions to prevent component damage.

### 6.3.5 Safety Actions and Protective Measures

In the presence of critical fault conditions, several safety actions can be activated to protect both the equipment and the operator.

These actions include:

- automatic shutdown of the electrical heater;
- EOP stop command;
- power cutoff through the electrical cabinet;
- activation of the emergency stop circuit.

The implemented safety logic is consistent with the hazard identification and risk assessment described in Chapter 5 and complies with the laboratory safety procedures adopted during experimental activity.

### 6.3.6 Test Interruption and Data Integrity

In the event of test interruption caused by system faults, safety shutdowns or operator decision, all measurement data acquired up to that point are preserved.

Data are stored in TDMS format, ensuring traceability of the executed test steps and allowing partial datasets to be analysed when required. Each interruption is documented by the operator, enabling correct interpretation of the recorded signals during the post-processing phase.

This approach guarantees data integrity while maintaining a high level of operational safety throughout the entire experimental campaign.

# Chapter 7

## Experimental Results and Discussion

This chapter presents and discusses the experimental results obtained using the newly developed thermal test rig. The experimental campaign was aimed at characterizing the behaviour of two electric oil pumps, identified as EOP1 and EOP2, under low-temperature operating conditions, as well as at validating the functionality and robustness of the test bench.

The experimental procedures and test methodologies adopted during the campaign are described in Chapter 6. In order to improve clarity and readability, only the most relevant results and performance indicators are discussed in this chapter, while complete pressure–flow maps, efficiency curves and detailed measurement plots are reported in the Appendix.

All supplier references have been anonymized and the pumps are identified exclusively as EOP1 and EOP2.

### 7.1 Experimental campaign overview

The experimental activity was conducted on two electrically driven oil pumps characterized by different internal architectures and control strategies. Both units were tested using the same hydraulic layout, instrumentation and thermal conditioning system in order to ensure comparable boundary conditions.

The main objectives of the experimental campaign were:

- evaluation of pump operability at low oil temperatures;
- characterization of pressure–flow behaviour over a wide operating range;
- analysis of efficiency trends as a function of temperature;
- identification of operational limits and failure modes;
- validation of the thermal test rig under representative conditions.

Table 7.1 summarizes the main characteristics of the performed tests.

Table 7.1. Overview of experimental tests

Parameter	EOP1	EOP2
Control interface	LIN	CAN
Tested temperature range	0°C to -40°C	0°C to -32°C
Pressure control device	Globe valve	Globe valve
Working fluid	Lubricating oil	Lubricating oil
Test configuration	Closed-loop system	Closed-loop system

All tests were performed under steady-state conditions after thermal stabilization of the oil circuit. The oil temperature measured at the tank outlet was used as reference temperature for result classification.

## 7.2 Results for EOP1

EOP1 was controlled through a LIN communication interface, allowing direct regulation of pump rotational speed. The pump was tested over a wide speed range at oil temperatures of 0°C, -10°C, -20°C, -30°C and -40°C.

The measured pressure–flow characteristics show the expected qualitative behaviour of an electrically driven positive-displacement pump. For all temperature levels, an increase in rotational speed resulted in a corresponding increase in delivered flow rate, while higher outlet pressures led to a reduction in flow.

As oil temperature decreased, a progressive reduction of the achievable flow range was observed, mainly due to the significant increase in lubricant viscosity. This effect became particularly evident below -20°C, where hydraulic losses increased markedly.

Complete pressure–flow maps for EOP1 at all tested temperatures are reported in Appendix A (Figures A.6–A.10).

The efficiency of EOP1 was evaluated by comparing the hydraulic output power with the measured electrical input power. The analysis revealed unusually high efficiency values at specific operating points, in some cases exceeding 60%.

Table 7.2 reports the maximum efficiency values extracted from the experimental data.

Table 7.2. Maximum measured efficiency values for EOP1

Oil temperature	Max efficiency [%]	Operating condition
0°C	62.2	Low pressure, low speed
-10°C	64.9	Low pressure, low speed
-20°C	59.3	Reduced flow regime
-30°C	52.1	Near minimum load
-40°C	47.6	Limited operating range

The efficiency values obtained for EOP1 are significantly higher than typical values reported for similar pump technologies. This behaviour can be mainly attributed to operation under very low hydraulic load conditions, where the electrical input power approaches the resolution limit of the current measurement system.

Additional contributing factors include reduced differential pressure across the pump and the influence of inverter and control electronics losses. For these reasons, the efficiency results for EOP1 should be interpreted primarily in a qualitative manner, with greater emphasis on trend evolution rather than absolute numerical accuracy.

A qualitative comparison with supplier reference data indicates that the experimentally measured flow rates are generally lower than nominal values, especially at low temperatures. This deviation is mainly related to increased oil viscosity and to the additional hydraulic resistance introduced by the integrated system configuration.

## 7.3 Results for EOP2

EOP2 was operated using a CAN-based communication interface and is characterized by a different internal architecture compared to EOP1. During testing, the pump exhibited more restrictive protection strategies under low-temperature conditions.

Stable operation was achieved at oil temperatures of 0°C, -10°C, -20°C and -30°C. Attempts to operate the pump below approximately -32°C consistently resulted in fault conditions that prevented continuous operation.

The pressure–flow behaviour of EOP2 shows a narrower operating envelope compared to EOP1. While stable performance was obtained at moderate temperatures, the achievable flow range decreased rapidly as oil temperature dropped below -20°C.

Complete characteristic curves for EOP2 are reported in Appendix B (Figures B.6–B.9).

Efficiency values measured for EOP2 remained within realistic ranges, with peak values between approximately 20% and 35% depending on the operating condition, as summarized in Table 7.3.

Table 7.3. Maximum measured efficiency values for EOP2

Oil temperature	Max efficiency [%]
0°C	33.1
-10°C	29.4
-20°C	24.7
-30°C	18.2

A monotonic reduction in efficiency was observed with decreasing oil temperature, consistent with the increase in viscous losses within the pump.

During low-temperature testing, EOP2 repeatedly activated internal stall protection mechanisms when oil inlet temperature approached -32°C. This condition resulted in automatic pump shutdown and required system reset before further operation.

Temperature measurements suggest that the operational limit was primarily related to internal motor and electronics thermal constraints rather than to purely hydraulic performance.



Figure 7.1. Conditions of the rig after reaching  $T = -40^{\circ}\text{C}$  without the EOP running.

## 7.4 Comparative analysis between EOP1 and EOP2

A direct comparison between the two tested pumps highlights substantial differences in terms of control strategy, hydraulic behaviour and low-temperature operability.

A first relevant distinction concerns the adopted control architecture. EOP1 is operated through a LIN-based interface that directly regulates pump rotational speed. This solution results in a classical behaviour in which the delivered flow rate varies continuously as a function of both speed and hydraulic load.

Conversely, EOP2 employs a CAN-based control strategy characterized by internal regulation algorithms aimed at stabilizing the delivered flow rate for each commanded operating point. This approach improves flow stability under nominal conditions but introduces stricter internal protection thresholds.

These differences are clearly reflected in the pressure–flow characteristics in the [A](#) (Figures A.6–A.10) and [B](#) (Figures B.5–B.8). EOP1 exhibits typical negatively sloped pressure–flow curves, where flow rate decreases progressively with increasing outlet pressure. This behaviour remains qualitatively consistent over the entire tested temperature range, although the operating envelope becomes increasingly limited as oil viscosity rises at low temperatures.

EOP2 shows flatter pressure–flow curves at moderate temperatures, indicating the presence of active internal compensation. However, once the maximum allowable torque or thermal threshold is reached, flow delivery collapses abruptly due to stall protection activation.

A consistent trend can also be observed in the operating point maps reported in the Appendix (see Figures A.1–A.5 and Figures B.1–B.4).

For EOP1, the maps clearly show a progressive reduction of delivered flow rate as the outlet pressure increases. This behaviour is characteristic of a speed-controlled positive-displacement pump, where the hydraulic load directly affects the effective flow delivery, resulting in the typical negative slope of the pressure–flow relationship.

Conversely, the operating point maps of EOP2 exhibit an almost constant flow rate over a wide pressure range, with only minor variations as the outlet pressure increases. This flattened trend indicates the action of internal control algorithms actively compensating the hydraulic resistance, maintaining the commanded operating condition until the protection limits of the system are reached.

The comparison of these maps therefore confirms that the different control architectures of the two pumps have a direct and measurable impact on the global hydraulic behaviour of the system.

From a low-temperature perspective, EOP1 demonstrated superior operability. Stable operation was achieved down to  $-40^{\circ}\text{C}$ , albeit within a reduced operating range. No irreversible fault conditions were observed, and pump operation could be restored by

adjusting operating parameters.

EOP2 was unable to operate below approximately  $-32^{\circ}\text{C}$ . Repeated test attempts at lower temperatures resulted in automatic shutdown caused by internal protection strategies. Temperature measurements indicate that this limitation is primarily associated with internal motor and electronic thermal constraints rather than with hydraulic instability.

These behaviours have relevant implications at system level. The broader operating range of EOP1 makes it potentially suitable for applications requiring guaranteed oil circulation during extreme cold-start conditions. In contrast, EOP2 offers more predictable efficiency values and stable behaviour under nominal operating conditions, but its restrictive protection logic limits its applicability in extreme environments.

A summary of the main performance differences observed during the experimental campaign is reported in Table 7.4.

Table 7.4. Comparison between EOP1 and EOP2

Aspect	EOP1	EOP2
Minimum operating temperature	$-40^{\circ}\text{C}$	$-32^{\circ}\text{C}$
Control interface	LIN	CAN
Maximum measured efficiency	$>60\%$ (anomalous)	$\sim 33\%$
Operational stability	Limited at low load	Stable until stall
Failure mode	Reset required	Stall protection
Overall robustness	Medium	High

Overall, EOP1 demonstrated superior low-temperature operability, while EOP2 exhibited more stable efficiency behaviour under nominal conditions but stricter operational limits at low temperatures.

## 7.5 Filter and HE results

In addition to pump characterization, the pressure losses introduced by the oil filter and the heat exchanger were monitored during the experimental campaign.

The flow rate versus pressure measurements reported in Appendix A (Figures A.20–A.24) and Appendix B (Figures B.17–B.20) show that both components introduce limited additional pressure drops within the investigated operating range. As expected, pressure losses increase with decreasing oil temperature due to higher fluid viscosity; however, no critical restrictions were observed even at the lowest tested temperatures.

The measured pressure differentials across the filter and the heat exchanger remained stable and repeatable throughout the test campaign, confirming that their integration did not compromise pump operation nor affect the validity of the experimental measurements.

These results demonstrate that the selected filter and heat exchanger are suitable for low-temperature testing and that their contribution to the overall hydraulic resistance of the circuit is compatible with the objectives of the experimental setup.

## 7.6 Validation of the thermal test rig

Beyond pump characterization, the experimental campaign confirmed the capability of the newly developed thermal test rig to operate reliably under severe low-temperature conditions.

The system demonstrated stable oil temperature control down to  $-40^{\circ}\text{C}$ , repeatable pressure regulation through the globe valve, reliable sensor operation across the entire temperature range and stable data acquisition without signal interruptions.

No oil leakages were detected during extended testing, confirming the effectiveness of the mechanical design solutions adopted for the hydraulic circuit.

Overall, the experimental results validate the developed test rig as a suitable and robust platform for low-temperature lubrication system testing and component development activities.



# Chapter 8

## Conclusion and additional steps for the future

This work addressed the development of a rig structure with the goal to allow the testing and characterization of three principal components, EOP, filter and HE for and electric PWT. The main result achieved as consequence of a successful design is the characterization of the EOP at cold temperatures. Ensuring reliable oil circulation in these conditions is essential for the durability and efficiency of modern electrified powertrains, yet it poses significant challenges due to the strong temperature dependence of lubricant properties and pump control strategies. The thermal test rig developed within this project has demonstrated reliable and repeatable operation over the entire investigated temperature range. Following the successful validation of the hydraulic layout, instrumentation and safety systems, and after obtaining CE marking certification, the setup is now considered a stable and mature experimental platform suitable for further testing activities beyond the scope of this thesis.

As a consequence, the rig is currently being reused for the characterization of additional electric oil pump prototypes supplied by external manufacturers. Two new pumps with different hydraulic and control characteristics have recently been delivered and are being evaluated using the same experimental methodology described in this work. The reuse of the validated setup ensures direct comparability between past and future measurements, while significantly reducing preparation time and development effort.

The test rig has been reinstalled inside the climatic chamber to enable extended low-temperature investigations. In order to improve thermal stability and measurement repeatability, the minimum ambient temperature has been limited to  $-40\text{ }^{\circ}\text{C}$ , while longer stabilization periods are adopted to guarantee that the lubricant reaches a uniform temperature before each acquisition. The temperature increase generated by pump operation during the tests is considered part of the natural operating behaviour and is not actively compensated.

Current testing activities focus on steady-state characterization at constant rotational speed, while progressively increasing oil temperature. This approach allows the influence of temperature-dependent viscosity variations on pump performance to be evaluated in a controlled manner, providing complementary information with respect to the constant-temperature mapping strategy adopted in the present work.

In addition, endurance and long-duration tests are planned to assess reliability and thermal robustness under continuous operation. Such tests were not previously feasible during the development phase of the rig, but are now enabled by the improved stability of the system and the validated safety features. These extended campaigns will allow the investigation of performance drift, thermal accumulation effects and potential degradation phenomena over time.

Overall, the availability of a certified and modular thermal test bench opens the possibility for systematic evaluation of future components, supporting both supplier benchmarking and advanced validation activities for next-generation lubrication systems.

# Appendix A

## Test EOP1

This appendix presents the experimental results obtained from the tests performed on EOP1. For each investigated temperature level, the operating point maps, pressure–flow curves, efficiency maps and filter and heat exchanger results are reported.

### A.1 Operating point maps

The operating point maps provide a graphical overview of the pump behaviour over the investigated pressure and temperature ranges. Each tested condition is represented using a colour code that indicates the ability of the pump to reach and maintain the commanded operating point.

The adopted colour convention is defined as follows:

- Green: operating point successfully reached and stable operation achieved;
- Yellow: operating point reached but stability compromised by control-related issues or error signals (e.g. inability to maintain the commanded RPM), typically associated with oscillations in pressure, flow rate or rotational speed;
- Red: operating point not reached or test condition not achievable.

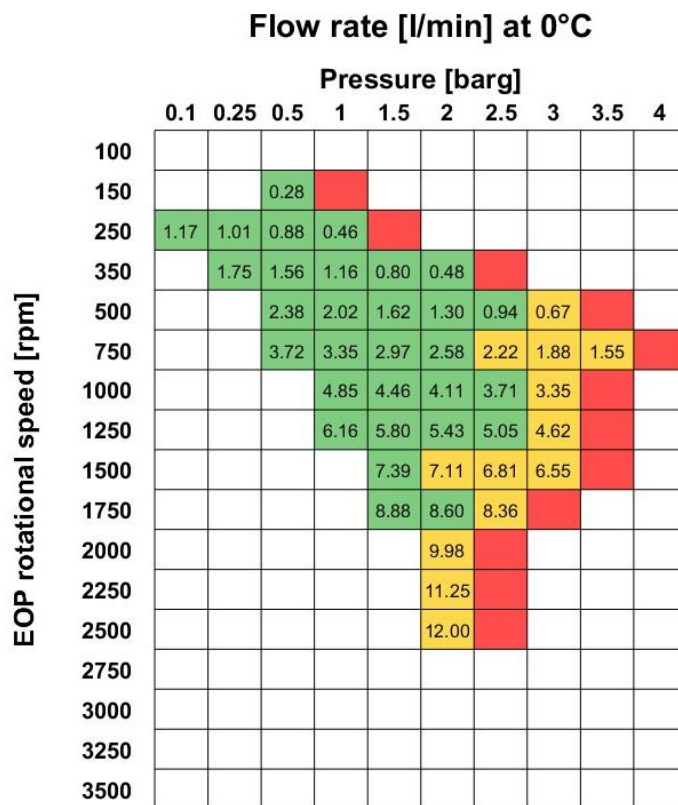


Figure A.1. EOP1 – Operating point map at  $T = 0^\circ\text{C}$ .

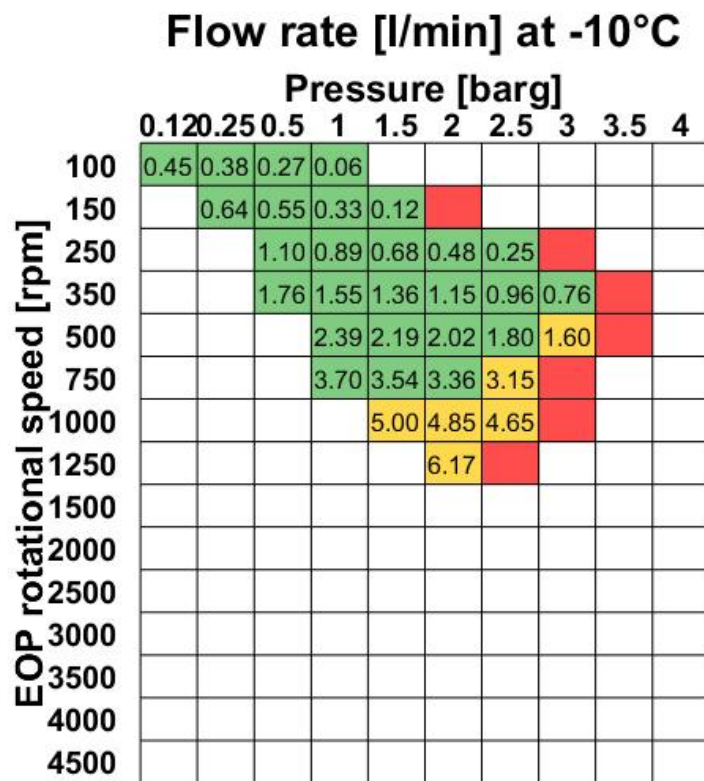


Figure A.2. EOP1 – Operating point map at  $T = -10^{\circ}\text{C}$ .

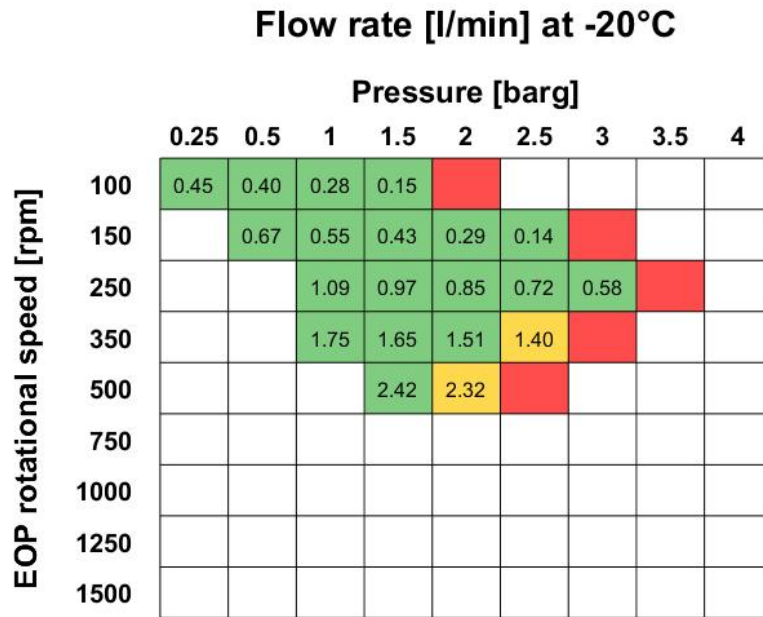


Figure A.3. EOP1 – Operating point map at  $T = -20^{\circ}\text{C}$ .

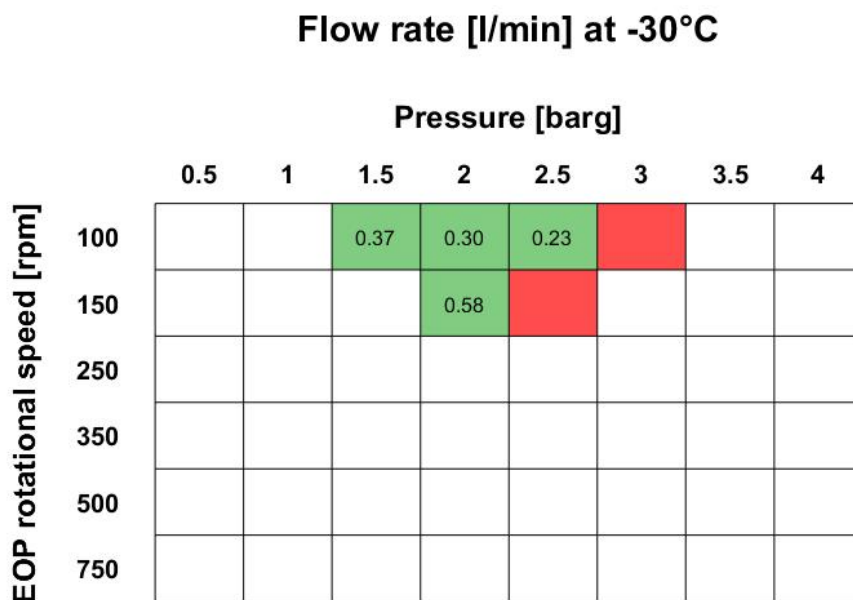


Figure A.4. EOP1 – Operating point map at  $T = -30^{\circ}\text{C}$ .

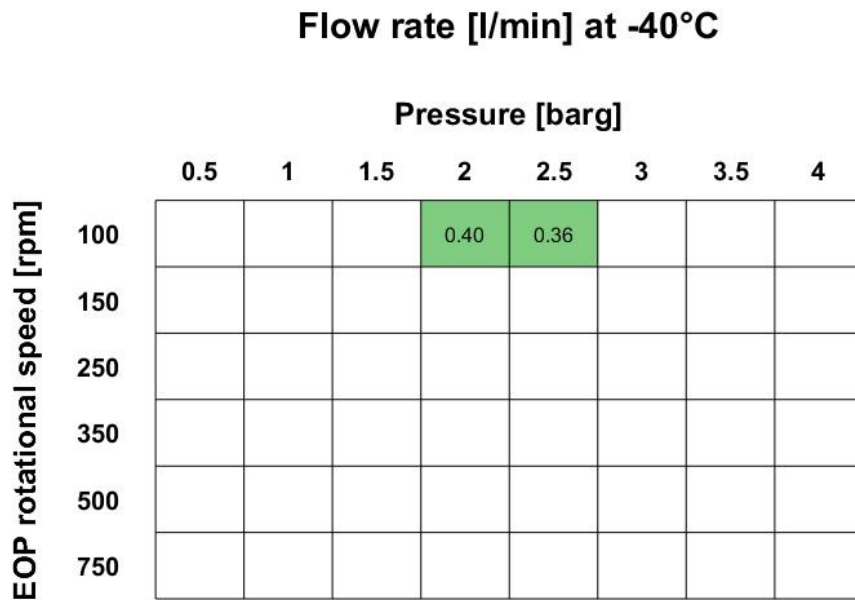


Figure A.5. EOP1 – Operating point map at  $T = -40^{\circ}\text{C}$ .

## A.2 Pressure–flow characteristic curves

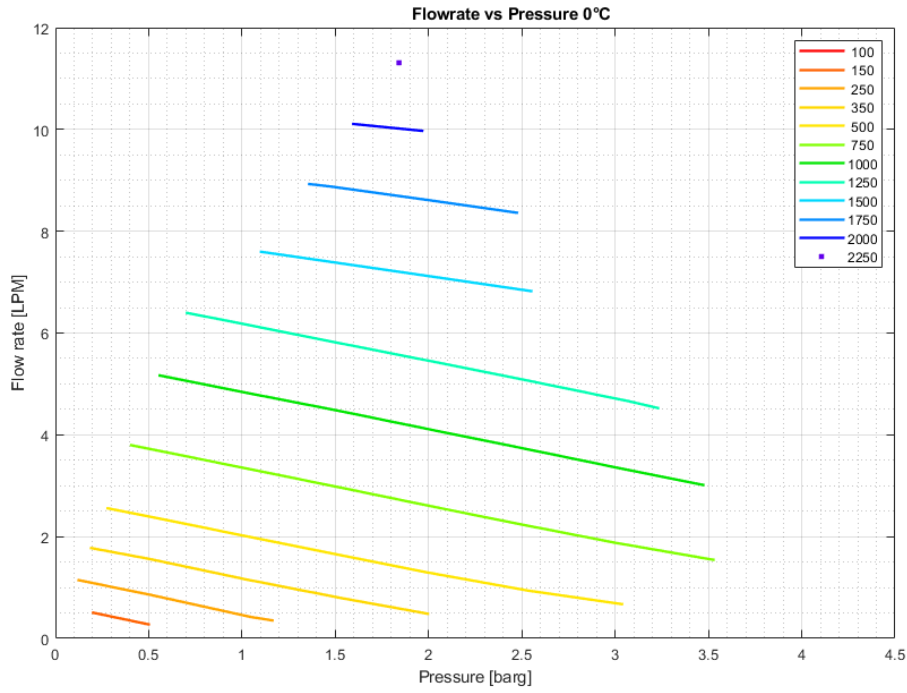


Figure A.6. EOP1 – Pressure–flow characteristic at  $T = 0^{\circ}\text{C}$ .

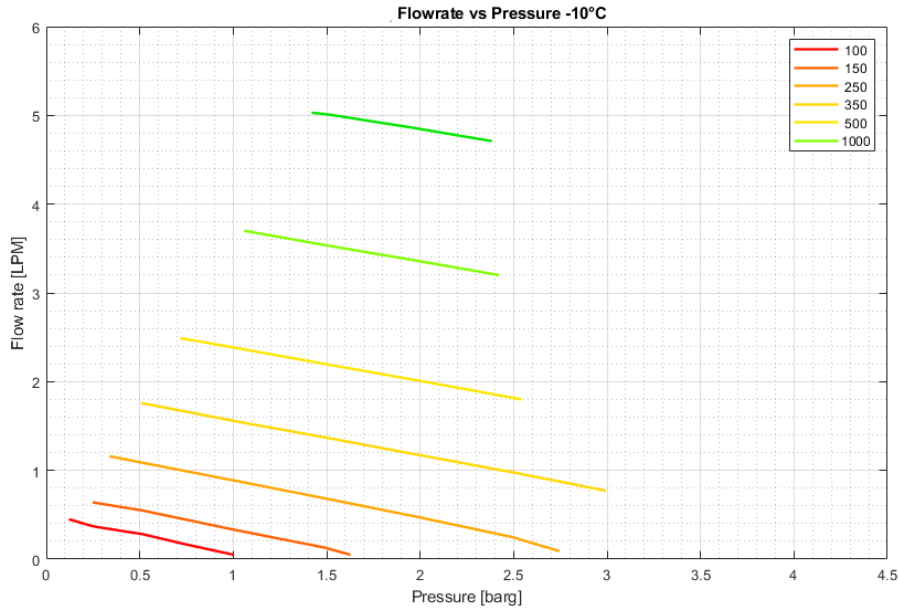


Figure A.7. EOP1 – Pressure–flow characteristic at  $T = -10^{\circ}\text{C}$ .

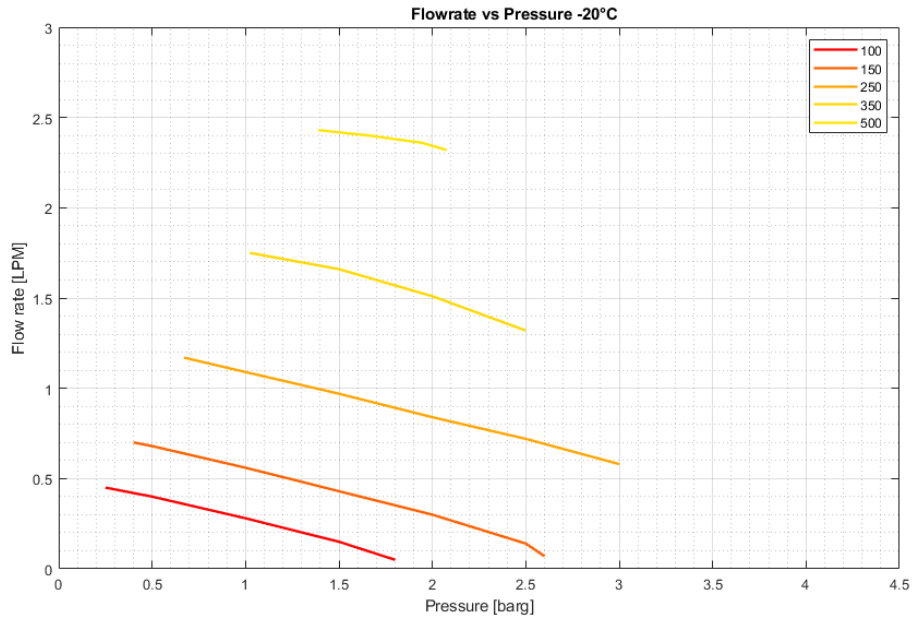


Figure A.8. EOP1 – Pressure–flow characteristic at  $T = -20^{\circ}\text{C}$ .

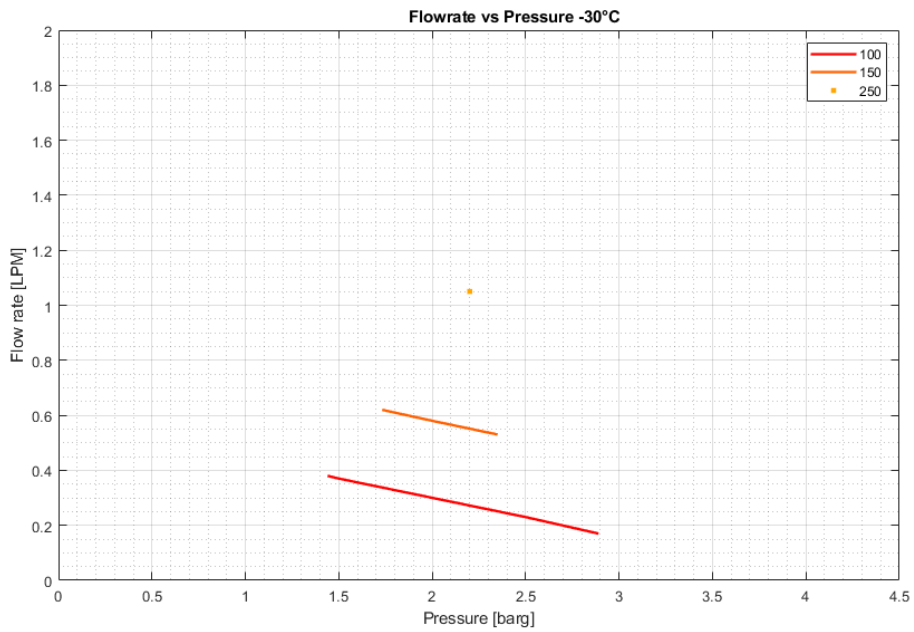


Figure A.9. EOP1 – Pressure–flow characteristic at  $T = -30^{\circ}\text{C}$ .

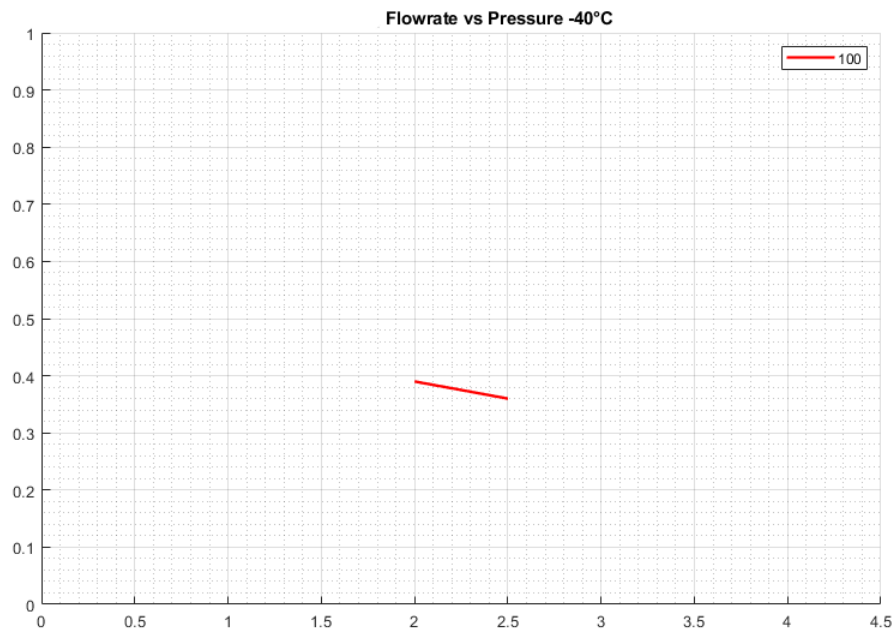


Figure A.10. EOP1 – Pressure–flow characteristic at  $T = -40^{\circ}\text{C}$ .

## A.3 Efficiency maps

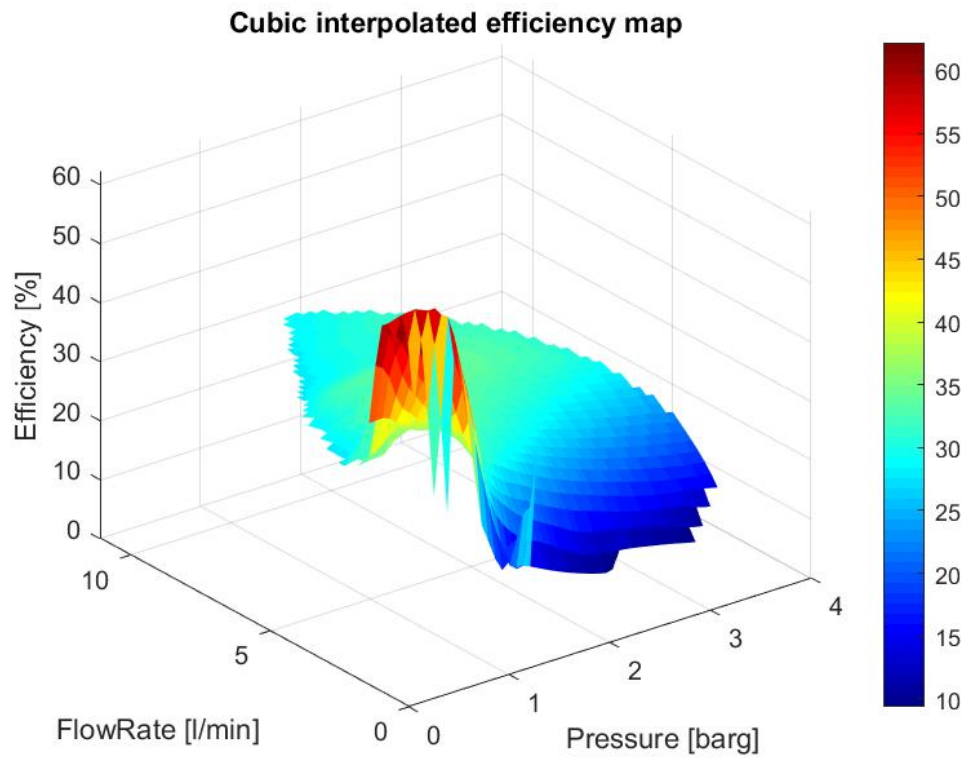


Figure A.11. EOP1 – Cubic efficiency map at  $T = 0^{\circ}\text{C}$ .

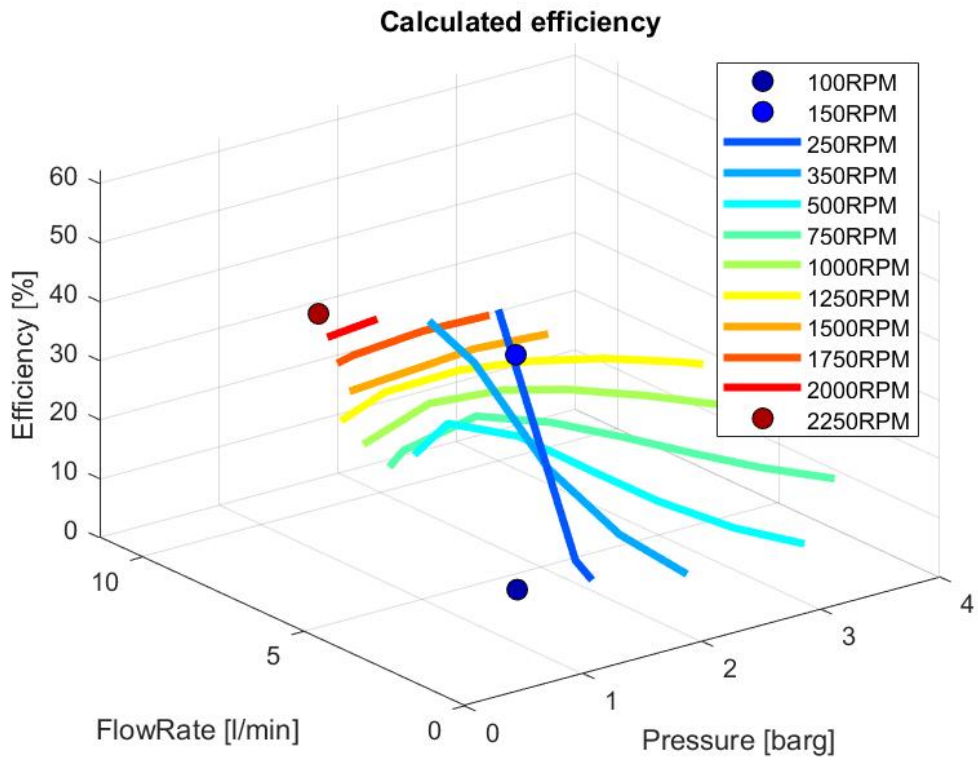


Figure A.12. EOP1 – Linear efficiency map at  $T = 0^{\circ}\text{C}$ .

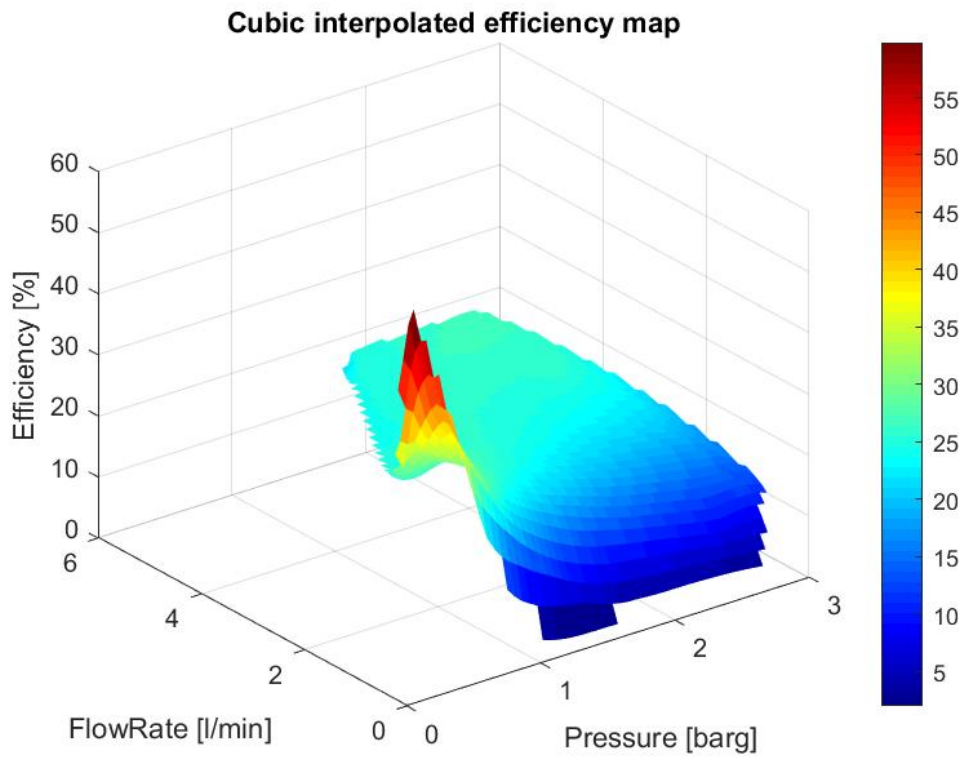


Figure A.13. EOP1 – Cubic efficiency map at  $T = -10^{\circ}\text{C}$ .

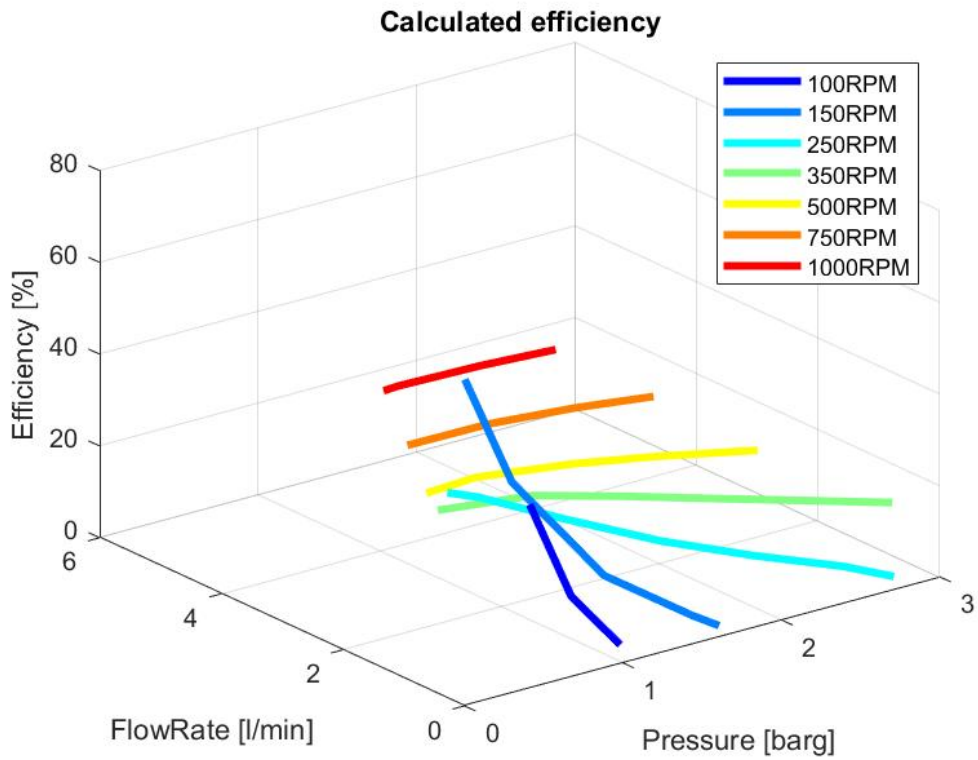


Figure A.14. EOP1 – Linear efficiency map at  $T = -10^{\circ}\text{C}$ .

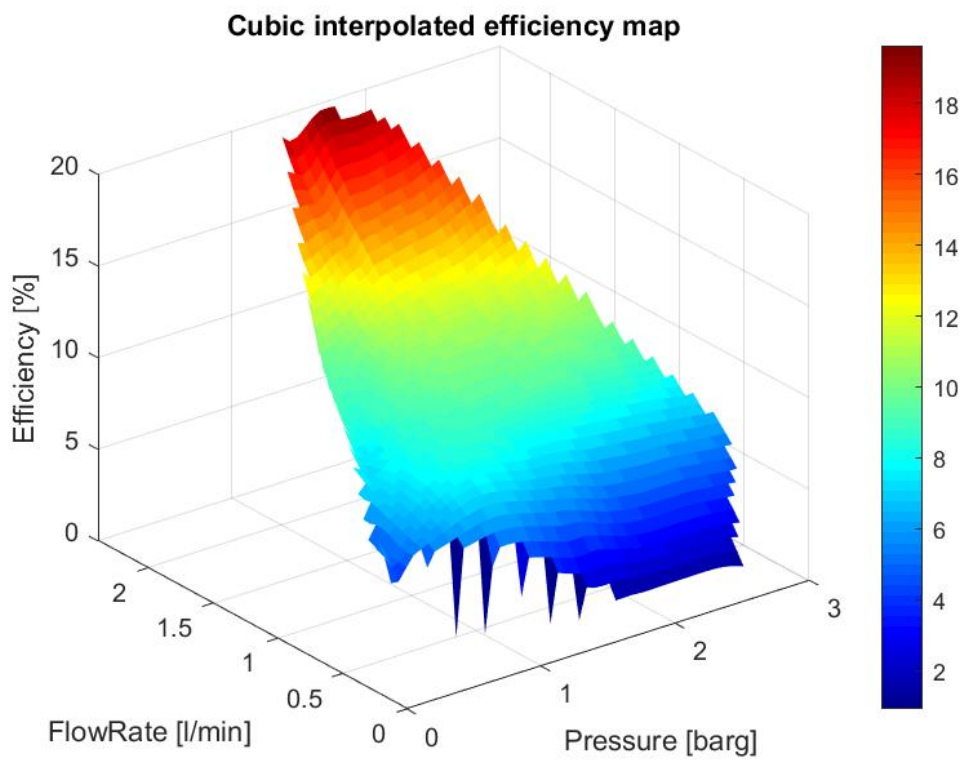


Figure A.15. EOP1 – Cubic efficiency map at  $T = -20^{\circ}\text{C}$ .

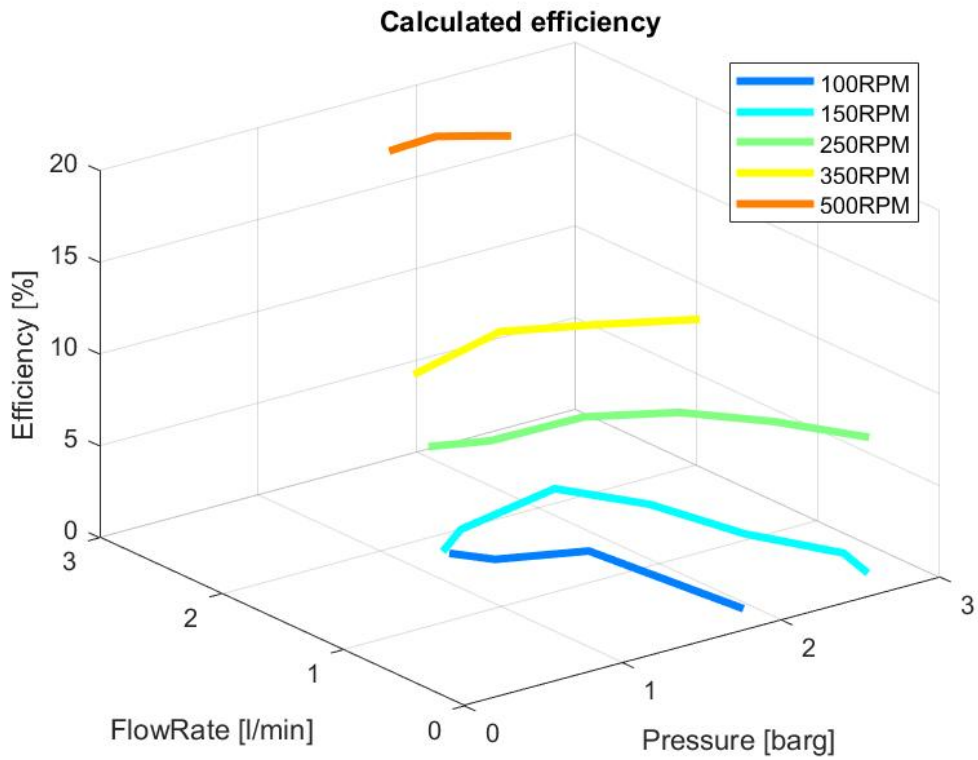


Figure A.16. EOP1 – Linear efficiency map at  $T = -20^{\circ}\text{C}$ .

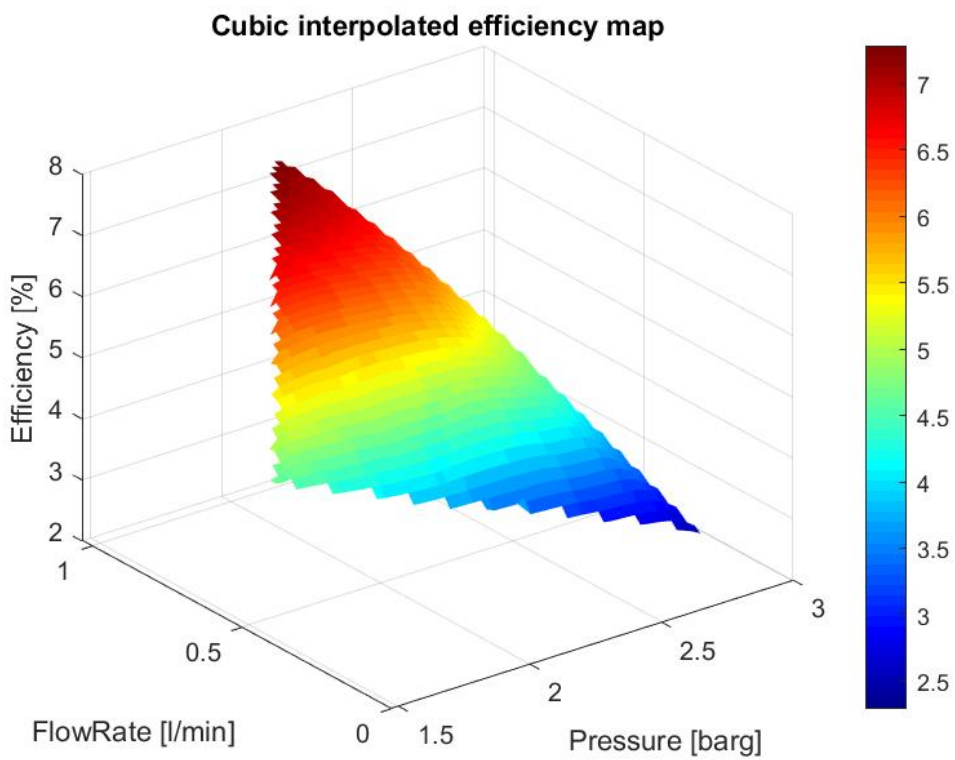


Figure A.17. EOP1 – Cubic efficiency map at  $T = -30^{\circ}\text{C}$ .

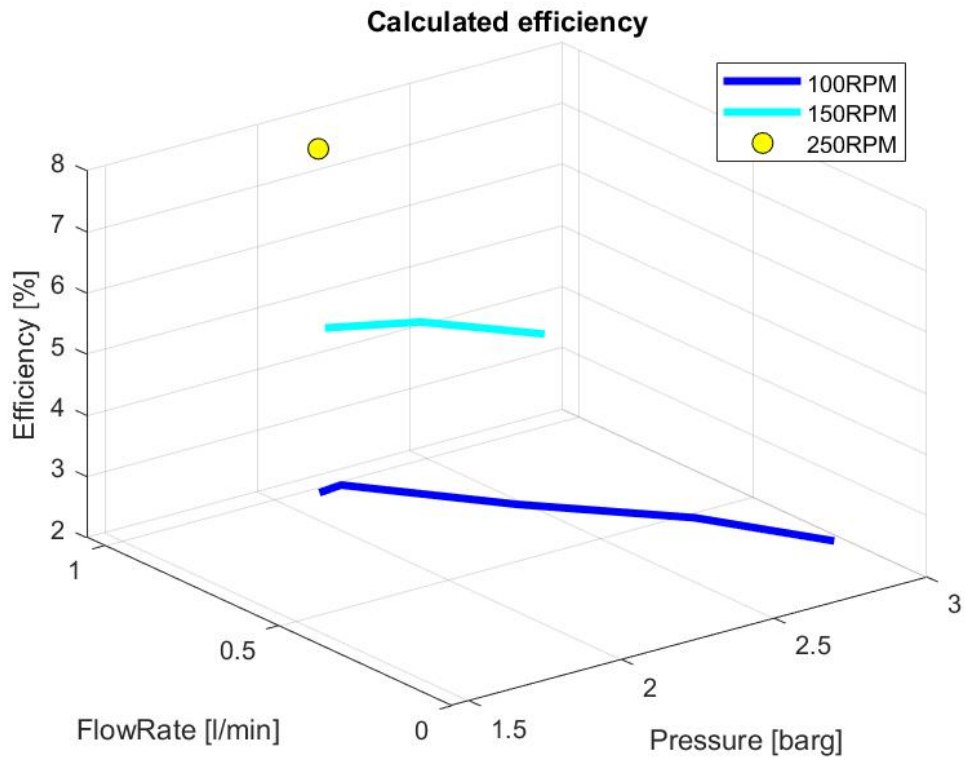


Figure A.18. EOP1 – Linear efficiency map at  $T = -30^{\circ}\text{C}$ .

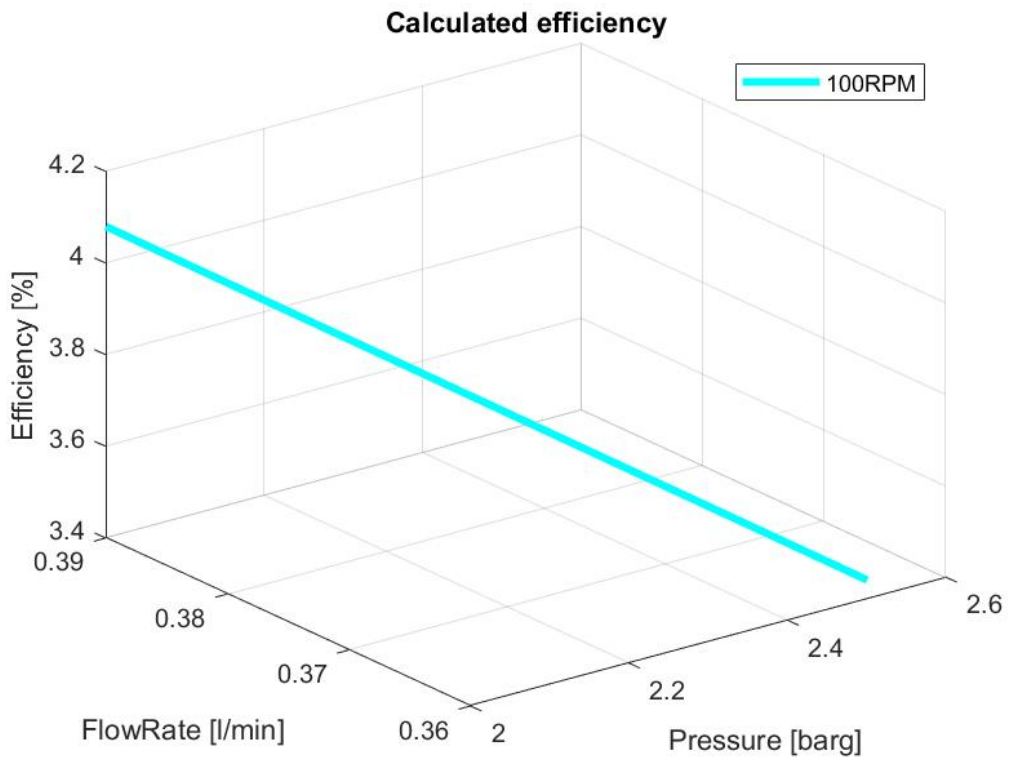


Figure A.19. EOP1 – Linear efficiency map at  $T = -40^{\circ}\text{C}$ .

## A.4 Filter and heat exchanger results

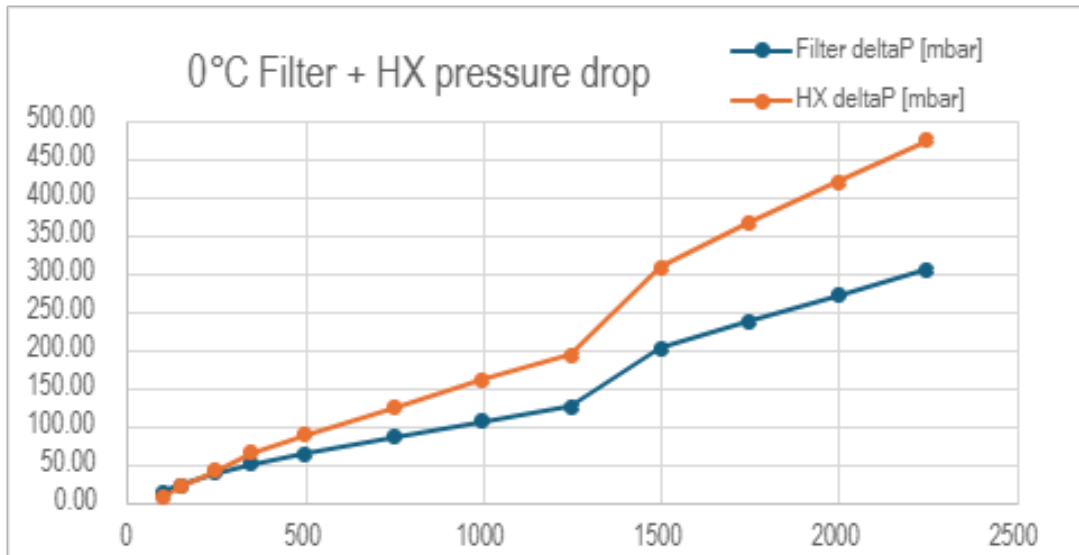


Figure A.20. EOP1 – Filter and heat exchanger results at  $T = 0^{\circ}\text{C}$ .

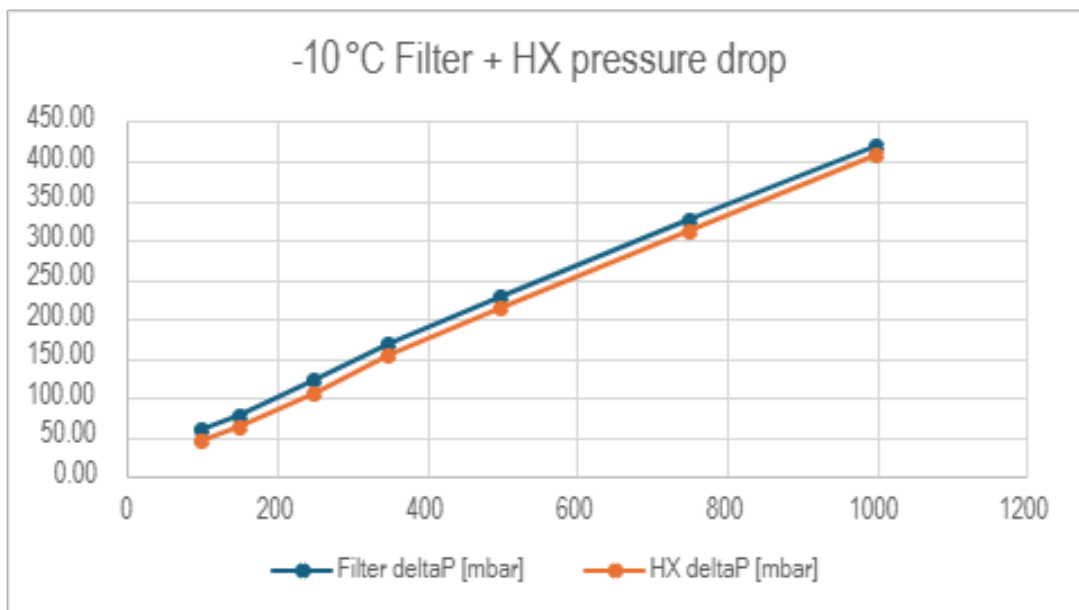


Figure A.21. EOP1 – Filter and heat exchanger results at  $T = -10^{\circ}\text{C}$ .

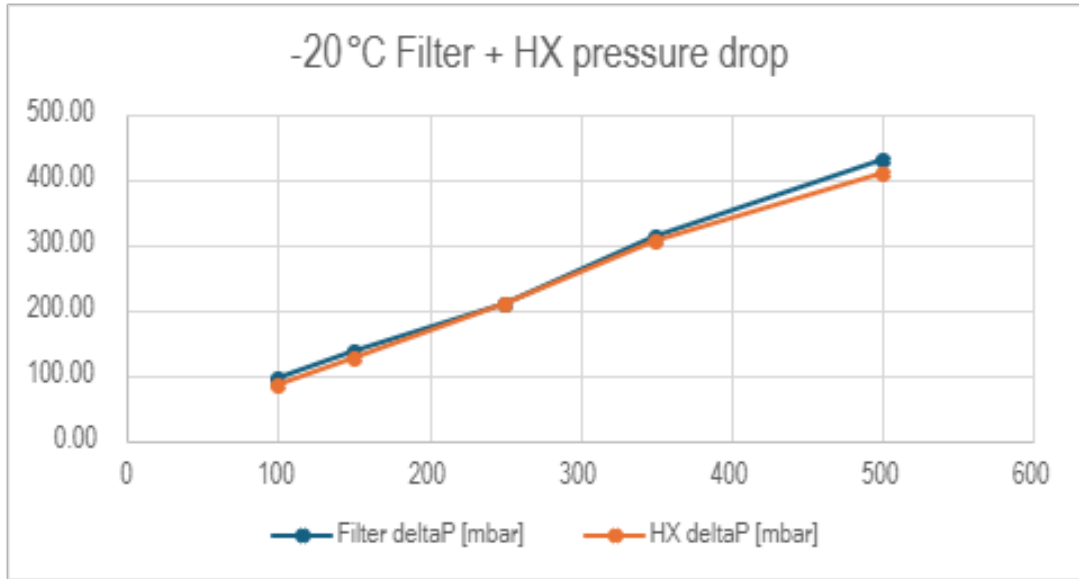


Figure A.22. EOP1 – Filter and heat exchanger results at  $T = -20^{\circ}\text{C}$ .

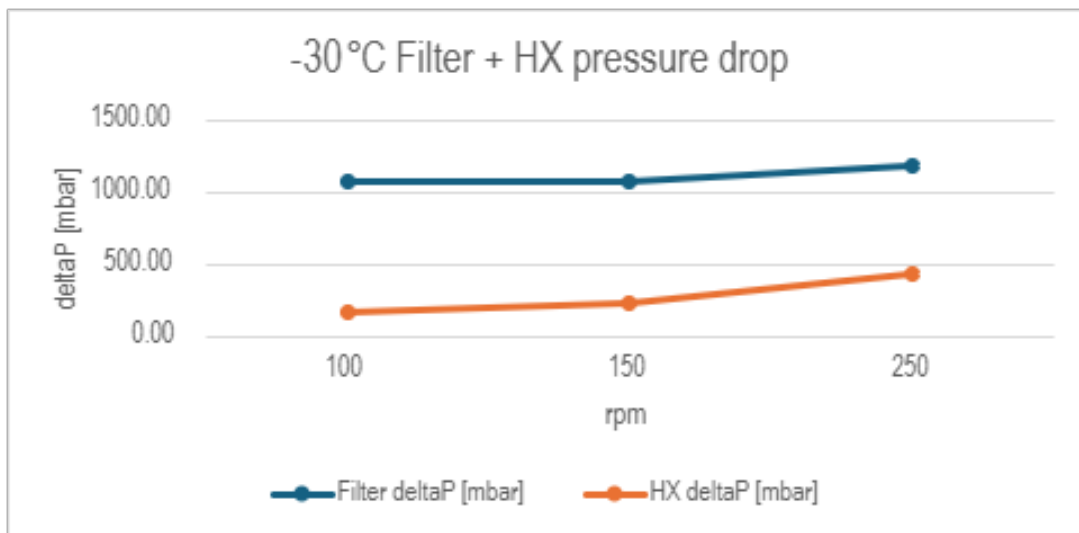


Figure A.23. EOP1 – Filter and heat exchanger results at  $T = -30^{\circ}\text{C}$ .

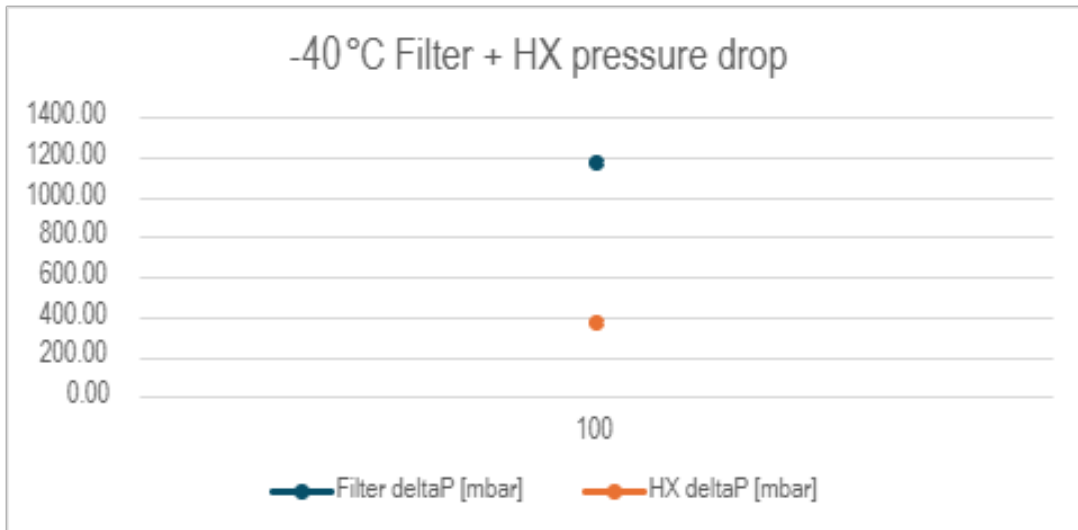


Figure A.24. EOP1 – Filter and heat exchanger results at  $T = -40^{\circ}\text{C}$ .

# Appendix B

## Test EOP2

This appendix presents the experimental results obtained from the tests performed on EOP2. For each investigated temperature level, the operating point maps, pressure–flow curves, efficiency maps and filter and heat exchanger results are reported.

### B.1 Operating point maps

The same colour coding described in Appendix [A](#) is adopted for the following operating point maps.

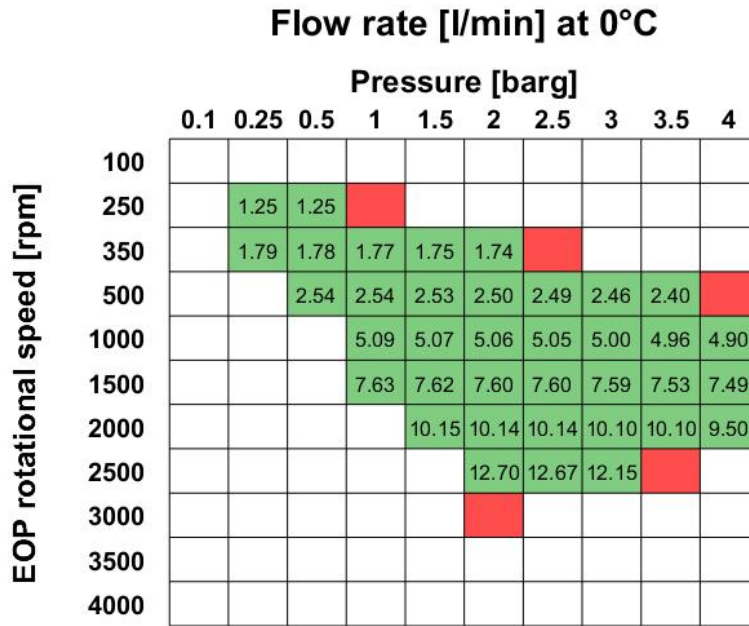


Figure B.1. EOP2 – Operating point map at  $T = 0^\circ\text{C}$ .

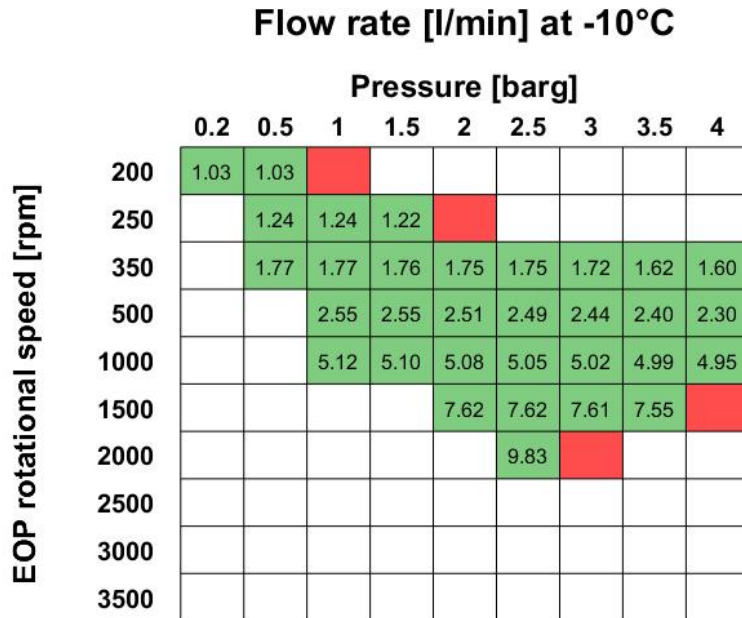


Figure B.2. EOP2 – Operating point map at  $T = -10^\circ\text{C}$ .

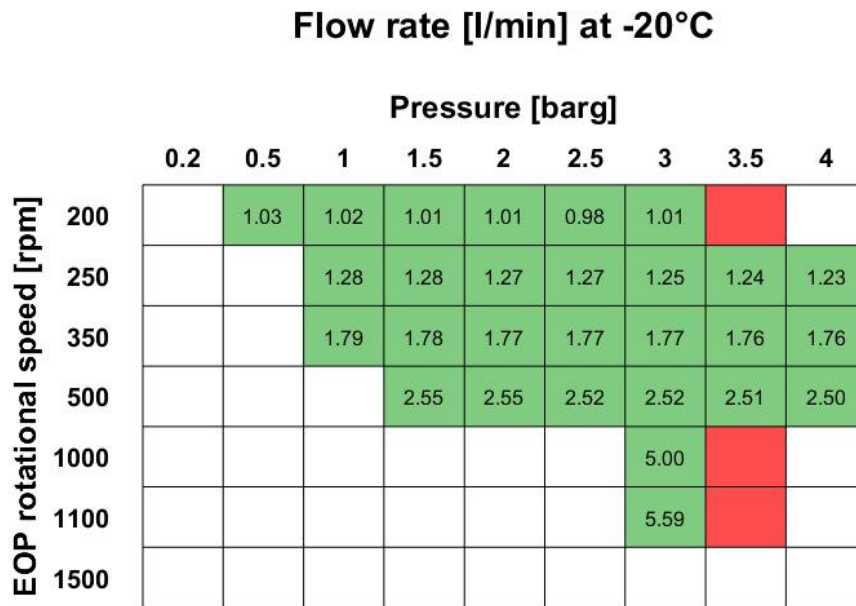


Figure B.3. EOP2 – Operating point map at  $T = -20^{\circ}\text{C}$ .

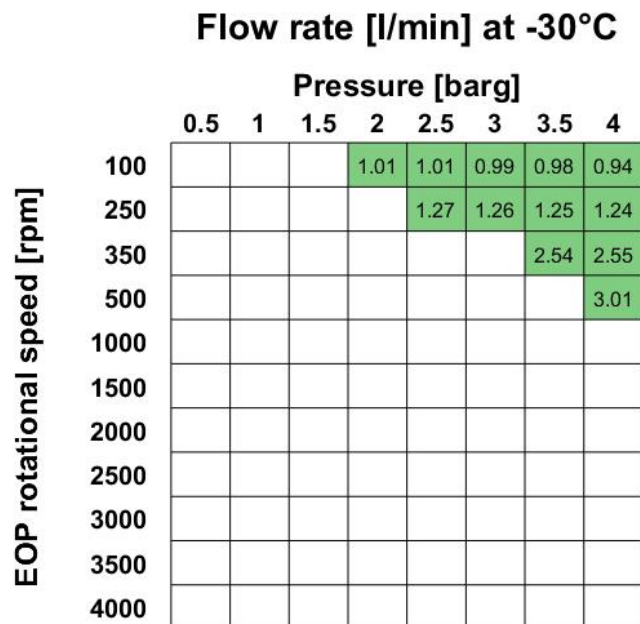


Figure B.4. EOP2 – Operating point map at  $T = -30^{\circ}\text{C}$ .

## B.2 Pressure–flow characteristic curves

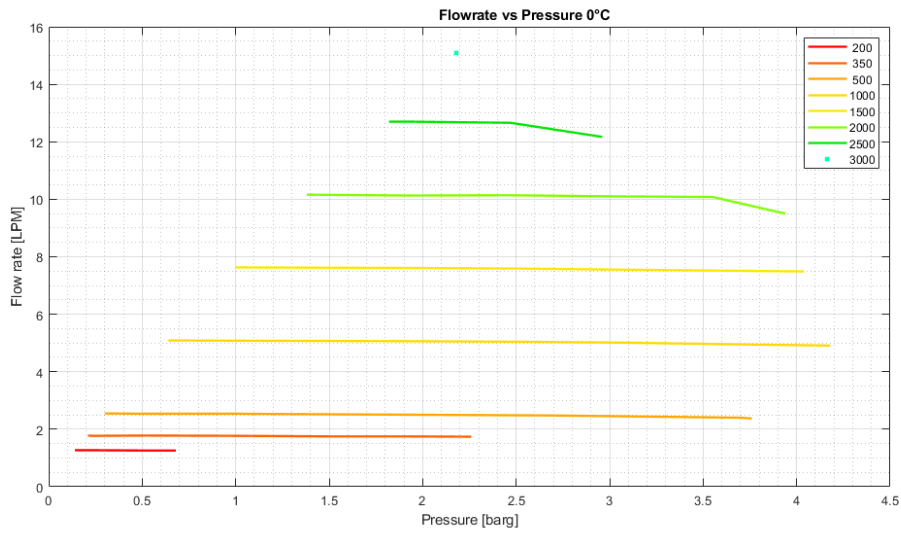


Figure B.5. EOP2 – Pressure–flow characteristic at  $T = 0^{\circ}\text{C}$ .

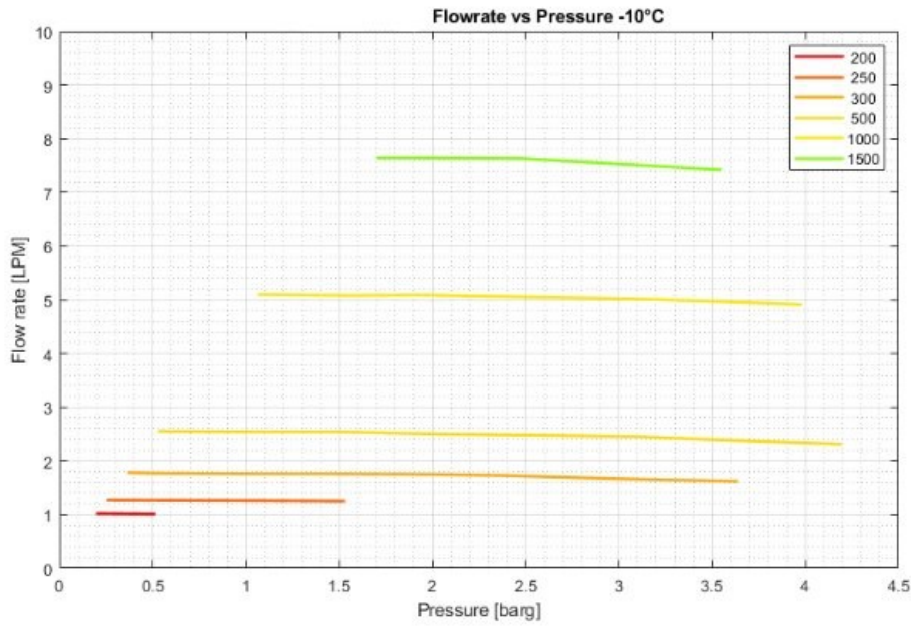


Figure B.6. EOP2 – Pressure–flow characteristic at  $T = -10^{\circ}\text{C}$ .

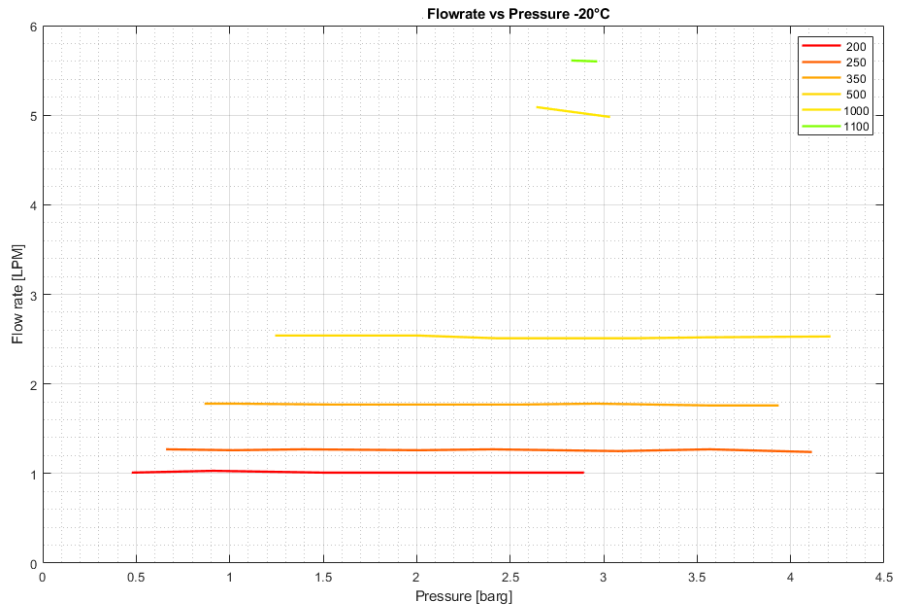


Figure B.7. EOP2 – Pressure–flow characteristic at  $T = -20^{\circ}\text{C}$ .

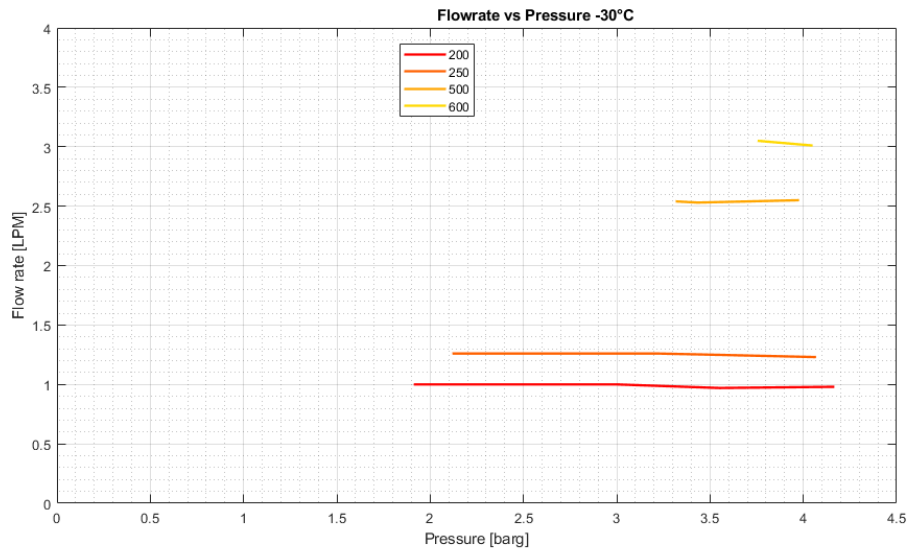


Figure B.8. EOP2 – Pressure–flow characteristic at  $T = -30^{\circ}\text{C}$ .

### B.3 Efficiency maps

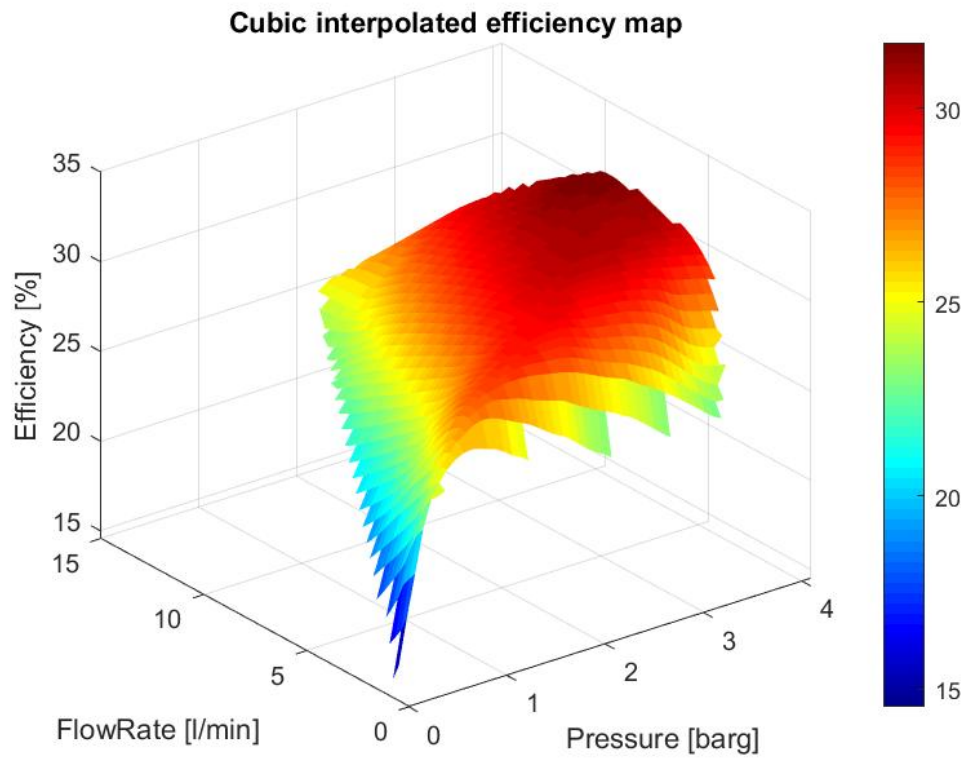


Figure B.9. EOP2 – Cubic efficiency map at  $T = 0^{\circ}\text{C}$ .

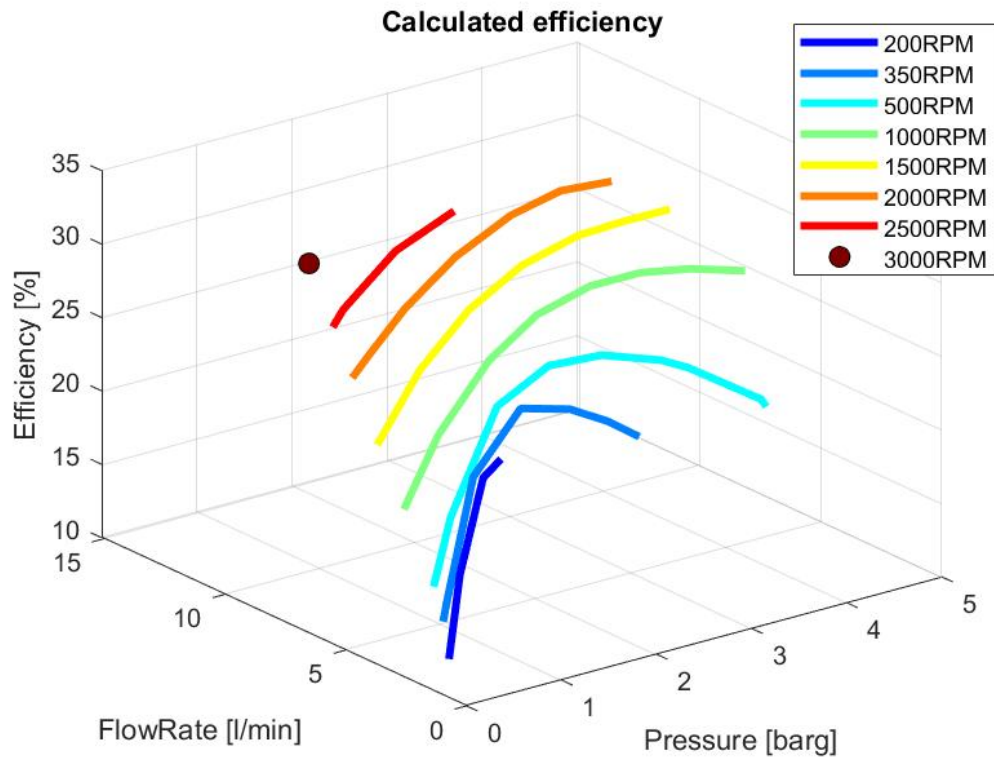


Figure B.10. EOP2 – Linear efficiency map at  $T = 0^{\circ}\text{C}$ .

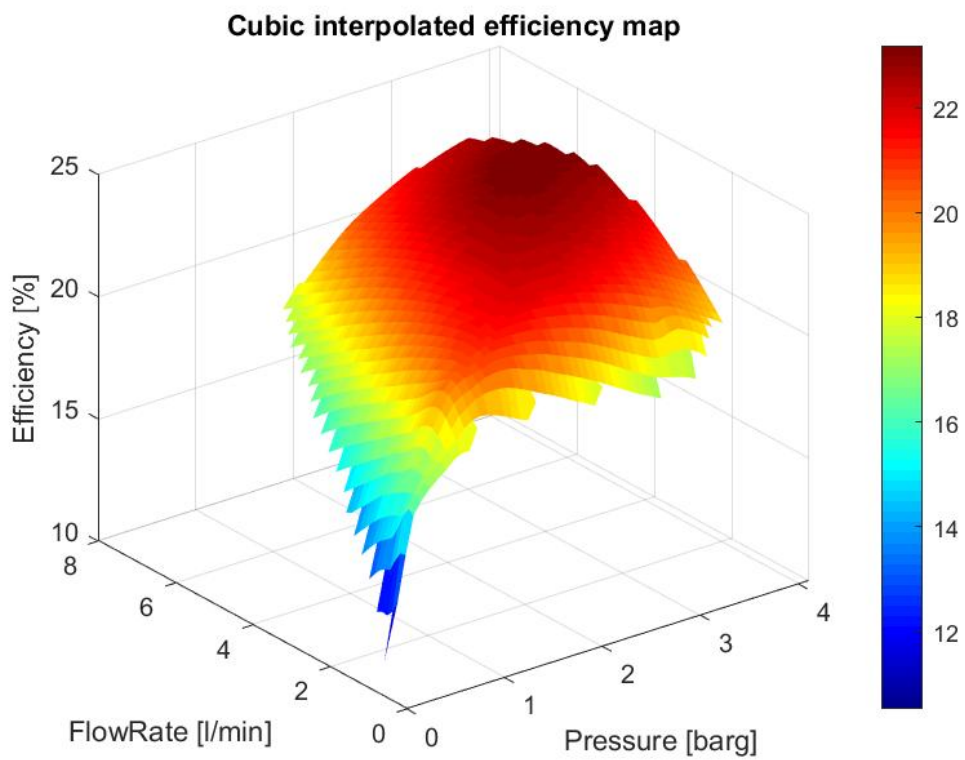


Figure B.11. EOP2 – Cubic efficiency map at  $T = -10^{\circ}\text{C}$ .

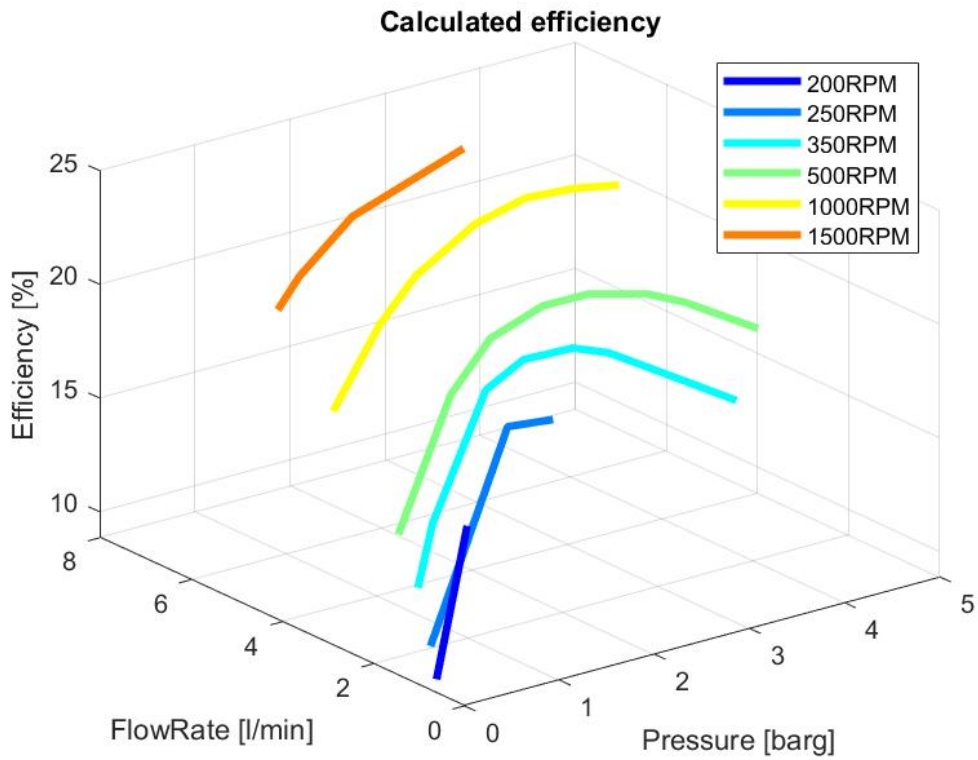


Figure B.12. EOP2 – Linear efficiency map at  $T = -10^{\circ}\text{C}$ .

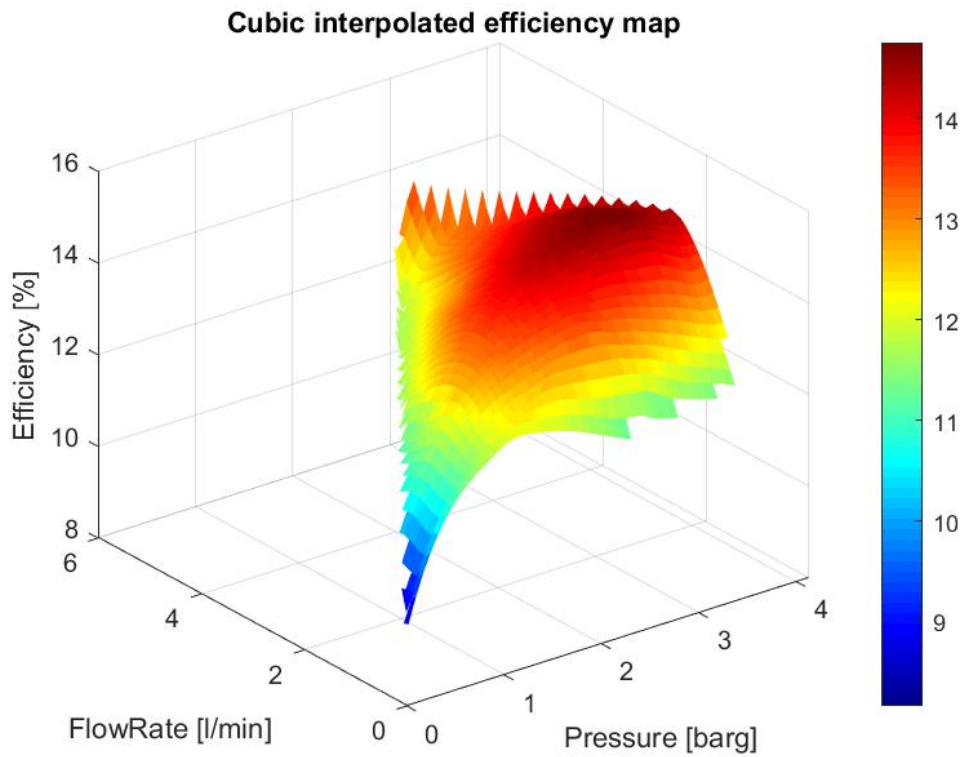


Figure B.13. EOP2 – Cubic efficiency map at  $T = -20^{\circ}\text{C}$ .

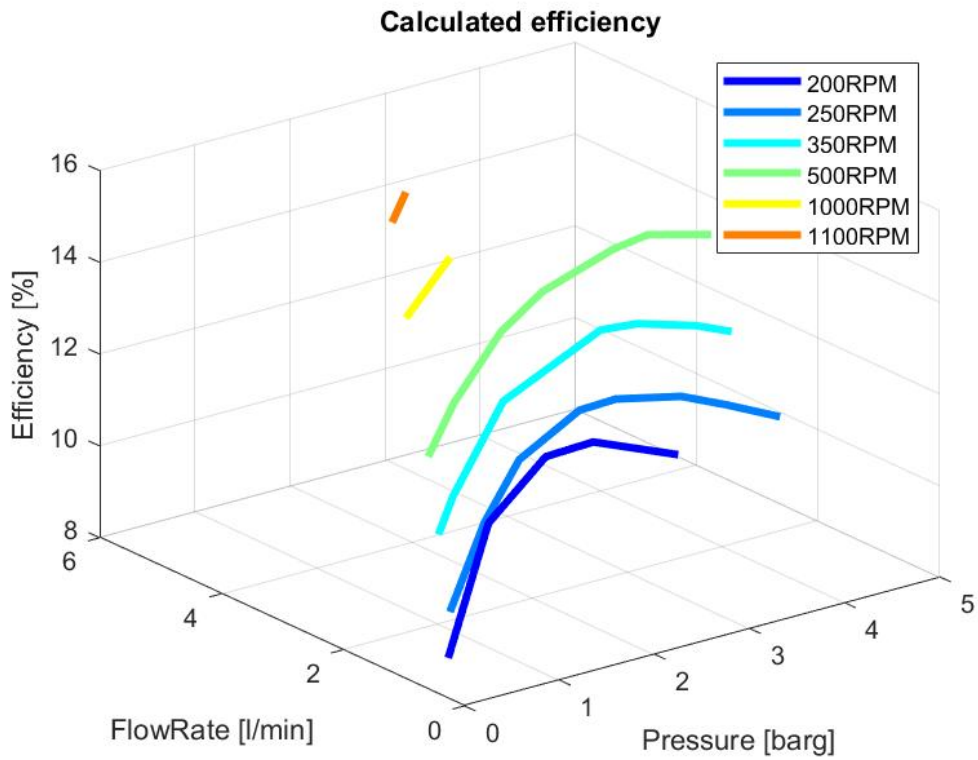


Figure B.14. EOP2 – Linear efficiency map at  $T = -20^{\circ}\text{C}$ .

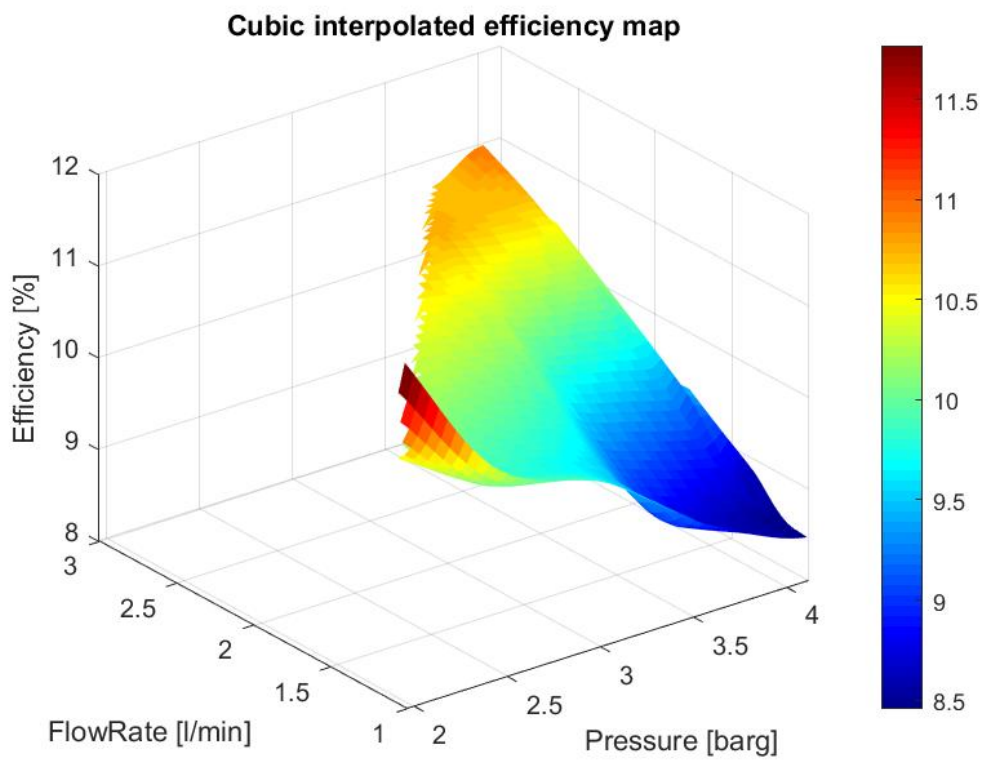


Figure B.15. EOP2 – Cubic efficiency map at  $T = -30^{\circ}\text{C}$ .

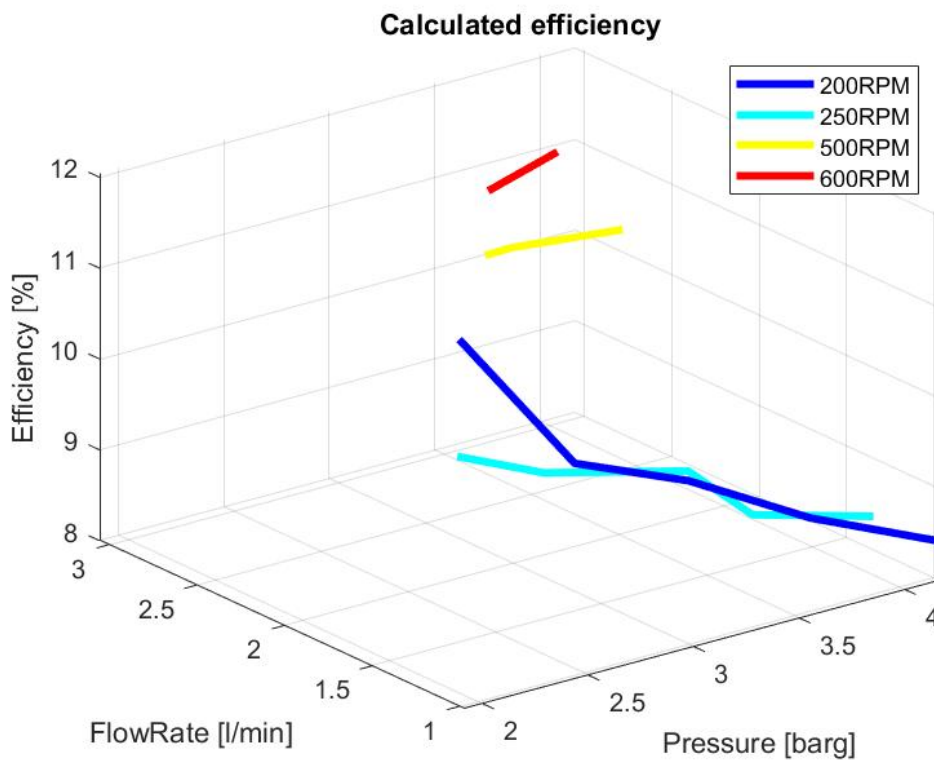


Figure B.16. EOP2 – Linear efficiency map at  $T = -30^{\circ}\text{C}$ .

## B.4 Filter and heat exchanger results

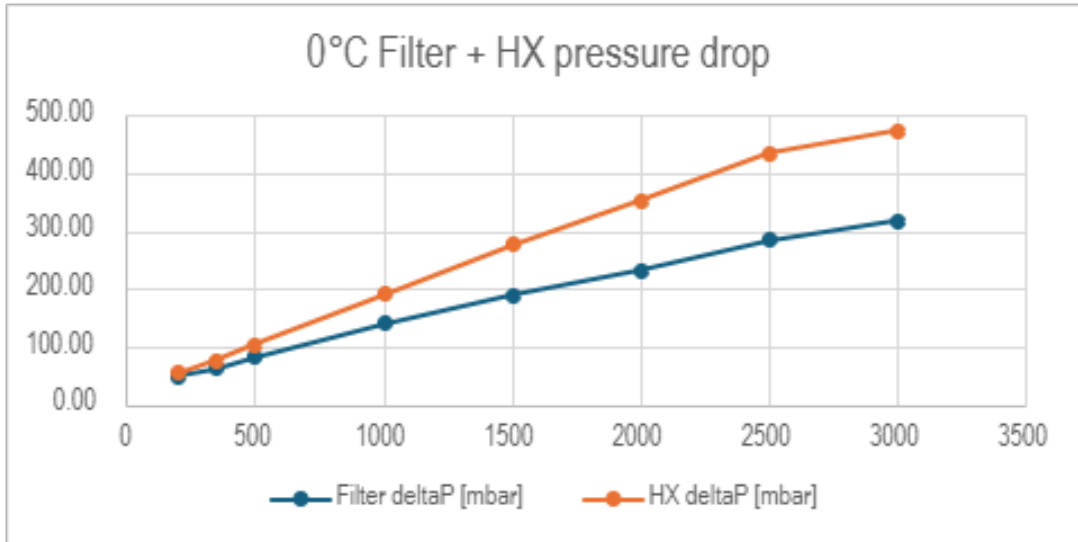


Figure B.17. EOP2 – Filter and heat exchanger results at  $T = 0^{\circ}\text{C}$ .

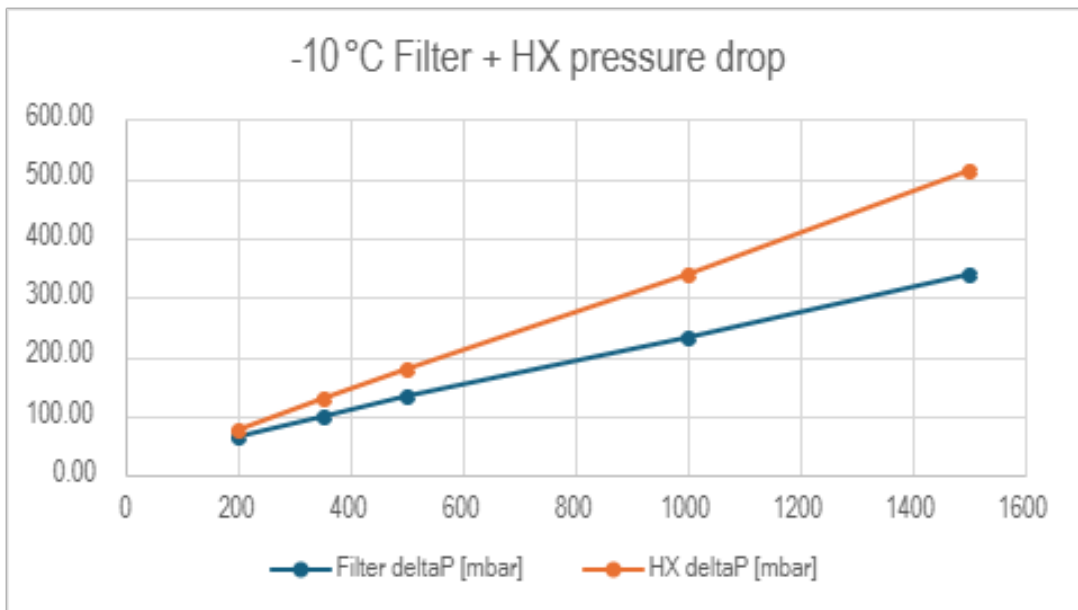


Figure B.18. EOP2 – Filter and heat exchanger results at  $T = -10^{\circ}\text{C}$ .

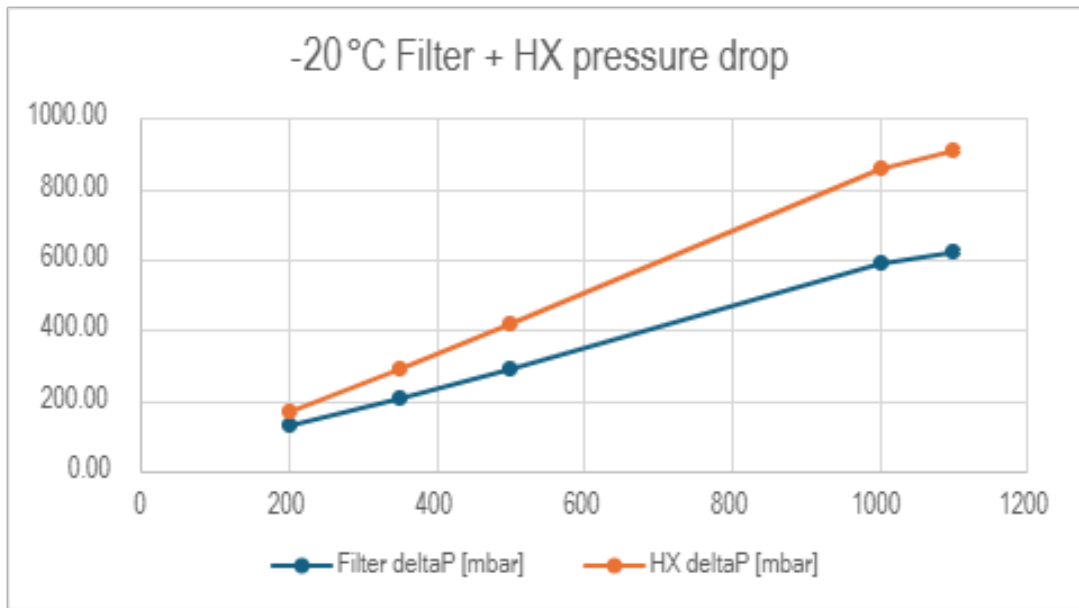


Figure B.19. EOP2 – Filter and heat exchanger results at  $T = -20^{\circ}\text{C}$ .

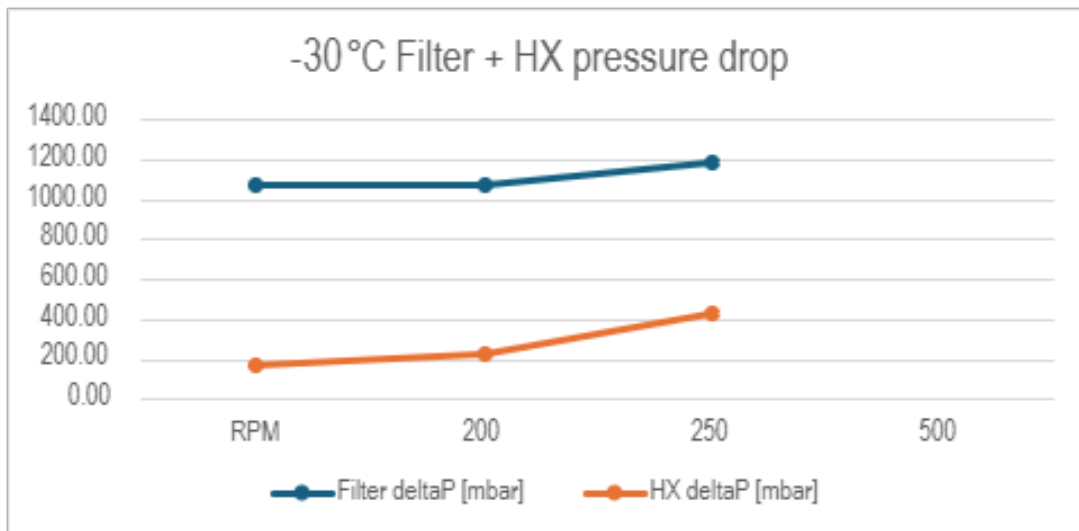


Figure B.20. EOP2 – Filter and heat exchanger results at  $T = -30^{\circ}\text{C}$ .

# Bibliography

- [1] Sara Franchina. Thermal test rig – test instruction. Internal technical document, 2025. Internal test instruction developed during the internship.
- [2] Sara Franchina. Thermal test rig development – project progress presentation. Internal presentation, 2025. Internal presentation summarizing the project development and test planning.
- [3] X. Gong and J. Smith. Effect of waveform and loading sequence on cyclic fatigue life. [https://www.researchgate.net/publication/245307987\\_Effect\\_of\\_Waveform\\_and>Loading\\_Sequence\\_on\\_Low-Cycle\\_Compressive\\_Fatigue\\_Life\\_of\\_Spruce](https://www.researchgate.net/publication/245307987_Effect_of_Waveform_and>Loading_Sequence_on_Low-Cycle_Compressive_Fatigue_Life_of_Spruce), 2003. Classic investigation showing that square waveforms accumulate damage more rapidly than triangular or sinusoidal waveforms.
- [4] M. Jimenez-Martinez. Waveform load analysis for fatigue in cyclic testing. <https://www.sciencedirect.com/science/article/pii/S2405844023056888>, 2023. Comparison of square, triangular, and sinusoidal load waveforms for cyclic fatigue tests and their effect on severity of cyclic loading.
- [5] Kun Li, Hao Zhang, and Qiang Wang. Influence of lubricating oil circulation characteristics on the performance of electric vehicle heat pump system under low temperature conditions. *Applied Thermal Engineering*, 218:119359, 2023.
- [6] Yang Liu, Xiaohui Zhang, and Shuang Wang. Electric oil pump design of hybrid continuously variable transmission. *IET Electrical Power Applications*, 13(8):1143–1151, 2019.
- [7] Garrett Motion. Garrett’s high-speed, high-power density e-powertrain advances the future of motion, May 2025. [Online; accessed 21-December-2025].
- [8] Garrett Advancing Motion. Health, safety and environment policy and cardinal safety rules, 2018. Internal company document, Brno Facility.
- [9] Garrett Advancing Motion. Machine risk assessment training (hsems 305), 2025. Internal company document, Health, Safety and Environment Management System.
- [10] National Instruments. *LabVIEW System Design Software*, 2023. Official documentation of the LabVIEW development environment.
- [11] National Instruments. Ni tdms file format – what is a tdms file? <https://www.ni.com/en/support/documentation/supplemental/06/the-ni-tdms-file-format.html>, May 2025. Official NI overview of the TDMS

- file format for structured, high-speed measurement data logging.
- [12] European Parliament. Directive 2006/42/ec of the european parliament and of the council on machinery. <https://eur-lex.europa.eu/eli/dir/2006/42/oj/eng>, 2006. Official EU legislative text defining machinery and essential requirements.
  - [13] E. G. Ribeiro, J. C. P. Gomes, and A. P. P. Ribeiro. Application of electric oil pumps on automotive systems. In *SAE Technical Paper*, number 2005-01-4086. SAE International, 2005.
  - [14] Massimo Rundo and Nicola Nervegna. Lubrication pumps for internal combustion engines: A review. *International Journal of Fluid Power*, 16(2):59–74, 2015.
  - [15] Pablo Daniel Simarra Mena. Study and modelling of an electric oil pump for automotive applications. Master’s thesis, Politecnico di Torino, 2023.
  - [16] European Union. Ce marking – product requirements, labels and markings. [https://europa.eu/youreurope/business/product-requirements/labels-markings/ce-marking/index\\_en.htm](https://europa.eu/youreurope/business/product-requirements/labels-markings/ce-marking/index_en.htm), December 2025. European Union official guidance on CE marking requirements.